Spring 2022

Cryptic Cryptophytes: The Plasticity in How Cryptophytes Respond to Changes in Resource Availability

Rachel Ann-Marie Schomaker

Cryptic cryptophytes: The plasticity in how cryptophytes respond to changes in resource availability

by

Rachel Ann-Marie Schomaker

Bachelor of Science
Florida Southern College, 2012

Submitted in Partial Fulfillment of the Requirements

For the Degree of Doctor of Philosophy in

Biological Sciences

College of Arts and Sciences

University of South Carolina

2022

Accepted by:

Jeffry L. Dudycha, Major Professor

Tammi L. Richardson, Committee Member

Jay Pinckney, Committee Member

Yen-Yi Ho, Committee Member

Xuefeng (Nick) Peng, Committee Member

Tracey L. Weldon, Interim Vice Provost and Dean of the Graduate School

DEDICATION

To my dad, Robert George Schomaker II, who would have celebrated the completion of my dissertation with a bologna sandwich and a fishing pole if he could have. I love and miss you with my whole heart. And to my mom, Anita Lynn Schneider, who has always been my biggest cheerleader. Thanks for being here through it all.

ACKNOWLEDGEMENTS

I am incredibly privileged to have worked with a wonderful team over the past few years, and to have been supported so thoroughly throughout the extent of my dissertation research. I'd like to thank Matthew J. Greenwold for his assistance on my bioinformatics and transcriptomic analysis journey, skills in which became an integral part of my dissertation. I'd also like to thank Kristin Heidenreich, Eric Lachenmeyer, and Brady Cunningham for their assistance growing and maintaining cultures and pigment analyses when I needed help throughout my first few years. To Savannah Simon, Emma Boyajieff, and Dylan C. Davis, I extend the greatest appreciation for their help with gene annotation and exploration, for taking many, many, *many* photos of cryptophyte cultures, for assisting in keeping experimental cultures alive, and for helping me collect population growth rate data, which saved my sanity throughout this journey. I also thank Trenton Agrelius, Lindsey Swartz, Jake Swanson, Dr. Gabriel Herrick, and Rachel Peters for their friendship and support throughout the duration of my graduate career (and undergraduate career, for some!). Last, I'd like to thank the National Center for Genome Analysis Support at Indiana University and University of South Carolina's Research Computing center for data storage, computing technology, and resources. My dissertation projects were funded by an award from the U. S. National Science Foundation's Dimensions of Biodiversity program (DEB 1542555) to TLR and JLD and the University of South Carolina's Support to Promote Advancement of Research and Creativity (SPARC) grant awarded to RAS.

ABSTRACT

Resource variability and availability often drives competition within ecosystems, which can lead to the diversification of organismal niches and physiological capabilities. In aquatic systems, common resources that photosynthetic organisms, such as algae, compete for are light and carbon. Both the spectral characteristics (color) and carbon concentrations of an aquatic system vary with time and space, which means that algae need to be able to respond to changes in resource availability to survive. Using a group of ubiquitous unicellular eukaryotes known as cryptophytes, we investigated both how cryptophytes respond to changes in the available light spectrum at a physiological and genetic level, and how they respond to changes in light and carbon availability.

First, we grew cryptophytes with different pigment complements (three phycoerythrin-containing and one phycocyanin-containing) under wide-spectrum, red, green, and blue light. We examined how these cryptophytes responded to changes in available light color, expecting that they would shift pigment physiology to maximize light capture as predicted by the theory of chromatic acclimation, and that gene expression would mirror any shifts in physiology. We found that pigment complement seems to be related to how cryptophytes respond to available spectra, and that light acclimation strategies related to habitat history may explain unexpected results observed in some species. Additionally, we found that post-transcriptional modification seems to play a role in genetic regulation of our physiological observations.

Second, we grew cryptophytes of varying sizes in habitats with varying light availability and carbon sources to examine the plasticity by which cryptophytes respond to changes in potential food supply. We expected that size would be a driver for carbon acquisition, and that cryptophytes would be able to survive in the darkness with added carbon to supplement photosynthetic losses. We found that growth, volume, and pigment concentrations all varied with species and treatment. Four species exhibited heterotrophy using glucose as a carbon source, and no cryptophytes were able to survive on bacteria in the dark. Both bacteria and glucose affected how cryptophytes grew in the light, but this varied with species. Overall, our results suggest that resource acquisition strategies are highly plastic in cryptophytes.

PREFACE

Organisms need a wide variety of resources to maintain growth, synthesize biomolecules, and perform necessary biochemical and metabolic processes. Microorganisms require sources of energy, carbon, vitamins and minerals, water, and electron donors, along with hospital conditions, such as an optimal pH, temperature, and gaseous environment. These requirements are well-studied in the field of microbiology, particular in prokaryotic systems. Multiple methods of resource acquisition strategies have been defined in relation to these various resource requirements. Carbon acquisition can be broken down into two general categories: autotrophy and heterotrophy. Autotrophy, which means “self-feeding”, means that an organism is able to use energy to synthesize their own organic compounds. Heterotrophy, which means “other-feeding”, is when an organism must acquire organic carbon from an external source because they cannot synthesize it themselves. In general, there are two types of heterotrophic function that unicellular organisms may exhibit: phagotrophy or osmotrophy. Phagotrophy is the process by which an organism engulfs an organic molecule (or a prey item; often, this is discussed in terms of bacteria and is called “bacterivory”) via phagocytosis and digests the molecule or individual to obtain organics. Osmotrophy is the process by which an organism absorbs dissolved organics from the external environment to use as an organic carbon source.

There is a third, less understood mechanism of carbon acquisition that is known as mixotrophy, where microorganisms are able to use a combination of both autotrophy and heterotrophy. The term “mixotroph” is often jumbled in the literature, sometimes being used to describe multicellular carnivorous plants which trap and consume insects to obtain nitrogen, while also being used to describe unicellular eukaryotes which use both autotrophic and heterotrophic means to acquire and assimilate organic carbon. Here, I will be defining a mixotroph as an organism that uses both autotrophy and heterotrophy for carbon acquisition and not for any other nutrient uptake.

Energy acquisition is also well defined in microorganisms. Some microorganisms, known as chemotrophs, can assimilate energy for biosynthesis by breaking chemical bonds, while others can capture light energy, known as phototrophs, to create organic molecules via photosynthesis. Photosynthesis has been well-characterized over the years in both multicellular and unicellular phototrophs, and we know that different photosynthetic organisms have evolved a host of photosynthetic pigments, and that different groups of organisms perform photosynthesis differently.

While we have a fundamental understanding of how carbon and energy are acquired and assimilated in microorganisms, the plasticity by which these various processes occur seems to vary with organismal group and the genetic plasticity is not well known. For example, there is a concept known as the Theory of Chromatic Acclimation, the idea that photosynthetic organisms can temporarily shift their pigment composition to maximize their photosynthetic efficiency dependent upon the available light intensity and color, which has been well-studied in cyanobacteria. Cyanobacteria maintain two main light-harvesting pigments (phycobiliproteins that can be classified as either

cyanobacteria-phycoerythrin and cyanobacteria-phycocyanin) that they can switch between depending on the available light spectrum, leading to a drastic phenotypic change in their coloration. However, we know less about whether this theory is applicable to other algal groups, particularly those that do not have multiple main light-harvesting pigments like cyanobacteria, such as cryptophytes. Cryptophytes are a wide-spread group of unicellular algae that can either have cryptophyte-phycoerythrin *or* cryptophyte-phycocyanin, but they cannot have both. Yet, they are found in a wide-variety of aquatic environments that vary in spectral characteristics. This begs the questions that my first two chapters of my dissertation aim to address: how has this diversity in pigmentation evolved, and how do cryptophytes with various phycobiliprotein types respond to different light spectra both at the physiological and genetic level?

The final chapter of my dissertation focuses less on photosynthetic plasticity and instead of the plasticity of carbon acquisition methods in cryptophytes. Cryptophytes have historically been considered autotrophic, but their evolutionary history that involved secondary endosymbiosis between an autotroph and a heterotroph leads me to believe that there is potential for plasticity in the cryptophyte lineage. Additionally, some species of cryptophytes have been suggested to be mixotrophic, and we do know of a few representatives that are strict heterotrophs, either because they never obtained the ability to photosynthesize (such as the *Goniomonas* clade) or because they lost the ability to photosynthesize over time (such as *Cryptomonas paramecium*). Just as cryptophytes occupy a wide variety of spectral habitats in nature, they also occupy a wide variety of habitats with different degrees of carbon availability, from freshwater ponds heavy in

dissolved organic matter to the open-ocean which has significantly less organic matter and a different population of potential bacterial prey. As such, the third chapter of my dissertation focuses on exploring the plasticity of carbon acquisition methods across the cryptophyte clade.

TABLE OF CONTENTS

LIST OF TABLES

LIST OF FIGURES

CHAPTER 1: CONSEQUENCES OF LIGHT SPECTRA FOR PIGMENT COMPOSITION AND GENE EXPRESSION IN THE CRYPTOPHYTE *RHODOMONAS SALINA*

Abstract

Algae with a more diverse suite of pigments can, in principle, exploit a broader swath of the light spectrum through chromatic acclimation, the ability to maximize light capture via plasticity of pigment composition. We grew *Rhodomonas salina* in wide-spectrum, red, green, and blue environments and measured how pigment composition differed. We also measured expression of key light-capture and photosynthesis-related genes and performed a transcriptome-wide expression analysis. We observed the highest concentration of phycoerythrin in green light, consistent with chromatic acclimation. Other pigments showed trends inconsistent with chromatic acclimation, possibly due to feedback loops among pigments or high-energy light acclimation. Expression of some photosynthesis-related genes was sensitive to spectrum, although expression of most was not. The phycoerythrin α-subunit was expressed two-orders of magnitude greater than the β-subunit even though the peptides are needed in an equimolar ratio. Expression of genes related to chlorophyll-binding and phycoerythrin concentration were correlated, indicating a potential synthesis relationship. Pigment concentrations and expression of related genes were generally uncorrelated, implying post-transcriptional regulation of pigments. Overall, most differentially expressed genes were not related to photosynthesis;

thus, examining associations between light spectrum and other organismal functions, including sexual reproduction and glycolysis, may be important.

Introduction

Photosynthesis is the remarkable metabolic process whereby organisms capture light energy and use it to fix carbon dioxide into organic carbon compounds. The evolution of photosynthesis resulted in an explosion of biodiversity across the globe, and understanding the functionality, plasticity, and ecological consequences of this process remains an area of substantial interest. Modern photosynthetic organisms have evolved to use chlorophyll-*a* in their reaction centers to funnel light energy through the photosynthetic pathway. Chlorophyll-*a* is excellent at absorbing blue (~400 – 490 nm) and red (~620 – 700 nm) wavelengths of the visible spectrum but it does not efficiently absorb the remaining wavelengths, leaving a wide range of potentially untapped energy that could be used for photosynthesis (Mackinney 1941).

Accessory pigments are light-absorbing compounds that differ among algal taxa and work in conjunction with chlorophyll-*a* by capturing light that chlorophyll-*a* absorbs poorly (Blinks 1954; Glazer 1977; Gantt 1980; Stengel *et al.* 2011). As a result, phytoplankton accessory pigments may open spectral niches that were not previously available, which can lead to increased biodiversity within ecosystems, altered community dynamics, and ecosystem functioning (Stengel *et al.* 2011; Sanfilippo *et al.* 2019). If the biodiversity of an aquatic ecosystem increases, the overall ecosystem productivity often increases, supporting the flow of carbon and energy between trophic levels (Balvanera *et al.* 2006; Cardinale *et al.* 2006; Ward & Follows 2016). Overall, the effects of niche differentiation and exploitation, whether caused by variation of absorption characteristics

via accessory pigment diversity or by other means, can have substantial downstream effects at both the community and ecosystem level.

The spectral characteristics of aquatic environments can vary substantially in time and space. Those rich in colored dissolved organic material (CDOM) tend to be dominated by red light because CDOM strongly absorbs blue and violet light (Blough and Del Vecchio 2002). Offshore oceans tend to be dominated by blue light because they have low CDOM and low phytoplankton concentrations (Kirk 1994; Blough & Del Vecchio 2002), while coastal oceans are often green in appearance, as nutrient inputs promote phytoplankton growth and hence high chlorophyll-*a* concentrations. As anthropogenic land-use, eutrophication, and CDOM input into aquatic environments rise, the amount of spectral variation across aquatic habitats may become more extreme (Roulet & Moore 2006; Kritzberg 2017; Dutkiewicz *et al.* 2019; Luimstra *et al.* 2020). These changes could force natural phytoplankton populations into new spectral environments, which can alter the ecosystem if the resident organisms are unable to effectively occupy them.

One way phytoplankton can respond to shifts in the spectral environment is by adjusting the ratio of various pigments in response to the spectral environment (Sanfilippo *et al.* 2019; Sebelik *et al.* 2020). Known as chromatic acclimation (or chromatic "adaptation"), this is a form of reversible phenotypic plasticity where photophysiology is adjusted to maximize light absorption (Engelmann 1883; Gaidukov 1903; Hattori & Fujita 1959a,b; Fujita & Hattori, 1960a,b, 1962a,b, 1963; Bennett & Bogorad 1973). Overall, it alleviates selection pressures imposed by variation of the available light spectrum or by competition for certain wavelengths (Toth and Palmer

2016). Chromatic acclimation is well-studied in cyanobacteria because many species maintain a diverse pigment complement, including the accessory pigments phycocyanin and phycoerythrin, which primarily absorb red (569-650nm) and green light (538-568nm) respectively, along with chlorophylls (Campbell 1996; Stengel *et al.* 2011; Xia *et al.* 2016). Cyanobacteria shift their pigment composition to best suit the light characteristics of their habitats, broadening their fundamental niche and giving them a competitive advantage where spectral variation occurs (Grossman 2003; Stomp *et al.* 2004; Stomp *et al.* 2007). Beyond cyanobacteria, physiological responses to light spectrum are widespread across many different eukaryotic phytoplankton (Wallen & Geen 1971; Rivkin 1989; Algarra et al. 1991; Figueroa et al. 1995; Granbom et al. 2001; Mouget et al. 2004; Vadiveloo et al. 2017), and light spectrum has been shown to effect not only pigment composition in eukaryotic phytoplankton, but growth rate, as well (Heidenriech & Richardson 2019), suggesting that light spectrum has major implications for phytoplankton fitness. However, the molecular mechanisms of these responses are poorly known and research on how gene expression in algae responds to changes in spectral irradiance is largely lacking; most such work in algae involves the effects of light intensity but not light spectrum (e.g., Ho et al. 2009; Park et al. 2010; Xiang et al. 2015; Nan et al. 2018; Li et al. 2019). Our aim is to begin remedying this gap for a eukaryotic alga that has multiple photosynthetic pigments.

Study System

Cryptophytes are a phylum of single-celled eukaryotic algae that are ubiquitous across nearly all aquatic habitats and exhibit remarkable diversity in visible pigmentation. Photosynthetic cryptophytes contain chlorophyll-*a* and also maintain the accessory

pigments chlorophyll-c_2, alloxanthin, α-carotene, and phycobiliproteins (cryptophyte phycoerythrin and cryptophyte phycocyanin). Unlike cyanobacteria, cryptophyte species each have only one type of phycobiliprotein (appearing either green or red), which are the main light-harvesting pigments in cryptophytes (Glazer 1983; Hill & Rowan 1989; Vesk *et al.* 1992; Blankenship 2002). These pigments are composed of two alpha and beta protein subunits, plus four chromophores known as phycobilins. The molecular structure of the protein-chromophore complex is directly related to the wavelengths of light the pigment can capture (Doust *et al.* 2004; Overkamp *et al.* 2014).

Phycobiliprotein evolution is associated with changes in light capture in cryptophytes (Greenwold *et al.* 2019), but studies examining chromatic acclimation are conflicting or differ greatly among clades. Some studies have suggested that cryptophytes exhibit only a weak chromatic acclimation response (Ojala 1993), while others suggest that cryptophytes exhibit some predicted changes in photophysiology in response to spectral availability (Kamiya & Miyachi 1984 a,b; Lawrenz & Richardson 2017; Heidenreich & Richardson 2019), but the responses vary with species and pigment composition. Our study aims to build off these previous observations in order to better understand cryptophytes' ability to respond to light spectrum and to investigate the molecular responses, which have not been studied previously.

Objectives

To better understand the mechanisms by which algae respond to light spectrum, we investigated the plasticity of pigment composition and gene expression (i.e., whether pigment composition and expression level changes) in the cryptophyte *Rhodomonas salina* (which has cryptophyte pycoerythrin-545) grown in different spectral

environments. We asked the following questions: 1) How do the concentrations of pigments change in response to different spectral irradiance but equal intensity? and 2) How does gene expression differ among spectral environments? We examined the pigment and transcriptional responses for experimental populations grown in blue, red, and green spectra. The blue vs. red light comparison represents the widest energy difference between spectra (as one blue photon is more energetic than one red photon) and reflects distinct habitats in the natural world. Green vs. red light also reflects distinct real-world habitats but maximizes the differences in the expected light absorption due to molecular physiology. In contrast, blue vs. green light comparisons represent distinct habitats that present more limited energetic and light absorption differences. We also collected data for the wide-spectrum environment our culture of *R. salina* had been growing in prior to the experiment as a baseline. Based on the theory of chromatic acclimation, we expected that *R. salina* would respond to maximize its capacity to capture available light; if *R. salina* was not plasticly responsive to light color, we expected to see no change in *R.* salina's physiology or gene expression across light spectra.

We investigated transcriptional responses at three different scales. First, we examined expression of transcripts that encode the peptide components of cryptophyte phycobiliproteins, predicting that they would correlate with concentration of the pigment and maximize available light capture. For example, we expected to see an increase in phycoerythrin concentration in green light, and we expected to see the genes encoding for the phycoerythrin subunit proteins to be upregulated in green light to mirror this shift in concentration. Assuming changes in concentration maximized light capture, we expected changes in concentration and gene expression to remain stable in order to maintain this

ability. Second, we examined expression of 99 genes that were *a priori* identified as participating in light capture or photosynthesis, predicting that these loci would be most sensitive to light spectrum, but the direction of regulation would be dependent upon each gene's function. Third, we examined genome-wide expression to identify molecular processes that interact with light spectrum but may not have obvious connections to light capture or photosynthesis. Because we do not know the specific function of every gene in the *R. salina* genome, we did not have any specific hypotheses for the direction of regulation we expected for many genes. We further sought to link our assessment of pigment plasticity (change in pigment composition) and expression plasticity (change in expression level) by testing for correlations between the two across our entire experiment.

Methods

Growth and Treatment Conditions

Baseline cultures. We grew five replicate cultures of *Rhodomonas salina* CCMP 1319 (from the National Center for Marine Algae and Microbiota at the Bigelow Laboratory for Ocean Sciences) in 150 mL of L1-Si media (Guillard & Ryther 1962) in a Conviron walk-in incubator (Controlled Environments, Inc., Manitoba, Canada) kept at 20°C. These replicate cultures were grown under a wide-spectrum light environment (LumiBar Pro LED Light strip, LU50001; LumiGrow, Emeryville, CA, USA) at ~30 µmol photons m^{-2} s^{-1} on a 12:12 hr light:dark cycle. Gas exchange and pH was not monitored, but all cultures were grown in the same experimental chamber and in the same media, so these conditions should not have varied. We swirled each replicate culture by hand daily to prevent settling and help aeration.

Experimental populations. Once the baseline cultures reached mid-exponential phase (5-7 days after inoculation), we used the five replicate cultures to inoculate four experimental populations from each by transferring 5 mL of the culture into 300 mL of fresh media for a total of 20 experimental populations. One experimental population derived from each replicate baseline culture was randomly assigned to each light spectrum treatment.

Treatment Conditions. We placed all experimental populations in four separate light environments: wide-spectrum; blue-dominated, green-dominated, and red-dominated, each maintained at ~30 µmol photons m^{-2} s^{-1} at 20°C, which is comparable to low-light conditions cryptophytes usually inhabit in nature. Like the wide-spectrum environment, the blue and red lights were maintained by LumiBar Pro LED light strips (LU50001; LumiGrow, Emeryville, CA, USA), but the green light environment was provided by an EvenGlow® RGB LED panel (Super Bright LEDs Inc., St. Louis, MO, USA). (Spectra for each environment can be found in Figure 1.6.) We left each population to acclimate in each treatment environment for 10 generations (assuming population intrinsic growth rates of 0.39, 0.43, 0.44, and 0.52, per day in wide-spectrum, green, red, and blue light respectively, as quantified by Heidenreich and Richardson 2019 in the same experimental chambers, meaning that the length of time to reach 10 generations for each treatment varied with growth rate). 10 generations is generally accepted as the minimum requirement for algal species to reach balanced growth conditions in new environments (Parkhill *et al.* 2001). During acclimation, we transferred the populations to new media after ~5 generations (~7 days) to ensure they remained in nutrient-replete conditions. After the populations were acclimated, we sampled for pigments and RNA.

Pigment Analyses

Cryptophyte Phycoerythrin Analysis. We calculated cryptophyte phycoerythrin concentrations using the freeze-thaw centrifugation method of Lawrenz *et al.* (2011). We took 15 mL aliquots of each experimental population and centrifuged them at 2,054 g in a Sorvall RC-4B centrifuge for 10 minutes. The supernatant was removed, and the cell pellet was resuspended in 0.1 M phosphate buffer (pH = 6). We then froze the samples at -20°C for a minimum of 24 hours. After freezing, we thawed the samples at 5°C for 24 hours. The thawed samples were then centrifuged at 11,000 g in a Beckman Coulter 18 Microfuge for 5 minutes to remove excess cell material. We measured the absorbance of the remaining supernatant against a phosphate buffer blank in a 1 cm quartz glass cuvette using a Shimadzu UV-VIS 2450 dual-beam spectrophotometer from 400 to 750 nm in 1 nm intervals. Data were scatter-corrected by subtracting the absorbance at 750 nm from the maximum absorption peak (Lawrenz *et al.* 2011). Concentrations (pg/cell) were calculated according to:

$$C = \frac{A}{\varepsilon * d}\ x\ MW\ x\ \frac{Vbuffer}{Vsample} x\ \frac{10^{12}}{N}$$

Where A = absorbance of sample, ε = the extinction coefficient for cryptophyte phycoerythrin (5.67 x 10^5 L ·mol^{-1} · cm^{-1}; MacColl et al. 1976), d = path length of the cuvette in cm, MW = molecular weight of cryptophyte phycoerythrin (45,000 Da; MacColl *et al.* 1973, 1976), V_{buffer} = volume of buffer in mL, V_{sample} = volume of sample in mL, and N = concentration of cells (cells/L). The 10^{12} is the conversion factor to convert the results into pg/cell from g/cell.

Non-Phycoerythrin Analyses. For determination of chlorophyll-*a*, chlorophyll-c_2, alloxanthin, and α-carotene concentrations, we filtered 5 mL of each experimental

population onto a 25 mm Whatman GF/C filter (GE LifeSciences, Buckinghamshire, UK). These samples were then processed using high performance liquid chromatography (HPLC) to obtain pigment concentrations for each sample. Details for analyzing phytoplankton pigment samples using HPLC can be found in Pinckney *et al.* (1996). Filters were freeze-dried overnight, then pigments were extracted for 24 h at -20°C with 750µL of 90% acetone with 50µL of a synthetic carotenoid as an internal standard. The extracted solution was filtered through a 0.45 µm syringe filter, and 250 µL was injected into a Shimadzu HPLC. Chromatograms were analyzed by comparing retention times and absorption spectra to known standards (HDI, Horsholm, Denmark). Phycobiliprotein concentration cannot be measured with HPLC, which is why the phycoerythrin and non-phycoerythrin pigment concentration measurements were conducted with different methods.

Statistical Analyses. We first checked the normality and homogeneity of our data using Shapiro-Wilk and Levene's tests. Then, we ran an Analysis of Variance (ANOVA) with a Tukey post-hoc comparison or a Kruskal-Wallis test with a Dunn's Multiple Comparison of Means post-hoc comparison to test for significant differences in pigment concentrations across all four treatments. An ANOVA was used for normally-distributed data (phycoerythrin), while the Kruskal-Wallis test was used if data were non-normally distributed (chlorophyll-*a*, chlorophyll-c_2, alloxanthin, and α-carotene).

RNA Extractions, Sequencing, and Transcriptome Assembly

After taking samples for pigment analyses, we spun the remainder of each culture (270 mL) in 500 mL centrifuge bottles at 3024g for 30 minutes (Beckman Coulter J2-21 centrifuge; JA-20 rotor) to pellet the cell material. The supernatant was removed, and the

remaining cell pellet was split into two pre-weighed 2 mL microcentrifuge tubes. We split each pelleted culture into two samples: 1) to ensure we had at least one sample for sequencing if the RNA from one extraction was of poor quality and 2) to allow us to send off technical replicates for sequencing to test for variation within biological replicates.

We spun the microcentrifuge tubes at 3000g (Beckman Coulter 18 Microfuge) for 12 minutes. The supernatant was removed, and then the pellets were weighed. If the pellet mass was between 50-100 mg, we lysed the cells with 1 mL of Bio-Rad PureZOL reagent; if the mass was less than 50 mg, we used 0.5 mL of reagent. The remainder of our extraction protocol followed the standard TRIzol RNA isolation procedure (detailed in the ThermoFisher Scientific Invitrogen TRIzol Reagent User Guide, Pub. No. MAN0001271, Rev. B.0), with the exception of adding a second ethanol wash step prior to elution to increase the purity of the RNA.

We sequenced each sample with 150bp paired-end Illumina sequencing, generating an average of 30,892,204 reads per sample after trimming. We built transcriptome assemblies with Trinity (Grabherr, et al 2011) and Velvet-Oases (Schulz, et al 2012), and combined them with EviGene (Gilbert 2013).

RNA quality control and RNA-sequencing

We checked the purity of the RNA using a Nanodrop 2000, obtained the concentration with a Qubit 4 Fluorometer, and checked the integrity of the RNA by running a sample of the extracted RNA on a 2% agarose gel at 60V for 1 hr. We considered high quality RNA samples to be those with 260/280 and 260/230 ratios greater than 1.8 and clear rRNA bands observed on the gel with no signs of degradation.

Samples were sent to the Duke University Genome Sequencing Information Manager for 150bp paired-end HiSeq 4000 sequencing targeting 30 million reads per sample. Library preparation was performed at Duke using the Illumina Tru-seq RNA sample library prep kit. We submitted RNA samples from each of the five biological replicates for each light environment. For three of those biological replicates, we submitted the sample divided into two technical replicates to ascertain technical variation. In total, we obtained sequences from 32 RNA samples [(5 biological replicates + 3 technical replicates) x 4 environments = 32 samples)].

Transcriptome Assembly and Quality Control

We checked the quality of the raw reads for each sample with FastQC (Andrews 2010), and then trimmed reads and removed adapter sequences using Trimmomatic (Bolger, *et al.* 2014) (Trimmomatic parameters: ILLUMINACLIP:TreSeq3-PE.fa:2:30:10 HEADCROP:20). After running Trimmomatic, we re-ran FastQC, and any remaining overrepresented adapter sequences observed were manually removed from each sample using cutadapt (Martin 2010). An average of 30,892,204 paired-end reads per sample remained after trimming, and we used these for transcriptome assembly.

We first created a transcriptome of all samples from all light treatments using Trinity (Grabherr, *et al.* 2011). Then, we created several assemblies using kmer lengths of 35, 45, 55, 65, 75, 85, and 95 with Velvet-Oases (Schulz, *et al.* 2012). We merged the separate Velvet-Oases assemblies using the Oases merge function to create one final Velvet-Oases assembly. We then combined the Trinity and Velvet-Oases assemblies with EvidentialGene mRNA transcript assembly software (EviGene; Gilbert 2013) with a kmer length of 75 to obtain a final transcriptome assembly. We used EviGene to correct

for the various biases attributed to the different assemblers, which ensured that we were left with a comprehensive and accurate transcriptome assembly.

We removed any remaining rRNA sequences from the final assembly by downloading the rRNA SSU and LSU subunits for *R. salina* from the SILVA database (Quast, *et al.* 2013) and blasting these sequences against our final *R. salina* assembly. Only 101 contigs hit to the rRNA subunits, and these were removed from the final assembly. We then used Benchmarking Universal Single Copy-Orthologs (BUSCO, version 3) to assess the completeness of the transcriptome by searching our assembly against the BUSCO Eukaryota_odb9 (creation date: 02/11/2016), Chlorophyta_odb10 (creation date: 01/12/2017), and Protists_ensembl (creation date: 11/15/2016) datasets (Simao, *et al. 2015*). We used a combination of BUSCO datasets to assess the completeness of our final assembly because *R. salina* does not fit neatly into any specific category. We used the Quality Assessment Tool for Genome Assemblies (QUAST) (Gurevich *et al.* 2013) to obtain descriptive statistics of the transcriptome assembly.

Gene Annotation

We used the *de novo* transcriptome annotator dammit (Scott 2018) to annotate our final assembly. This pipeline uses Transdecoder to build gene models and then searches the Pfam-A, Rfam, OrthoDB, and uniref90 protein databases for annotation information with an E-value cutoff of $1x10^{-5}$. The putative transcripts were also run through a gene ontology (GO) pathway analysis using OmicsBox (BioBam Bioinformatics 2019) to obtain functional annotation information.

Building the a priori *list of photosynthesis-related genes*

Prior to differential gene expression analysis, we compiled a list of 99 photosynthesis-related genes known to exist within cryptophyte genomes (Douglas and Penny 1998; Jarvis and Soll 2001; Gould *et al.* 2007; Koziol *et al.* 2007; Khan *et al.* 2007; Overkamp 2014; Takaichi 2011; Neilson *et al.* 2017). These included genes related to pigment synthesis (e.g., the phycoerythrin subunits, chlorophyll-binding proteins), photosystem assembly (e.g., photosystem I and photosystem II proteins), energy synthesis and use (e.g., ATP synthase subunits, cytochrome b6-f complex subunits), the dark reactions (e.g., RuBisCo subunits, light-independent reductases), and helper proteins (e.g., translocons, transport proteins) (Table 1.1).

We pulled the nucleotide sequences of these genes from cryptophyte genomes publicly available in the NCBI database. We then used blastn to independently search for these genes in our transcriptome assembly with an E-value cutoff of $1x10^{-5}$. These sequences were used in our differential gene expression analyses to investigate the plasticity of genes related to light capture and photosynthetic function with respect to spectral habitat.

Differential Gene Expression Analysis

We mapped trimmed paired-end reads back to the final transcriptome assembly and obtained read count data using kallisto (Bray *et al.* 2016). We first examined the distributions of counts across samples and treatments to determine if any samples needed to be removed from the analysis due to batch effects, and to compare data from our technical replicates. We used the technical replication to test for repeatability of the procedures that occurred during sequencing. There were no significant differences

between our technical replicates. Given these results, we dropped the technical replicates from the remaining analyses to keep the dataset approximately the same size for each biological replicate.

For each spectral comparison (blue vs. red, green vs. red, and blue vs. green), we used Degust (Powell 2019) to run edgeR with a false discovery rate (FDR) corrected *p*-value cutoff of 0.05 and a log fold-change (FC) cutoff of ±2. We ran this analysis at three different scales: first, we tested the expression of cryptophyte phycoerythrin-subunit genes to determine if they were differentially expressed among spectra; second, we tested the *a priori* list of photosynthesis-related genes to investigate photosynthetic pathways more broadly; third, we tested the complete gene set (the total number of contigs expressed in our assembly) to see whether other genes respond to differences in light spectrum. For the photosynthesis gene set, we performed additional analyses to guard against false negatives by relaxing FDR cutoffs to 0.1 and 0.2, as well. Gene expression levels are reported in transcripts per million (TPM).

Correlation Analysis

We used Pearson's correlation coefficients (and Spearman's rank correlation coefficients where data were non-parametric) to assess potential correlations between pigment concentrations and gene expression independent of light treatment (i.e., the correlations detailed below were performed across all 20 experimental populations, not across the 4 light spectra, to capture variation within treatments). We used the corr.test R command with a Holm-Bonferroni adjustment to control for multiple comparisons (part of the "stats" package) for running individual comparisons of interest, which included identifying potential correlations between the following: cryptophyte phycoerythrin

pigment concentration and phycoerythrin protein subunits' transcript expression (both alpha (α) and beta (β) subunits) and cryptophyte phycoerythrin and chlorophyll concentrations. We also did a correlation analysis of the photosynthesis-related genes to all pigment concentrations.

Results

Pigment Data

Total pigments. Overall, there were no significant differences in total pigment across spectra. Concentrations were highest in green light (10.80 pg/cell) followed by wide-spectrum cells, (7.40 pg/cell), then blue (7.40 pg/cell), and red light (7.10 pg/cell). In all spectral environments, cryptophyte phycoerythrin comprised the greatest percentage of the total pigment concentration, followed by chlorophyll-*a*, chlorophyll-c_2, alloxanthin, and α-carotene.

Phycoerythrin concentrations. We saw the highest cryptophyte phycoerythrin concentrations in cultures grown under green light (6.2 ± 0.60 pg/cell) and the lowest in those grown in red light (2.7 ± 0.60 pg/cell) (Figure 1.1a). Populations grown in blue light and the wide-spectrum light had average cryptophyte phycoerythrin concentrations of 4.6 ± 0.60 pg/cell and 3.8 ± 0.90 pg/cell, respectively (Figure 1.1a). The cryptophyte phycoerythrin concentrations were significantly different between populations grown in green and red light (p-value = 0.0069; F-value = 7.85; df = 2). We did not observe any other significant differences between the blue vs. red or blue vs. green comparisons. For wide-spectrum, blue, and green light environments, cryptophyte phycoerythrin comprised 50% or more of the total cellular pigment concentration (50.5%, 62.0%, and 57.4% for wide, blue, and green light, respectively). Cryptophyte phycoerythrin concentrations

comprised only 37% of the total cellular pigment for cultures grown in red light (Figure 2).

Non-PBP pigment concentrations. Chlorophyll-*a* concentrations were significantly different between populations grown in red (2.5 ± 0.40 pg/cell) and blue light (1.4 ± 0.20 pg/cell) (*p*-value = 0.045; Z = -2.00). Populations grown in green light had an average chlorophyll-*a* concentration of 2.6 ± 0.60 pg/cell, while those grown in the wide-spectrum environment had 1.7 ± 0.20 pg/cell (Figure 1.1b). While populations grown in green light exhibited the highest average chlorophyll-*a* concentrations compared to the other spectral habitats, there were no significant differences observed between green light chlorophyll-*a* concentrations and the other spectra. The percentage of total cellular pigment that is chlorophyll-*a* differed with environment, with wide-spectrum, blue, green, and red-light environments exhibiting chlorophyll-*a* percentages of 23.3, 18.6, 24.3, and 35.6%, respectively. Chlorophyll-c_2 concentrations differed slightly across the different spectral environments, but there were no significant differences between any spectral comparisons (Figure 1.2).

Alloxanthin and α-carotene concentrations (Figure 1.1c) were both significantly different between and red and blue treatments (alloxanthin *p*-value = 0.037; Z = -2.09; α-carotene *p*-value = 0.0061; Z = -2.74). Alloxanthin concentrations ranged from 4.0 ± 0.04, 3.1 ± 0.03, 4.4 ± 0.12, and 6.8 ± 0.07 pg/cell in wide-spectrum, blue, green, and red light, respectively, while α-carotene concentrations were 1.7 ± 0.04, 1.0 ± 0.02, 3.2 ± 0.13, and 6.7 ± 0.11 pg/cell.

Transcriptome Assembly

Our final transcriptome assembly contained 24,167 contigs, had an N50 of 2,431 bp, and had a GC content of 58.75%. Publicly available cryptophyte transcriptome assemblies of species from the *Hemiselmis, Proteomonas, Cryptomonas, Chroomonas, Guillardia*, and *Rhodomonas* clades (Marine Microbial Eukaryote Transcriptome Sequencing Project) range from 24,119 to 41,208 contigs with varying assembly metrics. Our *R. salina* assembly statistics thus fall within the expected published range of cryptophyte transcriptomes. A previously assembled *R. salina* transcriptome based on 50 bp reads assembled with Abyss (MMETSP1047-20130122) had 31,523 contigs and an N50 of only 1,650. Any disparities observed are likely due to differences in assembly methods, sequencing depth, read length, or species' biological variation.

Of the 24,167 contigs in our assembly, we were able to identify 13,170 (54.50%) transcripts by matching them to protein annotations from the Pfam-A, Rfam, OrthoDB, and uniref90 databases. The remaining transcripts did not return an annotation hit across the protein databases.

The results of our BUSCO analysis revealed that 63.0% of expected eukaryotic orthologs are present in our assembly, while 32.7% and 46.5% of the chlorophyte and protist BUSCOs were present, respectively (Table 1.1).

Differential Gene Expression Analysis and Exploration

We found that neither of the cryptophyte phycoerythrin subunit genes were significantly differentially expressed in any of our three spectral comparisons (FDR *p*-value < 0.05 and a $\log_2$ foldchange ≥ 2). To evaluate the potential for false negatives, we relaxed the FDR and foldchange; this had no effect on the outcome in the blue vs. red or blue vs. green comparisons. However, when the FDR cutoff was adjusted to 0.1 with a

foldchange of 1.5, then expression of the cryptophyte phycoerythrin β subunit gene was significantly downregulated in green light compared to red light – opposite the pattern of the pigment's concentration. The cryptophyte phycoerythrin α and β subunit gene expression patterns did not match that of the cryptophyte phycoerythrin concentrations. For the α-subunit gene(s), we observed the highest expression in wide-spectrum light (2,254 TPM) and the lowest in blue (1,306 TPM) and red light (1,301 TPM), but for the β subunit, red light cultures exhibited the highest expression (103 TPM), while the wide-spectrum, blue, and green light cultures were nearly the same (72, 71, and 65 TPM, respectively) (Figure 1.3).

When we performed these same comparisons for our *a priori* photosynthesis gene set, we found that very few photosynthesis-related genes were significantly differentially expressed between light spectra. With the standard FDR of 0.05, 9 genes were differentially expressed in the blue vs. red treatments, while there were none in either the green vs. red or green vs. blue comparisons. When we relaxed the FDR to 0.1 with a $\log_2$ foldchange ≥ 2, we saw 12 differentially expressed genes in blue vs. red, 5 for green vs. blue, and still none for green vs. red. We did not see any evidence for differential expression of photosynthetic genes in the green vs. red comparison until we reached an FDR of 0.14 with no specified $\log_2$ foldchange, where we then had 2 genes returned. The top annotated differentially expressed genes for each of our photosynthetic comparisons are outlined in Tables 1.3A-C.

When we ran the analysis for the complete gene set, we found that 1,290 genes were significantly differentially expressed in the blue vs. red comparison with an FDR *p*-value < 0.05 and a $\log_2$ foldchange ≥ 2. Of these, 990 were upregulated in blue light, while 300 were upregulated in red light (Figure 1.4; Figure 1.5; Figure S1.2a). Our gene

ontology results suggest that the genes upregulated in blue light were involved in a wide array of functions, including oxidation-reduction processes, translation, transmembrane transport, carbohydrate metabolic processes, transcriptional regulation, cell signaling, transduction, and communication, and various biosynthetic processes, such as phospholipid and nucleotide biosynthesis. Those upregulated in red light were primarily involved in translation, transmembrane proteins and ion transport, oxidation-reduction processes, and photosynthetic electron transport.

For the green vs. red comparison, 1,826 genes were significantly differentially expressed (FDR p-value < 0.05; $\log_2$ foldchange ≥ 2) (Figure 1.4; Figure 1.5; Figure S1.2b). Of these 1,826, only 232 were upregulated in red light and 1,594 were upregulated in green light. Both green- and red-light environments saw an upregulation of different genes involved in biological processes primarily involved in oxidation-reduction processes, transmembrane transport, and protein phosphorylation. Green light also upregulated genes involved in carbohydrate metabolic processes, transcription and translational regulation, DNA replication and repair, and multiple RNA processing mechanisms, including mRNA, rRNA, and tRNA processing, mRNA splicing, RNA polymerase regulation, and mRNA catabolism.

Only fifty genes were significantly differentially expressed between blue and green light. Of these, 39 were upregulated in blue light, while 11 were upregulated in green light (FDR p-value < 0.05; $\log_2$ foldchange ≥ 2) (Figure 1.4; Figure 1.5; Figure S1.2c). The fifty genes included ones that were functionally involved in methyltransferase activity, tyrosine phosphatase function, DNA binding, transcriptional regulation, and protein folding and transport.

Many of the top differentially expressed genes could not be identified across any of the protein databases used in our dammit annotation pipeline, nor when we tried identifying their potential annotation using the NCBI conserved domain database (CDD) (Lu *et al.* 2020). Thus, it is apparent that some transcriptionally active and spectrally responsive regions of the *R. salina* genome are currently unannotated and may require extension or deeper exploration.

Correlation Analysis

We found no significant correlations between cryptophyte phycoerythrin pigment concentration and protein subunit expression (both α and β subunits). When we tested for correlations among expression patterns of the photosynthetic gene set and the various pigment concentrations, we found a total of 14 genes were significantly (p-value < 0.05) correlated with chlorophyll-*a* and chlorophyll-c_2 concentration (Table 1.2). Most of these genes were related to PSI and PSII synthesis, chlorophyll binding proteins, or ATP synthesis, and two were related to cryptophyte phycoerythrin synthesis or function. One gene encoding for a chlorophyll A-B binding protein (transcript 22761 in our assembly), a protein that binds to chlorophyll to form light-harvesting complexes (Dittami *et al.* 2010; Hey and Grimm 2020), was significantly correlated with cryptophyte phycoerythrin concentration (coefficient = 0.499, p-value = 0.049). Twenty-four genes were significantly correlated with the photoprotective pigments (Table 1.3). Of these twenty-four, six were chlorophyll binding proteins that all exhibited negative correlations; five were related to ATP synthesis that all had positive correlations; nine were proteins for PSI or PSII synthesis and function, which were mostly positively

correlated; and one was the RuBisCo large subunit (rbcL), which had a significantly positive correlation.

Discussion

For aquatic photosynthetic organisms, light is often a major limiting resource and cause of competition, thus organisms efficient at exploiting a broader range of light colors should have an advantage over those with more limited absorption options. We examined the physiological plasticity in pigment composition and gene expression in *R. salina* grown in wide-spectrum, blue, green, and red light. We expected that differences in pigmentation would follow the general theory of chromatic acclimation (Engelmann 1883, 1902; Gaiducov 1902, 1903), where pigments (type and concentrations) adjust to optimize absorption of wavelengths of available light, and we expected gene expression of pigment-related genes to follow the same pattern. We also predicted that other photosynthesis-related genes would have high expression sensitivity to changes in light color, but we did not expect that many non-photosynthesis-related genes would respond to spectrum. Our data partially supported the theory of chromatic acclimation, but some deviations from expected pigment concentrations and the lack of clear drivers at the level of gene expression suggest that plastic responses to light spectrum are more complex than the theory assumes.

Are cryptophyte pigments maximizing their capacity to capture available light?

R. salina contains cryptophyte phycoerythrin 545, which efficiently absorbs green wavelengths of light (with a maximum absorption peak at 545 nm). Because of this, we expected that the absolute concentration of phycoerythrin would increase when *R. salina*

grew in a green-dominated environment. Our results supported this prediction. Because the cryptophyte phycoerythrin is the major light-harvesting pigment in *R. salina* and it absorbs green light better than chlorophylls do, this suggests that *R. salina* is maximizing its ability to capture light in green wavelengths. In red light, we saw that as a proportion of total cellular pigments cryptophyte phycoerythrin decreased by 12% compared to the wide-spectrum control; chlorophyll-*a* counterbalanced this with a 12% increase (though this was not statistically significant). This suggests that *R. salina* exhibited an investment tradeoff in pigment composition in red light, perhaps using chlorophyll-*a*, which absorbs red better than phycoerythrin does, as the primary photosynthetic absorption compound. These particular differences of pigment concentrations and ratios in green and red light were the strongest we observed and are consistent with the theory of chromatic acclimation.

Other patterns, however, cannot be explained by chromatic acclimation. For example, phycoerythrin was present in red light and both chlorophylls were present in green light even though these pigments do not efficiently absorb these corresponding wavelengths. It is unclear why these pigments were not degraded in environments where other pigments would be more useful. Second, pigment composition in a blue environment runs counter to expectations from chromatic acclimation. Chlorophylls absorb blue light better than cryptophyte phycoerythrin, yet in our blue environment *R. salina* produced a large amount of phycoerythrin and a modest amount of chlorophylls. Third, *R. salina* produced an unexpectedly large amount of chlorophyll-*a* in green light. While some chlorophyll-*a* is always necessary for photosynthesis (because chlorophyll complexes mediate the transfer of energy from phycoerythrin to photosystem II in cryptophytes; Scholes, *et al.* 2006), the lower amounts in blue and wide-spectrum light

suggest an excess is being produced in green light. Even though other aspects of pigments in red and green light support chromatic acclimation, the high chlorophyll-*a* in green light, the high phycoerythrin in red light, and the preferential presence of phycoerythrin in blue light shows that in some circumstances *R. salina* invests in producing pigments poorly suited to the ambient light environment.

After ten mitotic generations of acclimation in constant environments, it is implausible to attribute these ineffectual pigments to persistence from the past. We therefore examined possible relationships between pigment concentrations to evaluate the plausibility that connections between synthesis pathways could explain these observations. Our analysis did not reveal any significant correlations between chlorophyll and phycoerythrin concentrations, so linked biosynthesis pathways also cannot directly explain our patterns of pigment plasticity. However, we did find a suggestive correlation between transcription of a chlorophyll binding protein gene (chlorophyll A-B binding protein) and phycoerythrin concentration, and two genes related to phycoerythrin synthesis (a phycoerythrin lyase and a potential phycoerythrin α-subunit) correlated with chlorophyll concentrations. These genes are strong candidates for further study of how chlorophyll and phycoerythrin synthesis may be related at a molecular level. It is possible that chlorophyll synthesis may be partially linked to phycoerythrin synthesis in *R. salina*, even though this isn't reflected in the pigment concentrations themselves. While we have an understanding of how the synthesis pathways for the cryptophyte phycobilins and chlorophylls are structured (Hill & Rowan 1989; Gantt 1996; Scholes *et al.* 2006; Dammeyer & Frankenberg-Dinkel 2008; Overkamp *et al.* 2014), we do not know if or how these synthesis pathways may be co-regulated, particularly with respect to light spectrum.

The surprisingly low concentrations of chlorophylls in blue light point toward another mechanism contributing to pigment spectral plasticity: high-energy light acclimation of chlorophyll via a mechanism other than quantity. The absorption and photosynthetic efficiency of chlorophyll-*a* is influenced by light spectrum, such that the overall quantum yield of photosynthesis (measured by the amount of oxygen produced per quantum absorbed) increases in high-energy wavelengths, i.e., blue light (Yocum & Blinks 1957; Vadiveloo *et al.* 2015). As a result, there may be less chlorophyll-*a* when *R. salina* is grown in this environment because the chlorophyll-*a* itself became more efficient when acclimated to blue light compared to red or green light. This is consistent with Heidenreich and Richardson (2019), who saw a decrease in cellular chlorophyll concentrations when both phycoerythrin- and phycocyanin-containing cryptophytes were shifted from wide-spectrum to blue-spectrum light, suggesting a possible acclimation response similar to those induced by high light intensity.

Light interception by photoprotective pigments may also influence light available for capture by photosynthetic pigments, and thereby influence photosynthetic pigment composition. Cryptophyte photoprotective pigments, alloxanthin and α-carotene, have been shown to respond to high light intensities (Mendes *et al.* 2018; Kana *et al.* 2019), but less is known about how they respond to changes in light color. Even though alloxanthin and α-carotene both absorb blue wavelengths efficiently, we found the photoprotective pigment concentrations to be lowest in blue light. It is possible that, as with chlorophyll-*a*, absorption efficiency changes with spectrum, and fewer pigment molecules are then needed to absorb the same amount of energy in blue light as in longer wavelengths, but we know of no evidence to indicate whether that happens.

How do cryptophyte phycoerythrin genes respond to light spectrum at the transcript level?

We expected to see an increase in expression of the cryptophyte phycoerythrin α and β subunit genes in green light to drive chromatic acclimation, and we predicted that expression of these genes would show the same pattern as the pigment concentration. Although our estimate of α subunit gene expression was higher in green than blue or red light, this was not statistically significant, and the overall pattern did not match that of the phycoerythrin pigment. This suggests that post-transcriptional regulatory mechanisms are the primary determinants of phycoerythrin concentrations.

Most striking, however, was the expression disparity between the α and β subunits. The α subunit gene was expressed at a much higher level on average (~1,670 TPM) compared to the β subunit (~78 TPM) across all four treatments, and expression of the two subunits was not correlated. This is noteworthy since they compose the overall cryptophyte phycoerythrin structure in a 1:1 molar ratio (ααββ), and thus we expected them to be expressed at similar levels and to covary. This unexpected relationship between α and β subunit expression could be due to the differences in evolutionary history between the two subunit genes. The α subunit is encoded in the nucleus (Apt et al. 1995; Douglas & Penny 1999; Curtis et al. 2012), which originated from a hypothesized cryptophyte heterotrophic ancestor, and the β subunit is found in the chloroplast genome (Douglas & Penny 1999; Khan et al. 2007; Donaher et al. 2009; Harrop et al. 2014; Kim et al. 2015; Kim et al. 2017), originally descended from the red-algal endosymbiont. A combination of nuclear and plastid photosynthesis-encoding genes is common in many photosynthetic organisms, where genes located in the nucleus encoding proteins that must be imported into the chloroplast (Eberhard *et al.* 2008; Ute *et al.* 2013). Once these

proteins are in the chloroplast, they are assembled into larger complexes for full functionality (Celedon and Cline 2013). Proteins that must be assembled in the thylakoid luminal space must cross multiple barriers between the nuclear envelope and the chloroplast membranes. It is possible that increased expression of nuclear genes ensures that sufficient peptides make it to their final destination and any excess proteins are degraded (Eberhard *et al.* 2008), though Gould *et al.* (2007) showed that the phycoerythrin α-subunit isolated from the cryptophyte *Guillardia theta* was able to cross the five membranes between the nucleus where it is synthesized and the thylakoid lumen where it is processed. Alternatively, since chloroplast-encoded transcripts are long-lived (Hosler *et al.* 1989), it is possible that the chloroplast-encoded phycoerythrin β subunit does not need to be transcribed at the same level as the nuclear-encoded α subunit for the overall cryptophyte phycoerythrin protein complex to be synthesized and assembled (Hosler *et al.* 1989; Kim *et al.* 1993).

How do photosynthesis-related genes respond to light spectrum at the transcript level?

We saw changes in expression of phycoerythrin subunits and chlorophyll binding proteins in the different spectral environments as mentioned above, along with various photosystem I and II encoding proteins. Of the sixty-six transcripts annotated as potential chlorophyll binding proteins in our assembly, only three were significantly differentially expressed. We also had only three transcripts encoding for phycoerythrin subunits and lyases that were significantly differentially expressed in any of our spectral comparisons. Curiously, these genes did not have any consistent pattern (i.e., not all the chlorophyll binding proteins were upregulated in red or blue light; not all of the phycoerythrin subunits were upregulated in green light, etc.). Transcripts encoding various chlorophyll

binding proteins were upregulated in blue light, red light, and green light; transcripts encoding different phycoerythrin subunits and lyases were also upregulated in all three light spectra. Determining why this is so will require detailed functional investigation into the individual proteins.

We found that genes for the RuBisCo large subunit (rbcL) were significantly upregulated in red light compared to blue, even though the small subunit (rbcS) was not differentially expressed across any of the comparisons. RuBisCo is directly involved in carbon assimilation during photosynthesis and is considered the ultimate rate-limiting component in carbon fixation. Changes to RuBisCo subunit gene expression leads to a change in RuBisCo protein synthesis and overall carbon fixation (Pichard *et al.* 1993; Pichard *et al.* 1996; Patel and Berry 2008; Kim *et al.* 2014). Generally, RuBisCo activity and protein synthesis is directly related to light intensity, but spectrum has been suggested to influence RuBisCo gene expression and protein synthesis as well. Eskins *et al*. (1991) found that blue light enhanced protein synthesis and activity over red light in soybean plants, but that this effect was diminished with the addition of far-red light. In a study using *Chlorella vulgaris*, Kim *et al.* (2014) found that rbcL expression was higher in blue light compared to red or wide-spectrum light. Our results possibly differ from these previous studies because of differences in the study organisms and their corresponding pigment complements, leading to increased carbon fixation in red light compared to blue light. However, information on carbon fixation and photosynthesis rates would be needed to determine this with more certainty.

Overall, we did not see many significant differences in expression of pigment-related genes across the different treatments, which is somewhat unexpected in comparisons where we saw significant differences in pigment composition. This

discrepancy between the gene expression profile and pigment composition may be a result of post-transcriptional and post-translational modification (Rochaix 1992, 1996; Gruissem *et al.* 1993), which has been shown to occur in response to changes in light intensity and spectrum in plants (Deng *et al.* 1989). Also, decreasing the transcription of chloroplast-encoded genes does not always affect the rates of their corresponding protein synthesis, so it could be that the transcription levels for the pigment-related genes do not reflect the actual pigment concentrations for this reason (i.e., the mRNA transcript:translated protein product ratio is not necessarily 1:1 (Kim *et al.* 1993)). We note that we did not measure pigment concentration and gene expression at multiple time points to determine if the concentrations and levels of expression change over the length of exposure to the treatment environments, so we cannot conclude for certain that these discrepancies are a result of post-transcriptional or post-translational regulation or if this discrepancy is instead an acclimation response (i.e., perhaps at the time in which we sampled for gene expression, transcription of the genes was reduced, but the pigment concentrations still remained higher from previous generations since being placed in the new environments).

What other functions respond to light spectrum at the transcript level?

Last, we ran differential expression analysis of our complete gene set to test for significant differences in expression of non-photosynthetic genes across spectra. One particularly interesting gene encodes for a domain of an "algal minus-dominance protein," which is a protein related to the differentiation of mating types in other algal taxa. This gene was upregulated in blue light compared to all other spectral environments in our experiment. In the green alga *Chlamydomonas reinhardtii*, this gene is involved in

gametic differentiation and can be regulated by a combination of nitrogen starvation and blue wavelengths, where nitrogen starvation initiates gametogenesis and blue light triggers the completion of the process (Beck and Haring 1996; Ferris and Goodenough 1997; Lin and Goodenough 2007; Chardin *et al.* 2014). Additionally, our annotation pipeline identified 56 genes (though they were not differentially expressed with light spectra) with putative functions similar to the RWP-RK domain-containing transcription factors, which have been shown to be involved in regulating cell differentiation, sexual reproduction, and nitrogen responses in vascular plants, slime molds, and green algae (Konishi & Yanagisawa 2013; Chardin *et al.* 2014; Tedeschi *et al.* 2016; Ota *et al.* 2019). Cryptophytes reproduce asexually, but there has been speculation that sexual reproduction is possible due to observations of cellular fusions (Hoef-Emden & Archibald 2016; Kugrens & Lee 1988) and accounts of dimorphism in clonal cultures (Hill & Wetherbee 1986; Hoef-Emden & Melkonian 2003). Changes in cell signaling due to shifts in light spectra is a mechanism that has been shown to trigger reproductive switches in other algal groups (Dring 1987; Hoham *et al.* 1997; Hoham *et al.* 2000; Tardu *et al.* 2016) and may be a potential avenue of investigation for understanding switches between reproductive mechanisms in cryptophytes.

We also saw a change in glyceraldehyde 3-phosphate dehydrogenase (GAPDH) expression, which was upregulated in red light compared to green. GAPDH catalyzes the sixth step of glycolysis, though it can also be involved in mRNA regulation, tRNA export, and DNA replication or repair (Huang *et al.* 1989; Sirover 1998; Qiu *et al.* 2020). This shift in GAPDH expression may be indicative of a shift in carbon metabolism or trophic strategy, such as decreasing photosynthetic function in favor of heterotrophic function (i.e., performing mixotrophy). Mixotrophy has been suggested as a form of

metabolic function in cryptophytes (Kugrens & Lee 1990; Gervais 1997; Roberts & Laybourn-Parry 1999; Yoo et al. 2017), including in *R. salina* (Lewitus et al. 1991), though there would need to be more experimentation to investigate this in greater detail. Generally, trophic strategy modification and switches in carbon metabolism have been extensively studied with regard to light *intensity* (e.g. Lewitus *et al.* 1991; Caron *et al.* 1993; Rottberger *et al.* 2013; McKie-Krisberg *et al.* 2015), but there are fewer studies on the effects of light *spectrum* on carbon metabolism (e.g., Hamada *et al.* 2003; Das *et al.* 2011).

Many studies examining the physiological effects of red and blue spectral habitats exist (e.g. Figueroa *et al.* 1994; Hoham *et al.* 1997; Ullrich *et al.* 1998; Aguilera *et al.* 2000; Korbee *et al.* 2005; Kim *et al.* 2019), and gene expression work has increased over the years, including work with green algae (Hermsmeier *et al.* 1991; Lee *et al.* 2018; Li *et al.* 2020), brown algae (Deng *et al.* 2012; Wang *et al.* 2013), red algae (Lopez-Figueroa 1991; Tardu *et al.* 2016), and stramenopiles (Takahashi *et al.* 2007; Losi & Gartner 2008). In many of these gene expression studies, blue wavelengths result in a greater number of upregulated genes than red wavelengths, which we also observed in *R. salina*. In all our comparisons, the higher-energy wavelengths of each pairing (blue light in the blue vs. red; green light in the green vs. red; blue light in the blue vs. green) resulted in the greatest number of significantly upregulated genes, regardless of whether the genes were related to photosynthetic function or not. We are unsure if this is a result of high-energy acclimation or if this is simply because higher-energy light triggers a broader net of molecular pathways (potential photomorphogenesis, photoprotection, DNA repair, pigment biosynthesis, etc.) than the lower-energy wavelengths.

Additionally, blue light has been shown to upregulate genes involved in pigment biosynthesis, circadian rhythm, photoreactivation (DNA repair after exposure to UV-B light), regulation of reactive oxygenic species (ROS) during photosynthesis, and photomorphogenesis (growth and reproductive characteristics) (Wang *et al*. 2013; Tardu et al. 2016). Genes upregulated in red light commonly include genes involved in light-harvesting proteins and general photosynthetic function (Wang *et al.* 2013; Deng *et al.* 2012; Lee *et al.* 2018; Tardu *et al.* 2016; Losi & Gartner 2008; Takahashi *et al.* 2007; Hermsmeier *et al.* 1991; Li *et al.* 2020), which is consistent with what we have found in the present study. The potential effects of green light on algal transcriptomes compared to other light spectra is still a widely unexplored avenue of study, given that most of the existing work focuses on the physiological effects of green-light dominated habitats on different algal species and does not include the molecular consequences (Lopez-Figueroa 1991; Hoham *et al.* 1997; Heidenreich & Richardson 2019).

Conclusion

We quantified differences in pigment composition and gene expression by *R. salina* cultures grown in wide-spectrum, blue-, green-, and red-light environments. *R. salina* appeared to maximize its capacity to capture available wavelengths using its main light-harvesting pigment (cryptophyte phycoerythrin), but the other pigments exhibited more complex responses to light spectrum than can be predicted by the theory of chromatic acclimation. Additionally, cryptophyte phycoerythrin concentrations and expression of phycoerythrin genes are not directly correlated as we expected, and differences observed may be explained by the evolutionary origins of the subunits and by post-transcriptional regulation. We hypothesize that post-transcriptional and post-

translational regulatory mechanisms are responsible for discrepancies observed between broader photosynthetic-related gene expression and physiological results.

Overall, photosynthetic-related gene expression is not sensitive to light spectrum, while some non-photosynthetic genes are regulated by light color, which was unexpected. Of particular interest, we have found genes related to sexual reproduction in the *R. salina* transcriptome that could be investigated further. Sexual reproduction in cryptophytes is not well understood and has only been discussed in a handful of studies; thus, future work can use these genes to examine potential triggers of sexual reproduction and to further our understanding of this process in the cryptophyte group.

The mechanisms controlling photosynthetic gene expression and protein synthesis in *R. salina*, and more broadly in the phylum Cryptophyta overall, remains poorly understood. Because cryptophytes exhibit such a wide diversity of phycobilin types that are only partially associated with phylogenetic history, questions also remain concerning how cryptophytes with different pigment complements, and thus potentially different ecological niches, may respond to shifts in spectral habitat.

Availability of Supporting Data

Raw sequence data has been deposited in the Sequence Read Archive (SRA) under the accession PRJNA749794. This Transcriptome Shotgun Assembly project has been deposited at DDBJ/EMBL/GenBank under the BioProject accession PRJNA749794. The version described in this paper is the first version, PRJNA749794. Pigment and related data have been deposited in Dryad.

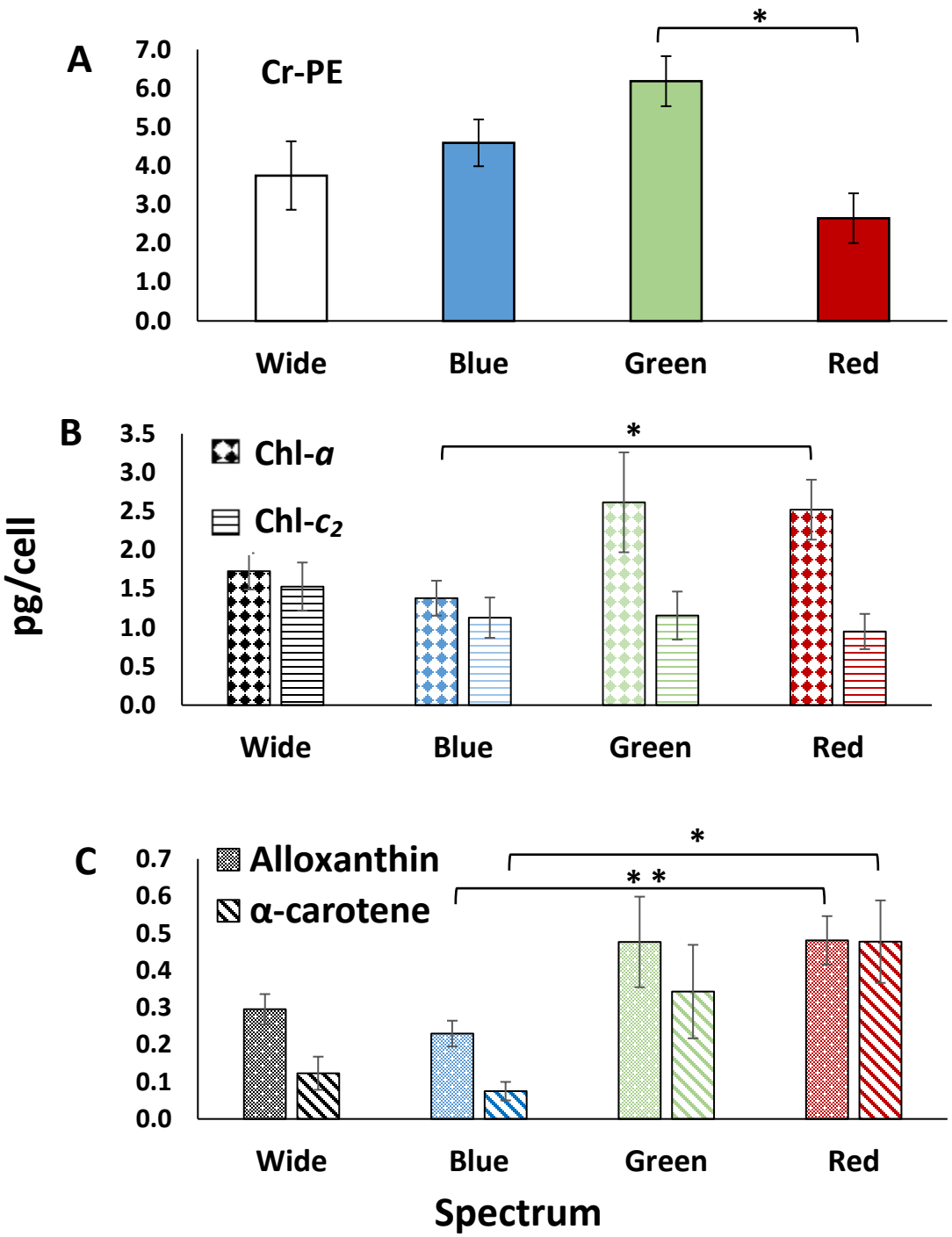

Figure 1.1: Average concentrations of all pigments in *R. salina* grown in wide-spectrum, blue, green, and red spectral environments. Error bars are standard error. Note the differences in the y-axis scale for all three graphs. **A)** Cryptophyte phycoerythrin (Cr-PE). **B)** Chlorophyll-*a* (chl-*a)* and chlorophyll-c_2 (chl-c_2). **C)** Alloxanthin and α-carotene.

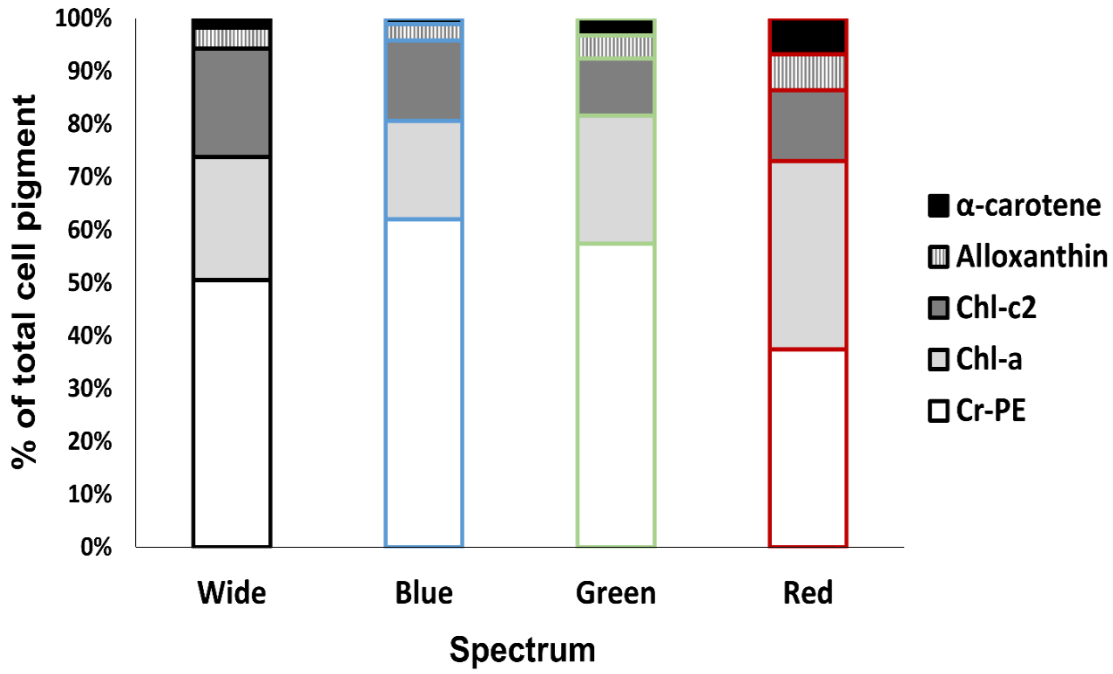

Figure 1.2: Relative pigment concentrations of pigments in *R. salina*. The figure includes α -carotene, alloxanthin, chlorophyll-c_2 (chl-c_2), chlorophyll-*a* (chl-*a*), and cryptophyte phycoerythrin (Cr-PE) across all four light treatments. Relative pigment concentrations were calculated on a mass/cell basis.

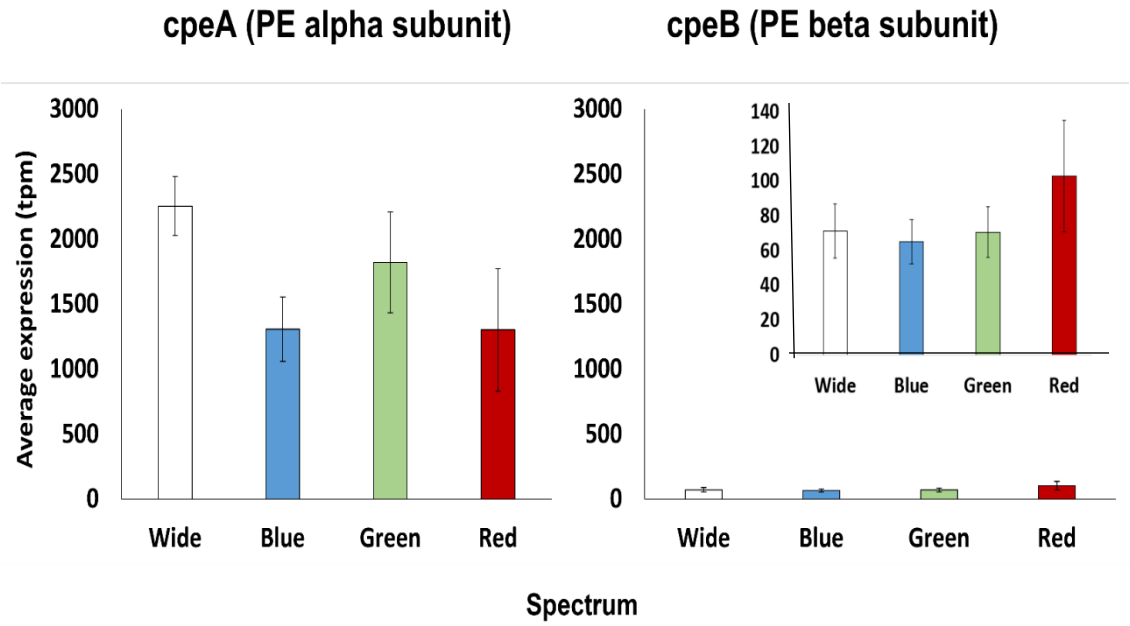

Figure 1.3: Expression of Cryptophyte phycoerythrin α and β subunits in *R. salina*. Expression values are reported in transcripts per million (tpm). There were no significant differences for either subunit across spectra. Note the difference in scales for the cpeB expression inset. Error bars represent standard error.

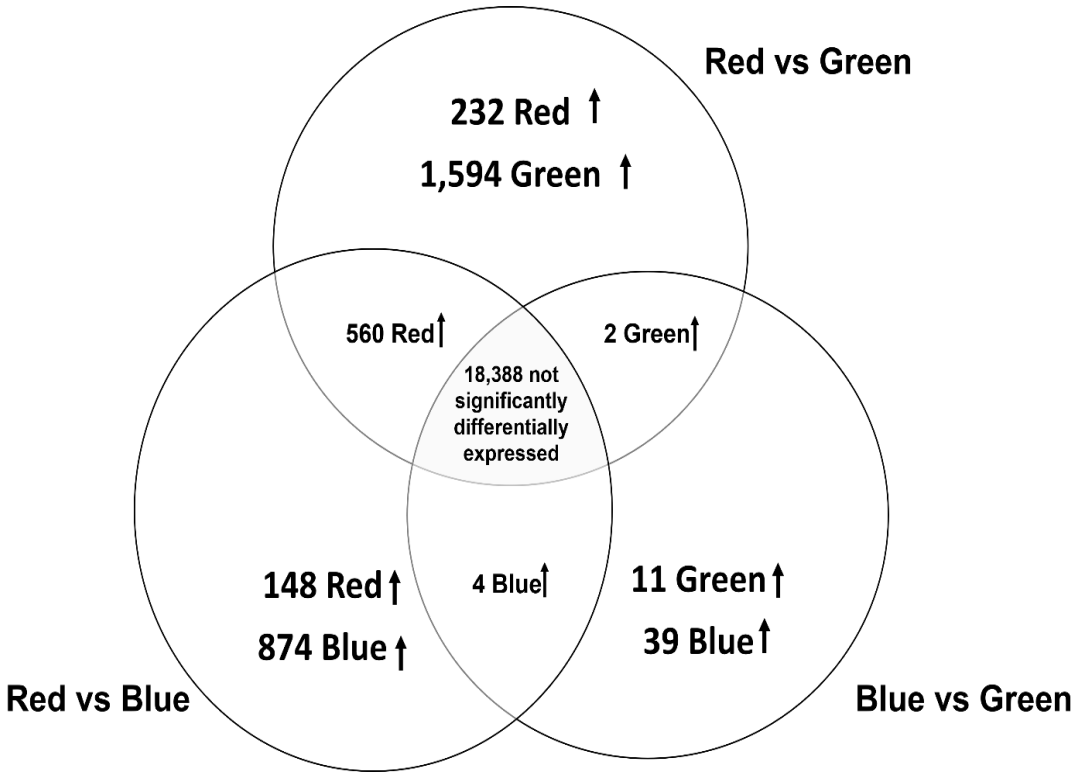

Figure 1.4: Venn diagrams for all gene expression comparisons in *R. salina*. Numbers shown in each comparison circle represent genes upregulated in each spectral environment compared to the other. Numbers displayed between comparisons represent genes upregulated in the given spectral environment regardless of which light environment was the opposing comparison. The value in the center represents the number of genes that were not significantly differentially expressed in any comparison.

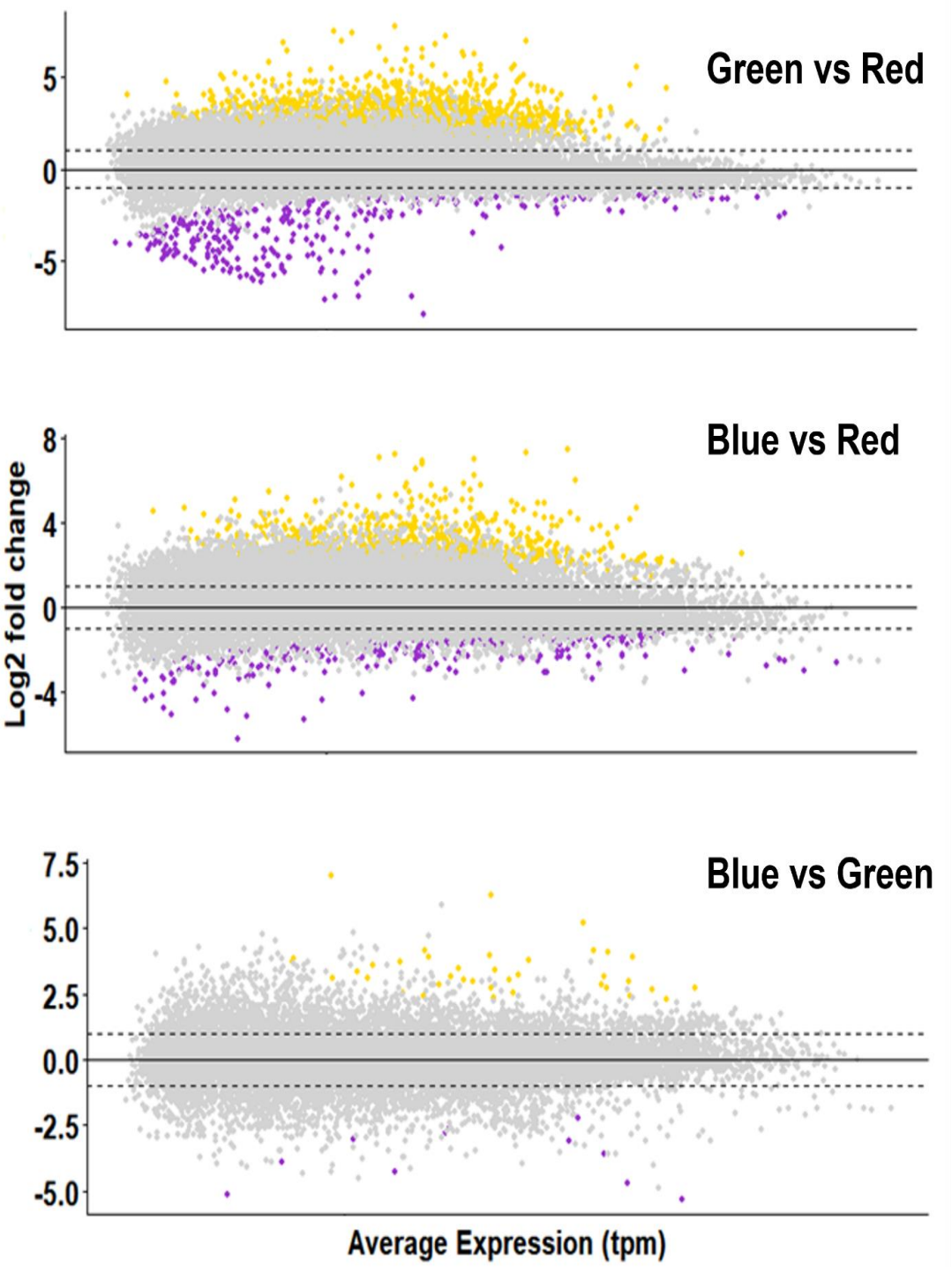

Figure 1.5. MA plots for all gene expression comparisons in *R. salina*. For Green vs Red, differentially expressed genes relative to expression in red light. For Blue vs Red, differentially expressed genes are relative to expression in red light. For Blue vs Green, differentially expressed genes are relative to green light. Yellow dots represent significantly upregulated genes; purple dots represent significantly downregulated genes. Grey dots represent expressed genes which were not significant. The FDR *p*-value cutoff was 0.05 with a $\log_2$ fold-change > ±2 (represented by the dashed horizontal lines).

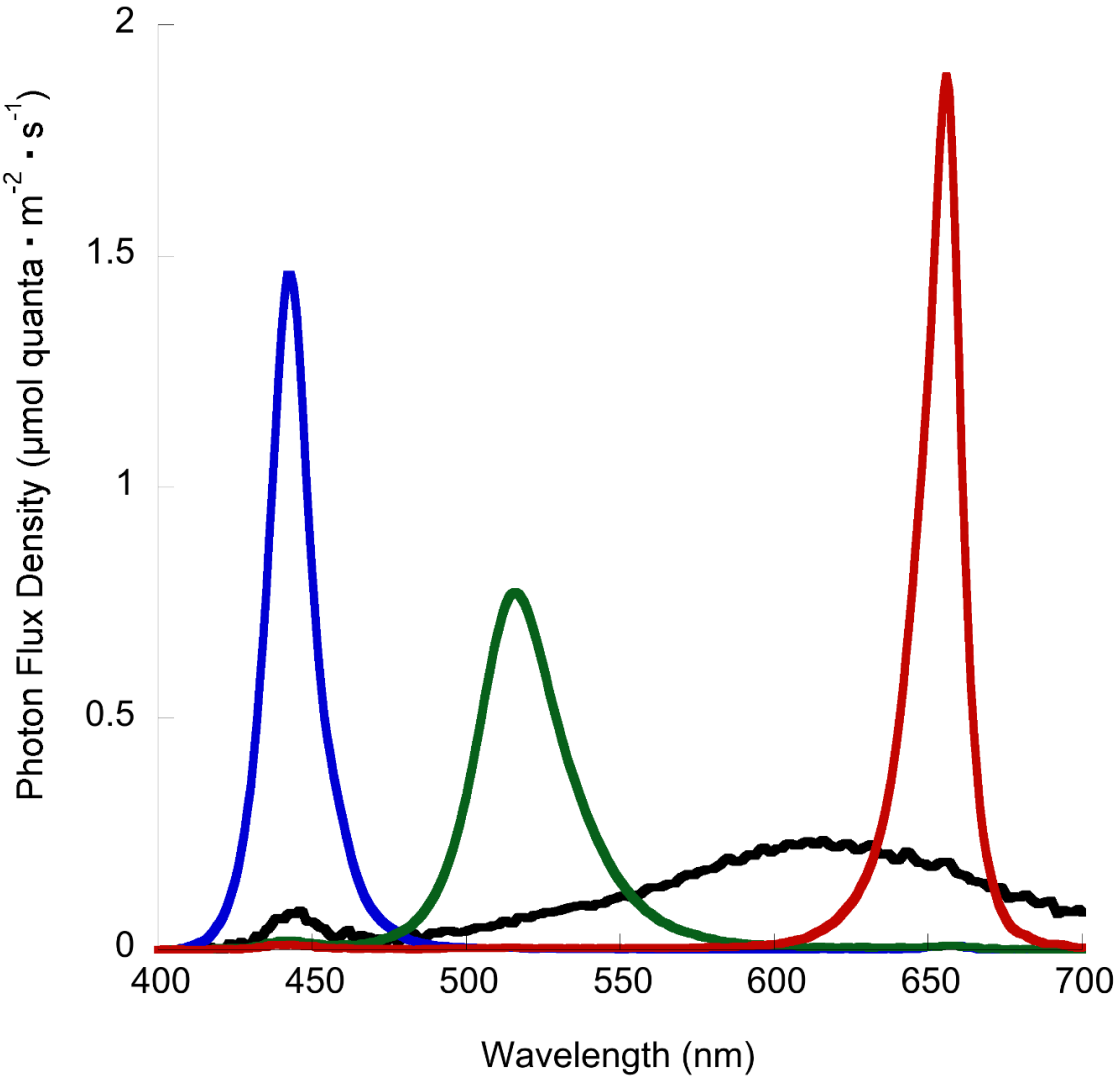

Figure 1.6: Spectra for growth chambers.

Table 1.1: Photosynthesis-related genes of interest.

Gene	**Symbol**	**GenBank Accession Number**
Magnesium-Chelatase Subunit, Chloroplastic	chlI	YP_009420404.1
Fucoxanthin Chl A/C Light-Harvesting Protein	lhcr/lhcc	XM_002292317.1
Heme Oxygenase	pbsA	ABO70806.1
Phycoerythrin Alpha Subunit	cpeA	CAC33091.2
Phycoerythrin Beta Subunit	cpeB	ABO70841.1
Phycoerythrin-Associated Linker Genes	cpeC	NC_005125.1
Phycoerythrin-Associated Linker Genes	cpeD	ABP99027.1
Phycobiliprotein/Chromophore Lyase	cpeS	EKX47022.1
Phycoerythrin Alpha Subunit Lyase	cpeZ	CAJ73184.1
Phycoerythrobilin Synthase	pebS	6QX6_B
Phycoerythrin Lyase	cpeT	AFP65495.1
Phycocyanin-Associated Linker Genes	cpcH2I2D2	AXB27150.1
Phycocyanin-Associated Linker Genes	cpcH3I3D3	ABQ85421.1
Phycocyanin Alpha Pcb-Like Lyase	cpcX	AIA66941.1
Carotenoid C2-Hydroxylase	crtG	AHB88556.1
Cis-Carotene Isomerase	crtH	QBE68568.1
Lycopene E-Cyclase	crtI	ADD79328.1
Leucopene Cyclase	crtL	ABW31007.1
Phytoene Desaturase	crtP	KAF0161346.1
Carotene Desaturase	crtQ	CAE7265831.1
B-Carotene Hydroxylase	crtR	AUC60050.1
Light Harvesting Apoproteins	LHCP	CAB1097287.1
Light Harvesting Complex	Lhcx	QIH55649.1
Light Harvesting Complex	Lhcz	CAM33414.1
15,16-Dihydrobiliverdin:Ferredoxin Oxidoreductase	pebA	6QX6_B
Peb:Ferredoxin Oxidoreductase	pebB	6QX6_A
Light Harvesting Protein 2	lhcb2	XP_005790942.1
Light Harvesting Complex Protein 8	lhcr8	BBO94014.1
Photosystem Ii Protein D1	psbA	ABO70840.1
Photosystem Ii P680 Chlorophyll A Apoprotein	psbB	YP_001293610.1
Photosystem Ii Cp43	psbC	YP_001293491.2
Photosystem Ii D2 Protein	psbD	YP_001293492.1
Cytochrome B559 Subunit Alpha	psbE	ABO70827.1
Cytochrome B559 Subunit Beta	psbF	YP_001293533.1
Photosystem Ii Reaction Center Protein H	psbH	YP_001293614.1

Photosystem Ii Reaction Center Protein I	psbI	YP_001293539.1
Photosystem Ii Reaction Center Protein J	psbJ	ALG63667.1
Photosystem Ii Reaction Center Protein K	psbK	YP_001293572.1
Photosystem Ii Reaction Center Protein L	psbL	YP_001293532.1
Photosystem Ii Reaction Center N Protein	psbN(A)	ABO70798.1
Photosystem Ii Reaction Center N Protein	psbN(B)	NP_050801.1
Photosystem Ii Reaction Center Protein T	psbT	YP_009420501.1
Cytochrome C-550	psbV	YP_001293523.1
Photosystem Ii Reaction Center Protein W	psbW	YP_001293482.1
Photosystem Ii Reaction Center X Protein	psbX	YP_001293524.1
Photosystem Ii Protein Y	psbY	YP_001293497.1
Photosystem I P700 A Apoprotein A1	psaA	YP_001293576.1
Photosystem I P700 A Apoprotein A2	psaB	NC_009573.1
Photosystem I Iron-Sulfur Center	psaC	YP_001293507.1
Photosystem I Subunit Ii	psaD	YP_001293570.1
Photosystem I Reaction Center Subunit Iv	psaE	YP_001293615.1
Photosystem I Subunit Iii	psaF	YP_001293526.1
Photosystem I Reaction Center Subunit Viii	psaI	YP_001293530.1
Photosystem I Subunit Ix	psaJ	ALG63666.1
Photosystem I Reaction Center Subunit Psak Precursor	psaK	YP_009420251.1
Photosystem I Reaction Center Subunit Xi	psaL	ALG63562.1
Photosysystem I Reaction Center Subunit Xii	psaM	NP_050701.1
Atp Synthase Subunit Alpha	atpA	ALG63566.1
Atp Synthase Subunit A	atpB	NP_050748.1
Atp Synthase Gamma Chain 1	atpC	NP_050748.1
Atp Synthase Subunit Beta	atpD	YP_001293544.1
Atp Synthase Subunit C	atpE	ALG63580.1
Atp Synthase Subunit B	atpF	YP_001293545.1
Atp Synthase Gamma Chain	atpG	YP_001293546.1
Atp Synthase Cf0 C Subunit	atpH	YP_001293547.1
Atp Synthase Protein I	atpI	YP_001293548.1
Ferredoxin Thioreductase, Beta Subunit	ftrB	YP_001293529.1
Cytochrome F Precursor	petA	YP_001293562.1
Cytochrome B6	petB	YP_001293480.1
Cytochrome B6/F Compex Subunit 4	petD	ABO70864.1
Ferredoxin, Chloroplastic Precursor	petF	YP_001293609.1
Cytochrome B6-F Complex Subunit 5	petG	ABO70761.1
Cytochrome B6-F Complex Subunit 6	petL	NP_050725.1
Cytochrome B6-F Complex Subunit 7	petM	ABO70756.1
Cytochrome B6-F Complex Subunit 8	petN	NP_050755.1

Cytochrome B559 Subunit Alpha	pbsE	WP_011124483.1
Cytochrome B559 Subunit Beta	pbsF	QXE46209.1
Cytochrome C-550 Precursor	pbsV	WP_011057125.1
Cytoplasmic Polyadenylation Element Binding Protein 1	cpeB1	JAO39450.1
Putative Septum Site-Determining Protein Mind Homolog, Chloroplastic	minD	YP_001293500.1
Cell Division Topological Specificity Factor Homolog, Chloroplastic	minE	ABO70851.1
Atp-Dependent Zinc Metalloprotease Ftsh 1, Chloroplastic	ftsH	ABO70796.1
Twin Arginine Transport	TAT	ABO70753.1
Er-Associated Degradation-Like Machinery	ERAD-like	ACS36235.1
Translocon At Inner Membrane Of Chloroplast (Tic)	TIC	KAA8499901.1
Translocon At Outer Membrane Of Chloroplast (Toc)	TOC	XP_002509092.1
Secretory Translocon	SEC	NP_050750.1
Acetate Permease A	acpA	ABO70762.1
Light-Independent Protochlorophyllide Reductase Subunit B	chlB	EU233748.1
Light-Independent Protochlorophyllide Reductase Iron-Sulfur Atp-Binding Protein	chlL	EU233749.1
Light-Independent Protochlorophyllide Reductase Subunit N	chlN	EU233756.1
Acetolactate Synthase Isozyme 1 Large Subunit	ilvB	ABO70722.1
Acetolactate Synthase Isozyme 3 Small Subunit	ilvH	ABO70838.1
Nad-Dependent Dihydropyrimidine Dehydrogenase Subunit Prea	preA	YP_009497974.1
Anthranilate Synthase Component 2	trpG	YP_009498064.1
Rubisco (Ribulose 1,5 Bisphosphate Carboxylase/Oxygenase), Large Chain	rbcL	ABO70740.1
Rubisco, Small Chain	rbcS	ABO70741.1
High Light Inducible Protein	hlip	ABO70729.1
Chlorophyll binding protein	cab	NP_050676.1

Table 1.2: Significant genes correlated with chlorophylls in *R. salina.*

Gene	Chl-*a* *p*-value	Chl-*a* Correlation Coefficient		Gene	Chl-c_2 *p*-value	Chl-c_2 Correlation Coefficient
atpH	0.009	0.150		CpeT	0.000	-0.892
psbV	0.009	0.032		Chl_bind32	0.012	-0.613
psbY	0.024	-0.116		psbW	0.035	-0.529
chlI	0.042	-0.055		PE_ab2	0.037	0.523
psaA	0.043	0.096		Chl_bind19	0.043	0.510
atpG	0.044	-0.207		Chl_bind8	0.048	-0.502
atpF	0.044	-0.207				
psbH	0.045	-0.115				

Table 1.3: Significant genes correlated with photoprotective pigments in *R. salina.*

Gene	**α-carotene *p*-value**	**α-carotene Correlation Coefficent**		**Gene**	**Alloxanthin *p*-value**	**Alloxanthin Correlation Coeffcient**
atpA	0.002	0.709		psbV	0.008	0.634
psbB	0.003	0.691		atpH	0.01	0.622
petF	0.003	0.684		psbY	0.038	-0.523
petG	0.005	0.667		chlI	0.042	0.514
atpH	0.006	0.650		psaA	0.048	0.501
rbcL	0.007	0.648				
atpB	0.010	0.623				
Chl_bind33	0.016	-0.590				
psbK	0.017	0.586				
psbD	0.018	0.584				
psbC	0.018	0.584				
Chl_bind3	0.023	-0.564				
Chl_bind11	0.023	-0.562				
Chl_bind27	0.035	-0.529				

Chl_bind 21	0.039	-0.521				
atpI	0.039	0.521				
PSII.Co mponent 1	0.041	-0.515				
Chl_bind 30	0.046	-0.506				
psbA	0.047	0.503				

CHAPTER 2: LET THERE BE LIGHT: CONSEQUENCES OF LIGHT SPECTRA FOR PIGMENT COMPOSITION AND GENE EXPRESSION IN CRYPTOPHYTES WITH DIFFERENT PHYCOBILIPROTEINS

Abstract

Aquatic environments vary in spectral characteristics across time and space. The pigment complement, or the type of pigments which photosynthetic organisms have, allows them to absorb various colors of light which can then be used for photosynthesis. Theoretically, photosynthetic organisms with a more diverse pigment complement should be able to exploit a wider array of light spectra, and should be able to survive in a broad range of light habitats by prioritizing pigments that maximize their capacity for light capture in the given environment (known as the theory of chromatic acclimation). We aimed to investigate how cryptophytes with different pigment complements and different natural habitats respond to different light spectra at both the physiological and molecular level. We grew three phycoerythrin-containing (*Rhodomonas salina, Hemiselmis andersenii*, and *Cryptomonas ovata)* and one phycocyanin-containing cryptophyte (*Hemiselmis tepida*) in wide-spectrum, blue, green, and red light and measured how pigment composition differed. We also examined the gene expression profile of each cryptophyte grown within each light environment, with a particular interest in genes that we identified as a part of the photosynthesis pathway *a priori.* Our results varied with species, with similarities between the phycoerythrin-containing cryptophytes that differed from the phycocyanin-containing one. The phycobiliprotein pigment concentration for

each species followed what we expected via the theory of chromatic acclimation; however, for all four species, we saw surprising differences between the phycobilin α and beta subunits even though the peptides are required in an equimolar ratio, suggesting post-transcriptional and post-translational regulation of these important proteins. *C. ovata* exhibited the greatest sensitivity and plasticity to light spectrum when examining photosynthesis-related genes, which may be related to its natural habitat history. We identified many non-photosynthesis-related genes that were sensitive to light spectrum in multiple species, suggesting that light color regulates more than the photosynthetic pathways in cryptophytes.

Introduction

Photosynthetic organisms capture light energy to create organic molecules using various types of pigments, and each pigment has different light absorption characteristics. Chlorophyll-*a* (chl-*a*), for example, which all modern photosynthetic organisms have, is efficient at absorbing blue (~400-520 nm) and red (~630-750 nm) wavelengths but is inefficient at capturing green wavelengths (~520-565 nm). Other pigments, such as carotenoids, which capture blue light, and phycobiliproteins, which capture either red or green light, allow photosynthetic organisms to capture a broader range of wavelengths that chl-*a* does not, increasing the range of light that can be used for photosynthesis (Blinks 1954; Glazer 1977; Gantt 1980; Stengel *et al.* 2011). However, not all photosynthetic organisms maintain the same pigment complement, and thus the absorption capabilities of different organisms can vary.

This diversity in pigment complements and absorption characteristics has the potential to influence the spectral niches that organisms occupy in various habitats. This is particularly important for algae and phytoplankton in aquatic habitats because the

spectral characteristics of aquatic ecosystems can vary and can change over time. Freshwater ecosystems tend to be red-dominated because they are rich in colored dissolved organic material (CDOM) that attenuates blue light quickly, and marine systems tend to be green or blue-dominated because the water and phytoplankton absorb red wavelengths quickly (Kirk 1994; Blough & Del Vecchio 2002),). Not only is there variation in spectral characteristics across habitats, but the available colors of light that are available can vary with depth. Closer to water's surface, there is a larger range of wavelengths available for photosynthesis, but as depth increases, lower-energy colors of light such as reds, oranges, and yellows are attenuated quickly by the water, CDOM, and phytoplankton throughout the water column, leaving the higher-energy green and blue wavelengths available (Schwarz & Markager 1999).

This variation within spectral habitats means that phytoplankton may be exposed to a wide variety of spectral shifts over time. Algal species that have a more diverse pigment complement should be able to occupy a wider range of spectral niches by shifting their pigment composition to maximize their capacity for light capture and photosynthesis dependent upon the colors of light available. This is known as the theory of chromatic acclimation (historically known as chromatic "adaptation") (Engelmann 1883; Gaidukov 1903), where algae alter their pigment composition to prioritize synthesis of pigments that are more efficient in the given spectral environment. This is not a permanent process, and the pigment composition could be altered again if the spectral availability were to change. This process of chromatic acclimation has been well-documented in cyanobacteria (Grossman 2003; Stomp *et al.* 2004; Stomp *et al.* 2007), a group of phytoplankton which maintain a diverse pigment complement, but is less understood in eukaryotic algae. Those studies which have examined the theory of

chromatic acclimation in eukaryotic algae have focused primarily on physiological responses to changes in light spectrum, but little work has been done examining the molecular responses (Wallen & Geen 1971; Rivkin 1989; Mouget et al. 2004; Vadiveloo et al. 2017).

Cryptophytes are unicellular eukaryotes which can be found in a wide variety of aquatic ecosystems. Their pigment complements are composed of chlorophyll-*a* (chl-*a),* chlorophyll-c_2 (chl-c_2)*,* alloxanthin, α-carotene, and a type of phycobiliprotein, which is their main light-harvesting pigment (Glazer 1983; Hill & Rowan 1989; Vesk *et al.* 1992; Blankenship 2002). Cryptophyte phycobiliproteins include cryptophyte phycoerythrin (denoted by Cr-PE) and cryptophyte phycocyanin (Cr-PC), but to date, each individual cryptophyte has been found to have only one type of phycobiliprotein. Cryptophyte phycoerythrin absorbs in the green and yellow (~545-566 nm) regions of the visible light spectrum and cryptophyte phycocyanin absorbs in the orange and red region (~569-645 nm). However, the specific wavelengths that each phycobiliprotein absorbs most efficiently varies with its chromophore attachments and configurations. Cryptophyte phycobiliproteins are composed of two α and two beta protein subunits, along with four phycobilin chromophore attachments, and these protein-chromophore complexes are directly related to the wavelengths of light the pigment can capture (Overkamp *et al.* 2014). For example, *Rhodomonas salina* and *Cryptomonas ovata* both have cryptophyte phycoerythrin, but *R. salina* has Cr-PE 545 while *C. ovata* has Cr-PE 566 (Cunningham *et al.* 2019). This means that *R. salina's* phycoerythrin has a maximum absorption peak at 545 nm in the visible light spectrum, while *C. ovata* has a maximum absorption peak at 566 nm (indicated by the 545 and 566 following "Cr-PE" for each species, respectively, leading to Cr-PE 545 and Cr-PE 566). These differences in absorption characteristics are

due to the type of chromophores that are attached to the protein subunits which make up the phycobiliprotein complex: *R. salina* has 15, 16 dihydrobiliverdin and phycoerythrobilin attached to its protein subunits, while *C. ovata* has bilin 584 and phycoerythrobilin (Apt *et al.* 1995). This is also seen in the cryptophyte phycocyanins which have different absorption maxima, such as Cr-PC 569, Cr-PC 577, Cr-PC 612, and Cr-PC 645 (Hill and Rowan 1989; Hoef-Emden and Archibald 2016).

Cryptophytes that have the same phycobiliprotein type can be found in different aquatic ecosystems. For example, *Chroomonas mesostigmatica* is a Cr-PC 645 cryptophyte that is found in marine ecosystems, while *Komma caudata*, in the same clade as *C. mesostigmatica*, is a Cr-PC 645 cryptophyte found in freshwater ecosystems. There are also Cr-PE cryptophytes that reside in different types of habitats, such as *C. ovata* (freshwater) and *R. salina* (marine), both which have Cr-PE, and there is variation in phycobiliprotein type even within the same type of aquatic system (e.g., *R. salina* with Cr-PE 545, *Hemiselmis andersenii* with Cr-PE 555, and *Falcomonas daucoides* Cr-PC 569, all which are marine species) (Hoef-Emden 2008, Hoef-Emden and Archibald 2016). Additionally, there is no distinct phylogenetic relationship between Cr-PE cryptophytes and Cr-PC cryptophytes (i.e., not all Cr-PE cryptophytes group together in one clade and not all Cr-PC cryptophytes group together) (Hoef-Emden 2008, Hoef-Emden and Archibald 2016). There are even clades that exhibit both types of phycobiliprotein, such as the *Hemiselmis* clade which has species such as *H. andersenii* (Cr-PE 555) and *H. tepida* (Cr-PC 612) (Cunningham *et al.* 2019). Thus, there does not appear to be any obvious link between pigmentation and habitat type or clade. This begs the question: how has this pigment diversity evolved?

Because cryptophytes with the same phycobiliprotein type can be found in habitats with drastically different spectral characteristics, it is possible that different phycobiliproteins may have plastic responses to changes in light color, and this variation in spectral habitat may be related to the evolution of the wide array of pigmentation observed in cryptophytes. In this study, we sought to test the plasticity by which cryptophytes with different pigment complements respond to light spectrum. We used four cryptophyte species: *Rhodomonas salina* (Cr-PE 545), *Hemiselmis andersenii* (Cr-PE 555), *Cryptomonas ovata* (Cr-PE 566), and *Hemiselmis tepida* (Cr-PC 615). For each species, we tested how the pigment composition and gene expression profiles changed in response to wide-spectrum, blue-dominated, green-dominated, and red-dominated light. We expected to see changes in pigment concentrations in each species following expectations predicted by the theory of chromatic acclimation to maximize the capacity to capture available spectra. For *R. salina, H. andersenii,* and *C. ovata,* all species which have a Cr-PE that absorbs well in green light, we expected to see an increase in Cr-PE concentration in green light compared to the other four light environments. For *H. tepida*, we expected to see an increase in the phycobiliproteins shifted towards the higher wavelengths.

For our transcriptome comparisons, we examined the gene expression at three different scales. We first examined the expression of transcripts that encode the peptide components of cryptophyte phycobiliproteins. Second, we investigated the expression of 99 photosynthesis-related genes which were identified *a priori,* predicting that these loci would be responsive to light color. Last, we examined the genome-wide expression to determine if other functions and molecular processes that are not obviously related to photosynthesis were responsive to light spectrum. We expected to see the cryptophyte

phycobiliprotein and photosynthesis-related gene expression mirror any shifts in cellular pigment protein concentrations, and that cryptophytes with similar colorations and pigment complements would have similar gene expression patterns across spectra.

Methods

Growth and Treatment Conditions

Baseline cultures. We grew five replicate cultures of *Cryptomonas ovata* UTEX 2783 (from the Culture Collection of Algae at the University of Texas-Austin; Cr-PE 566), *Hemiselmis tepida* CCMP 443 (from the National Center for Marine Algae and Microbiota (NCMA) at the Bigelow Laboratory for Ocean Sciences; Cr-PC 615, *Rhodomonas salina* CCMP 1319 (from NCMA; Cr-PE 545) and *Hemiselmis andersenii* CCMP 644 (from NCMA; Cr-PE 555). Each replicate was grown in 150 mL of the species' stock media, which included MWC+Se, L1-Si+NH4, Li-Si, and K (Guillard & Ryther 1962) for *C. ovata*, *H. tepida, R. salina,* and *H. andersenii* respectively. All cultures were grown in a Conviron walk-in incubator (Controlled Environments, Inc., Manitoba, Canada) kept at 20°C. These replicate baseline cultures were grown under a wide-spectrum light environment (LumiBar Pro LED Light strip, LU50001; LumiGrow, Emeryville, CA, USA) at ~30 µmol photons m^{-2} s^{-1} on a 12:12 hr light:dark cycle. We swirled each replicate culture by hand daily to prevent settling and help aeration.

Experimental populations. Once the baseline cultures reached mid-exponential phase (5-7 days after inoculation), we used the five replicate cultures to inoculate four experimental populations from each by transferring 5 mL of the culture into 300 mL of fresh media for a total of 20 experimental populations per species. One experimental population derived from each replicate baseline culture was randomly assigned to each light spectrum treatment.

Treatment Conditions. We placed all experimental populations in four separate light environments: wide-spectrum; blue-dominated, green-dominated, and red-dominated, each maintained at ~30 µmol photons m^{-2} s^{-1} at 20°C, which is comparable to low-light conditions cryptophytes usually inhabit in nature. Like the wide-spectrum environment, the blue and red lights were maintained by LumiBar Pro LED light strips (LU50001; LumiGrow, Emeryville, CA, USA), but the green light environment was provided by an EvenGlow® RGB LED panel (Super Bright LEDs Inc., St. Louis, MO, USA). We left each population to acclimate in each treatment environment for 10 generations (assuming population intrinsic growth rates as quantified by Heidenreich and Richardson 2019 in the same experimental chambers; see Table 1.1 for more details). During acclimation, we transferred the populations to new media after ~5 generations (~7 days for *R. salina, H. andersenii*, and *H. tepida,* and ~12 days for *C. ovata*) to ensure they remained in nutrient-replete conditions. After the populations were acclimated, we sampled for pigments and RNA.

Pigment Analyses

Cryptophyte Phycobiliprotein Analysis. We calculated cryptophyte phycobiliprotein concentrations using the freeze-thaw centrifugation method of Lawrenz *et al.* (2011). Briefly, took 15 mL aliquots of each experimental population and centrifuged them at 2,054 g in a Sorvall RC-4B centrifuge for 10 minutes. The supernatant was removed, and the cell pellet was resuspended in 0.1 M phosphate buffer (pH = 6). We then froze the samples at -20°C for a minimum of 24 hours. After freezing, we thawed the samples at 5°C for 24 hours. The thawed samples were then centrifuged at 11,000 g in a Beckman Coulter 18 Microfuge for 5 minutes to remove excess cell material. We measured the absorbance of the remaining supernatant against a phosphate

buffer blank in a 1 cm quartz glass cuvette using a Shimadzu UV-VIS 2450 dual-beam spectrophotometer from 400 to 750 nm in 1 nm intervals. Data were scatter-corrected by subtracting the absorbance at 750 nm from the maximum absorption peak (Lawrenz *et al.* 2011). Concentrations (pg/cell) were calculated according to:

$$C = \frac{A}{\varepsilon * d} \; x \; MW \; x \; \frac{Vbuffer}{Vsample} x \; \frac{10^{12}}{N}$$

Where A = absorbance of sample, ε = the extinction coefficient for cryptophyte phycobiliprotein (phycoerythrin = 5.67 x 10^5 L ·mol^{-1} · cm^{-1}; phycocyanin = 5.70 x 10^5 L ·mol^{-1} · cm^{-1}; MacColl et al. 1976), d = path length of the cuvette in cm, MW = molecular weight of cryptophyte phycoerythrin (45,000 Da; MacColl *et al.* 1973, 1976), V_{buffer} = volume of buffer in mL, V_{sample} = volume of sample in mL, and N = concentration of cells (cells/L). The 10^{12} is the conversion factor to convert the results into pg/cell from g/cell.

Non-Phycoerythrin Analyses. To determine the chlorophyll-*a*, chlorophyll-c_2, alloxanthin, and α-carotene concentrations, we filtered 5 mL of each experimental population onto a 25 mm Whatman GF/C filter (GE LifeSciences, Buckinghamshire, UK). These samples were then processed using high performance liquid chromatography (HPLC) to obtain pigment concentrations for each sample. Details for analyzing phytoplankton pigment samples using HPLC can be found in Pinckney *et al.* (1996). Briefly, filters were freeze-dried overnight, then pigments were extracted for 24 h at -20°C with 750µL of 90% acetone with 50µL of a synthetic carotenoid as an internal standard. The extracted solution was filtered through a 0.45 µm syringe filter, and 250 µL was injected into a Shimadzu HPLC. Chromatograms were analyzed by comparing retention times and absorption spectra to known standards (HDI, Horsholm, Denmark).

Statistical Analyses. We first checked the normality of our data using Shapiro-Wilk tests. Then, we ran a two-way Analysis of Variance (ANOVA) with a Tukey post-hoc comparison to test for significant differences in pigment concentrations across all four treatments and across species.

When we examined pigment (and transcriptome) responses to light spectrum, we performed statistical analyses using the data from experimental populations grown in blue, red, and green spectra. The blue vs. red light comparison represented the widest energy difference between spectra (as one blue photon is more energetic than one red photon) and reflected distinct habitats in the natural world (open-ocean marine vs. freshwater). Green vs. red light also reflected distinct real-world habitats (coastal marine vs. freshwater) but maximizes the differences in the expected light absorption due to molecular physiology. In contrast, blue vs. green light comparisons represented distinct habitats (open-ocean marine vs coastal marine) that present more limited energetic and light absorption differences. Experimental cultures grown in the wide-spectrum environment gave us a baseline for what the cultures were growing in prior to the beginning of the experiment.

RNA Extractions, Sequencing, and Transcriptome Assembly

After taking samples for pigment analyses, we spun the remainder of each culture (270 mL) in 500 mL centrifuge bottles at 3024g for 30 minutes (Beckman Coulter J2-21 centrifuge; JA-20 rotor) to pellet the cell material. The supernatant was removed and the pellet was transferred to a microcentrifuge tube, and then we spun the microcentrifuge tubes at 3000g (Beckman Coulter 18 Microfuge) for 12 minutes. The supernatant was removed, and then the pellets were weighed. If the pellet mass was between 50-100 mg,

we lysed the cells with 1 mL of Bio-Rad PureZOL reagent; if the mass was less than 50 mg, we used 0.5 mL of reagent. The remainder of our extraction protocol followed the standard TRIzol RNA isolation procedure (detailed in the ThermoFisher Scientific Invitrogen TRIzol Reagent User Guide, Pub. No. MAN0001271, Rev. B.0), with the addition of a second ethanol wash step prior to elution to increase the purity of the RNA.

All species were sequenced using 150bp paired-end sequencing. Raw reads were quality trimmed and filtered using Trimmomatic (Bolger, Lohse, & Usadel 2014), and then we built transcriptome assemblies for each species using Trinity (Grabherr *et al*. 2011) and Velvet-Oases (Schulz, *et al*. 2012), and then we combined them using EviGene (Gilbert 2013). This allowed us to correct for biases that each assembler exhibits, leaving us with a comprehensive and robust final assembly. After the transcriptomes were complete, we used TransRate (Smith-Unna *et al.* 2016) and BUSCO (Simao *et al.* 2020) as quality control metrics to assess the completeness of our assembly and obtain basic assembly stats. Further quality control, RNA-sequencing details and specifications, and transcriptome assembly protocols are detailed in Chapter 1.

Gene Annotation

For each of the assemblies, we used the *de novo* transcriptome annotator dammit (Scott 2018) to annotate putative gene transcripts. This pipeline uses Transdecoder to build gene models and then searches the following protein databases for annotation matches (using an E-value cutoff of 1x10-5): Pfam-A, Rfam, OrthoDB, and uniref90.

Building the a priori *list of photosynthesis-related genes*

The details for how we chose and obtained our photosynthesis-related genes prior to the experiment can be found in Schomaker, Richardson, and Dudycha (unpublished). Briefly, we compiled a list of photosynthesis-genes from existing cryptophyte genomes

(Douglas and Penny 1998; Jarvis and Soll 2001; Gould *et al.* 2007; Koziol *et al.* 2007; Khan *et al.* 2007; Overkamp 2014; Takaichi 2011; Neilson *et al.* 2017) and pulled the nucleotide sequences of these genes from the genomes available in the NCBI database. We used blastn to search for these sequences in our transcriptome assemblies using an E-value cutoff of 1x10-5, and then these sequences were used in our differential gene expression analysis to investigate the plasticity of photosynthesis and light capture across spectra at the level of gene expression.

Differential Gene Expression Analysis and Exploration

For each of the four species, we mapped the trimmed paired-end reads back to the final transcriptome assembly to obtain our read count data using kallisto (Bray *et al.* 2016). Then, we ran the differential gene expression analyses for each species using Degust (Powell 2019) to run edgeR with a false discovery rate (FDR) corrected *p*-value cutoff of 0.05 and a log fold-change (FC) cutoff of ±2. We examined the differences in gene expression at three different scales. First, we investigated the expression of the cryptophyte phycobilin-subunit genes to determine if they were differentially expressed among spectra. Second, we tested the *a prior* list of photosynthesis-related genes to investigate the plasticity of photosynthesis more broadly. Third, we tested the complete gene set (the total number of contigs expressed in our assembly) to see whether genes that are not directly related to photosynthesis function were regulated by light spectrum. All gene expression levels for each comparison are reported in transcripts per million (TPM).

Results

Pigment Data

Phycobiliprotein concentrations. For *R. salina,* we saw the highest Cr-PE 545 concentrations in cultures grown under green light (6.20 ± 0.60 pg/cell), which was significantly higher in green light (p-value = 0.0069; F-value = 7.85; df = 2) than populations grown in red light that exhibited the lowest Cr-PE 545 concentrations (2.70 ± 0.60 pg/cell). Populations grown in blue light and the wide-spectrum light had average cryptophyte phycoerythrin concentrations of 4.60 ± 0.60 pg/cell and 3.80 ± 0.90 pg/cell, respectively. There were no significant differences observed between the red vs blue and the blue vs green comparisons (Figure 2.1A).

H. andersenii exhibited the highest Cr-PE 555 concentrations when grown under green light (5.41 ± 0.29 pg/cell) and the lowest in blue light (1.84 ± 0.19 pg/cell). This difference between Cr-PE 555 concentrations was significant (p-value = 0.021, df = 3, F-value = 3.97). No other comparisons were significantly different (Figure 2.1B). Our second *Hemiselmis* species, *H. tepida,* had the highest phycobiliprotein content in red light, where Cr-PC 615 was measured at 1.51 ± 0.40 pg/cell, followed by blue light (1.14 ± 0.26 pg/cell), wide-spectrum (0.82 ± 0.28 pg/cell), and green light (0.47 ± 0.14 pg/cell). None of the *H. tepida* Cr-PC 615 concentrations across treatments were significantly different (Figure 2.1C).

C. ovata exhibited the highest Cr-PE 566 concentration in blue light (62.54 ± 0.53 pg/cell) followed by green light (45.56 ± 0.64 pg/cell), wide-spectrum (38.21 ± 0.91 pg/cell) and red light (34.21 ± 0.81 pg/cell). There was a significantly higher concentration of Cr-PE 566 in blue light compared to *C. ovata* cultures grown in red and green light (p-value = 0.021, df = 3, F-value = 2.405 and p-value = 0.003, df = 3, F-value

= 2.405 respectively), and there was no significant difference in Cr-PE 566 concentrations between cultures grown in green and red light (Figure 2.1D).

Non-PBP pigment concentrations. The concentration of non-PBP pigments varied with species and spectra. In general, all the pigments followed similar trends in concentration across spectra within each species (Figure 2.2 and Figure 2.3). For example, chl-*a* concentrations in *H. tepida* were highest in red, followed by blue, green, and wide-spectrum cultures. Alloxanthin and α-carotene followed this same trend, being highest in red, followed by blue, green, and wide-spectrum light in *H. tepida.* This occurred in all four species.

There were no significant differences observed in chl-*a*, chl-c_2, alloxanthin, or α-carotene concentrations for *H. andersenii* cultures grown in the four different spectra (Figure 2.2A). *H. andersenii* cultures grown in wide-spectrum light had the highest average chl-*a* concentrations (2.40 ± 1.08 pg/cell), followed by cultures grown in blue, green, and red light (with averages of 2.12 ± 0.86, 1.88 ± 0.94, and 1.72 ± 0.60 pg/cell, respectively). Chl-c_2 concentrations all sat around 0.40 pg/cell for wide-spectrum, blue, and green light, but was 0.30 pg/cell on average for cultures grown in red light. Alloxanthin concentrations (Figure 2.3A) were highest in blue and wide-spectrum light (0.62 ± 0.25 and 0.64 ± 0.29 pg/cell, respectively), followed by green light (0.53 ± 0.30 pg/cell) and red light (0.45 ± 0.16 pg/cell). α-carotene concentrations for *H. andersenii* cultures grown in wide-spectrum, blue, and green light ranged from 0.25 – 0.30 pg/cell, while cultures grown in red light had an average concentration of 0.16 ± 0.05 pg/cell.

For *R. salina*, we saw a significant higher concentration of chl-*a* in cultures grown in red light compared to those grown in blue, and we saw a significant lower concentration of both alloxanthin and α-carotene for cultures grown in blue light

compared to red (Figure 2.2B and Figure 2.3B). Surprisingly, the highest chl-*a* concentrations were observed in *R. salina* cultures grown in green light, and we also saw high concentrations of alloxanthin and α-carotene in green and red light.

H. tepida (Figure 2.2C and 2.3C) chl-c_2 concentrations were low across all for spectra (ranging from 0.13 – 0.14 pg/cell), and there were no significant differences observed between any of the other pigments grown across spectra. Chl-*a* concentrations were highest in red light (5.43 ± 1.48 pg/cell), followed by blue (4.18 ± 1.75 pg/cell), green (3.42 ± 0.90 pg/cell), and wide-spectrum light (2.76 ± 0.22 pg/cell), and alloxanthin and α-carotene concentrations followed this same pattern, being highest in red light, followed by blue, green, and wide-spectrum light, ranging from 0.56 - 1.09 pg/cell and 0.30 – 0.63 pg/cell for alloxanthin and α-carotene, respectively.

C. ovata (Figures 2.2D and 2.3D) cultures had the greatest concentration of each pigment per cell, most likely attributed to its large cell size compared to the other species. Chl-c_2 concentrations were negligible (ranging from 0.51 – 1.14 pg/cell) compared to the other pigments. Chl-*a* was highest in blue light (24.53 ± 35.42 pg/cell), followed by wide-spectrum (22.54 ± 17.14 pg/cell), green (19.8 ± 9.19 pg/cell), and red light (14.58 ± 10.80 pg/cell). Alloxanthin was highest in wide-spectrum light (5.08 ± 3.81 pg/cell), followed closely by blue light (4.62 ± 6.20 pg/cell), green (4.60 ± 2.62 pg/cell), and red light (3.01 ± 1.75 pg/cell). A-carotene followed a similar trend, though concentrations were slightly higher in blue light (2.91 ± 4.31) than wide-spectrum light (2.39 ± 1.98 pg/cell), followed then by green (2.02 ± 1.28 pg/cell) and red light (1.61 ± 1.50 pg/cell). There were no significant differences across any spectral comparisons for any non-PBP pigments for *C. ovata.*

Transcriptome Assembly

Our final transcriptome assemblies ranged from 20,553 to 155,790 contigs dependent upon the species (Table 2.2). Our average contig length range from 820bp to 1,560bp, and our GC content ranged from 58.8% to 62.8%. The percentage of annotated genes were we able to identify with our annotation pipeline varied with species (Table 2.2). Our lowest annotation percentage was 24.6% for *C. ovata*, where we were able to identify 38,324 protein annotations out of the total 155,790 contigs in the assembly. For *H. andersenii* and *H. tepida,* we were able to annotate 42.2% and 43.9% of the respective assemblies (16,551 of 39,221 contigs for *H. andersenii* and 9,023 of 20,553 contigs for *H. tepida*). We were able to annotate the greatest number of contigs for *R. salina* at 54.2% (13,171 of 24,167 contigs). The remaining transcripts for each assembly did not return an annotation hit across the protein databases.

Our BUSCO analysis revealed that our *R. salina* transcriptome 63.0% of the expected eukaryote orthologs and 46.5% of the expected protist orthologs. *H. andersenii* exhibited 66% of the expected eukaryote orthologs and 61.0% of the protist ones, while *H. tepida* contained 40.4% and 41.9% of the eukaryote and protist BUSCOs respectively. *C. ovata* had the highest BUSCO matches with 85.9% of the eukaryote and 80.5% of the protist orthologs recovered (Tables 2.3 and 2.4).

Differential Gene Expression Analysis and Exploration.

Phycobiliprotein subunit gene expression. We saw similar expression trends in *R. salina* and *H. andersenii* when looking at the phycobiliprotein subunit gene expression. In *R. salina*, we found that neither of the cryptophyte phycoerythrin subunit genes were significantly differently expressed across spectra (FDR p-value < 0.05 and a

$\log_2$foldchange ≥ 2), but they were expressed at drastically different levels. The α subunit expression ranged from 1,306 TPM to 2,254 TPM while the beta ranged from 65 TPM in green light to 103 TPM in red light (Figure 2.4A). The expression of both the α and beta subunits in *H. andersenii* were much lower, but the trend of the α and beta subunits being unequally expressed remained. For *H. andersenii,* there were again no significant differences in the phycoerythrin peptide genes observed across spectra, but the α subunit was expressed at a much higher level (15 TPM) than the beta subunit (1 TPM) (Figure 2.4B).

We saw different expression trends for the phycobiliprotein peptide subunits in *H. andersenii* and *C. ovata* compared to *R. salina* and *H. rufescens*. In *C. ovata* the beta subunit was expressed at an average of 177,558 TPM while the α was expressed at an average of 21,406 TPM, which is much higher and the opposite trend of subunit expression that we observed in the other two cryptophytes (Figure 2.4C). We also observed that both α and beta phycoerythrin subunits were significantly downregulated in blue light compared to the other light environments (green vs. blue α subunit *p*-value = 0.00023, green vs. blue beta subunit *p*-value = 2.89×10^{-11}; red vs. blue α subunit *p*-value = 0.00012, red vs. blue beta subunit *p*-value = 1.62×10^{-10}) even though the phycoerythrin concentrations were highest in blue light for *C. ovata.* This was true for both subunit expression in blue light compared to wide-spectrum light as well, even though this was not one of our main comparisons (wide vs blue α subunit *p*-value = 2.48x10-11; wide vs. blue beta subunit *p*-value = 2.48×10^{-11}). For our second green cryptophyte, *H. tepida,* we also saw significantly greater expression of the beta subunit compared to the α subunit, with the beta having an average expression of 11,410 TPM and the α having an average

of 511 TPM, though none of the comparisons across light spectra were significant (Figure 2.4D).

Photosynthesis-related gene expression. For *R. salina*, we found very few photosynthesis-related genes were significantly differentially expressed across light environment (p-value < 0.05 and $\log_2$ foldchange ≥ 2). 9 genes were significantly differentially expressed in the blue vs. red treatments, but there were none found when comparing expression in blue vs. green light or when comparing expression in red vs. green light. For *H. andersenii*, we again saw few significantly differentially expressed genes across spectra, but in both the green vs. blue and the green vs. red comparisons, we found an ATP synthase subunit which was upregulated in green light in both comparisons (and it was also significantly upregulated in green light compared to wide-spectrum light).

We also did not see many significantly differentially expressed genes for any of the comparisons performed using *H. tepida* all of the photosynthesis-related genes. We found one significantly differentially expressed gene when comparing photosynthesis-related genes in red and blue light for *H. tepida*, which was a gene coding for photosystem I subunit X and was significantly upregulated in blue light compared to red (p-value = 0.0017). However, for *C. ovata*, we observed 26 genes which were significantly differentially expressed in every comparison. Of these 26, 14 were downregulated in blue light no matter what other light environment they were compared to, and 12 were consistently upregulated in blue light compared to other light spectra. Those that were constantly downregulated in blue light included both phycoerythrin subunit genes, the RuBisCo large subunit gene (rbcL), genes related to photosystem I and II protein components, and one gene coding for a cytochrome b6-f complex subunit. Of

the 12 that were consistently upregulated in blue light in *C. ovata*, 4 were genes coding for cytochrome b6-f complex proteins, 3 were genes coding for photosystem II protein complexes, and the others included the RuBisCo small subunit gene (rbcS), a high-light inducible protein, a sec translocase gene, and a gene coding for magnesium chelatase.

Complete gene set expression. When comparing expression of the complete gene set across the different light spectra, the results varied greatly with species. In *R. salina*, 1,290 genes were significantly differentially expressed in the blue vs. red comparisons. 990 of these genes were upregulated in blue light, while 300 were upregulated in red light (Figure 2.5). Genes that were upregulated in blue light were involved in oxidation-reduction processes, translation, transmembrane transport, carbohydrate metabolic processes, transcriptional regulation, cell signaling, transduction, and communication. Those upregulated in red light were involved in translation, transmembrane transport, oxidation-reduction processes, and photosynthetic electron transport. 1,826 genes were significantly differentially expressed in the green vs. red comparison, with 232 upregulated in red light and 1,594 upregulated in green light. Both green and red light upregulated genes involved in oxidation-reduction processes, transmembrane transport, and phosphorylation, and green light also upregulated genes involved in carbohydrate metabolic processes, transcription and translational regulation, DNA replication and repair, and many different functions related to RNA processing, splicing, and catabolism. For the green vs. blue comparison, only 50 genes were significantly differentially expressed, 39 of which were upregulated in blue light and 11 which were upregulated in green light (Figure 2.5). These fifty genes included functions involved in methyltransferase activity, tyrosine phosphatase function, DNA binding, transcriptional regulation, and protein folding and transport.

In *H. andersenii*, we saw far less significant differential gene expression in the complete gene set. When comparison blue vs. red light, we had 193 significantly differentially expressed genes, where 188 were upregulated in blue and 5 were upregulated in red. Many of the genes upregulated in blue light compared to red were related to RNA processing and ribosomal function and synthesis. Two of the 5 genes that were significantly upregulated in red were annotated: one was related to RNA methylation and the other was related to RNA transport. For the red vs. green comparison, there were 10 significantly differentially expressed genes, and for the green vs. blue comparison, there were 11. For both the red vs. green and the green vs. blue comparisons, the majority of significantly differentially expressed genes were significantly upregulated in the higher-energy light (green in the red vs. green comparison and blue in the green vs. blue comparison) (Figure 2.5).

We saw the greatest number of significantly differentially expressed genes for *H. tepida* in the red vs. blue comparison, where we found 972 genes which were significantly differentially expressed. Of these, 495 were upregulated in blue, while 729 were upregulated in red. For the green vs. red comparison, we had 108 significantly differentially expressed genes. Of these 108, 103 were upregulated in green light, while 5 were upregulated in red light (Figure 2.8). Of the 5 that were upregulated in red light, one was a RWP-PK gene, which codes for a domain that is part of algal minus dominance proteins. Of the genes upregulated in green light compared to red, there were many related to methylation and photosynthetic electron transfer and transport. For the green vs. blue comparison, there were 53 significantly differentially expressed genes. Eight of these were upregulated in green while the remaining 46 were up in blue. The genes upregulated in green light had putative functions related to protein interactions, DNA-

binding, and protein transfer, while those upregulated in blue light had functions including DNA regulation, phosphorylation, protein transfer, and oxidation-reduction processes.

For *C. ovata,* we saw no significant gene expression for any genes in the green vs. red comparison and the red vs. blue comparison (Figure 2.8). For the green vs. blue comparison, we found two unannotated genes that were significantly differentially expressed with a FDR *p*-value of 0.05 and a $\log_2$ foldchange of ≥ 2. For the red vs. blue comparison, only 6,607 of the ~155,000 total contigs in the assembly had a $\log_2$ foldchange ≥ 2, suggesting that many of the genes in the *C. ovata* transcriptome are lowly expressed. When we removed the cutoff of a $\log_2$ foldchange of ≤ 2 but kept the FDR *p*-value of 0.05, we still saw no significant differential expression. We didn't observe any significant differential expression until we went up to a *p*-value of 0.01, which gave us only one significantly differentially expressed gene (which had an unknown annotation). Even going up to a FDR *p*-value of 0.9 yielded only 27 significantly differentially expressed genes in the red vs. blue comparison (with no $\log_2$ foldchange cutoff). This suggests that the *C. ovata* transcriptome assembly is so large that we lose the power to detect significant expression when correcting for multiple comparison biases.

For all of species, a large percentage of our top differentially expressed genes were unable to be identified across any of the protein databases used in our dammit annotation pipeline. Thus, there are many genes that are transcriptionally active and spectrally responsive across all of our cryptophyte genomes that are currently unannotated and may require further exploration.

Discussion

Aquatic ecosystems vary in light spectrum, and as consequence, aquatic photosynthetic organisms can be exposed to different colors of light. Theoretically, algae with a wider variety of pigments which are able to adjust their pigment complement to maximize light capture when the light environment shifts should be able to exploit more spectral niches and acclimate to environmental plasticity more readily. We examined both the physiological and transcriptomic plasticity of cryptophytes with different pigment complements grown in wide-spectrum, blue-, green-, and red-dominated light environments. We expected that each cryptophyte would exhibit physiological shifts in response to light spectrum as predicted by the theory of chromatic acclimation, where the pigment composition (type and concentrations) would be adjusted to optimize light capture in the given environment. We also expected that cryptophytes that appear the same color and have similar pigment complements would respond in a similar manner. On a transcriptomic level, we expected that photosynthesis-related genes would be sensitive to light spectrum, and that the expression of genes related to pigment proteins would mirror shifts observed in the pigment composition for each cryptophyte. Our results partially supported these hypotheses and the expectations given from the theory of chromatic acclimation, but some observations in pigment shifts and gene expression cannot be explained by this idea and lack clear drivers as to why they were responsive to light spectrum.

How do the transcriptomes assemblies across different cryptophytes compare?

Our transcriptome assemblies ranged from ~20,000 contigs to ~156,000 contigs with GC contents around 60.0% and a N50 ranging from 1,154bp to 2,431bp. These

results are comparable to other cryptophyte transcriptome assemblies. An *R. salina* CCMP 1319 transcriptome assembly assembled as part of the Marine Microbial Eukaryote Transcriptome Sequencing Project (MMETSP) had 31,523 contigs with a N50 of 1,650, while *H. andersenii* CCMP 644 assembled had 38,813 contigs with a N50 of 1,314bp, both which are similar to our results for our assemblies of these same species. While there are no freshwater assemblies of *Cryptomonas* species to our knowledge, the marine heterotrophic cryptophyte, *C. paramecium* CCAP 977/2a transcriptome assembly had 43,247 contigs and a N50 of 1,280bp and *C. curvata* CCAP 979/52 had 38,064 contigs with a N50 of 1,427bp. While our *C. ovata* assembly has more contigs than our other cryptophyte assemblies and other cryptophyte transcriptomes that are currently available, this high contig number for algal species is not uncommon. This is particularly common in dinoflagellate species and species that tend to be mixotrophic, which have assembly sizes ranging from 118,304 to 202,600 contigs (Zhang *et al.* 2014; Wang *et al.* 2019; Menghini and Aubry 2021). Additionally, given that our BUSCO results revealed a high percentage of expected orthologs in our assembly and our pipeline is designed to create a robust and comprehensive transcriptome, we are confident in our assembly results.

Are cryptophyte pigments maximizing their capacity to capture available light across species?

There were no significant differences between cryptophyte phycobiliprotein concentrations when examining the concentrations observed across treatments without taking into consideration species differences. This suggests that light spectrum on its own does not lead to a significant difference in phycobiliprotein concentrations and that

species' differences play a large role in the changes observed across treatments. When we examined the differences in pigment concentrations across species, we did find significant differences between cryptophyte phycobiliprotein concentrations across species regardless of light environment. *C. ovata* exhibited significantly higher phycobiliprotein concentrations compared to all other species (*p*-value = 1.15×10^{-11}, *p*-value = 1.18×10^{-11}, and *p*-value = 1.25×10^{-11} compared to *H. andersenii, H. tepida,* and *R. salina* respectively). There were no significant differences between *H. andersenii, H. tepida*, and *R. salina* phycobiliprotein concentrations. It is important to note here that *C. ovata* is a much larger cryptophyte species compared to the others, with an average cell volume of 1,079 ± 453 μm^3 (Cunningham *et al.* 2019), while *H. andersenii, H. tepida,* and *R. salina* are all much smaller, having cell volumes that range from 23 - 213 μm^3 (Cunningham *et al.* 2019). While we did not measure cell volumes in this particular study, this is the most likely explanation for significant differences observed in phycobilin concentration across species regardless of light spectrum.

When we did within-species comparisons of each species grown in the different treatments, we saw that, in general, the cryptophytes appear to be adjusting their phycobilin concentration to respond to changes in available light spectra. Both *R. salina* and *H. andersenii* exhibited the highest Cr-PE concentrations in green light compared to the other light environments, and *H. tepida* had the highest concentration of Cr-PC 615 in red light. For each of these species, the phycobiliprotein concentration was highest in the spectrum in which it is the most efficient at light capture (Cr-PE 545 and 555 in green light, and Cr-PC 615 in red light). *C. ovata* exhibited the highest Cr-PE 566 concentration in blue light, followed by green and wide-spectrum light, with the lowest concentration observed in red light. While it was unexpected that the phycoerythrin concentration

would be so high in blue light, we do see the same trend where the phycobiliprotein concentration is higher in light that it is more efficient at absorbing (green light) compared to the one it is least efficient at absorbing (red). The high concentration of Cr-PE 566 observed in blue light in *C. ovata* could be explained by a significant change in cell volume in blue light compared to the other light environments, but we would need to measure biovolume across spectra to test this hypothesis to determine if light spectrum is correlated with cell volume. Overall, it appears that cryptophytes do exhibit shifts in the concentration of their main light-harvesting pigments to maximize their potential for light capture in different spectra as expected via the theory of chromatic acclimation.

Non-PBP pigments also varied across species and spectra. Interestingly, while we do see shifts in chlorophyll concentrations that we may expect via the theory of chromatic acclimation, e.g., concentrations of chl-*a* are highest in *H. tepida* cultures grown in red and blue light, which chl-*a* absorbs efficiently, we also see that all four species have higher concentrations of chlorophyll in green light than would be predicted by the theory of chromatic acclimation because chlorophyll does not efficiently absorb green light. For all four species, chlorophyll concentrations are comparable to or greater than those in blue and red light. In *R. salina* and *H. tepida,* these concentrations are even higher than the wide-spectrum control environment, suggesting that chlorophyll is being produced in green light vs. remaining in the cell because it hasn't been degraded. We see similar trends in photoprotective pigment concentrations, where they are comparable or higher than concentrations in the blue light environment where we'd expect them to be most active because blue light is the highest-energy light available in our study. For *H. tepida* and *C. ovata*, all of the pigments have similar trends across spectra, including the major-light harvesting phycobiliprotein. For example, all non-PBP pigments and the PBP in *H.*

tepida are highest in red light, followed by blue, green, and wide-spectrum light. All of the pigments in *C. ovata* are highest in blue light, followed by wide-spectrum, green, and red light. This suggests that these two species adjust all of their pigments in a similar manner across spectra, and that instead of following the theory of chromatic acclimation where pigments are adjusted to maximize absorption efficiency for photosynthesis, *H. tepida* and *C. ovata* adjust their pigmentation in a different manner. We hypothesize that the biochemical pathways for these pigments may all be linked and as consequence, they all respond to light spectrum in similar manners, but more detailed analysis into the molecular pathways would be necessary to confirm this.

R. salina and *H. andersenii*, our two "red" cryptophytes, on the other hand, do not seem to follow this pattern. While chl-*a,* chl-*c2,* alloxanthin, and alpha-carotene for both species follow similar trends, the phycoerythrin concentrations vary from the rest of the pigments and are adjusted in a manner we would expect via the theory of chromatic acclimation. For both *R . salina* and *H. andersenii,* phycoerythrin concentrations were highest in green light, which the pigment is most efficient at absorbing, and concentrations were lower in red light compared to the wide-spectrum control. This suggests that there is variation in how cryptophytes with different phycobiliprotein types respond to variation in light spectrum. It seems that cryptophytes with a narrower phycobiliprotein absorption spectrum such as *R. salina* and *H. andersenii* may be more plastic in their pigment response to light color, while cryptophytes with a wider spectrum, such as *H. tepida* and *C. ovata,* while still shifting pigment concentrations, adjust all of the pigments in the same manner.

How do different cryptophyte phycobilin genes respond to light spectrum at the transcript level?

We examined the change in gene expression of the phycobiliprotein-related genes to determine if there were any shifts in expression between phycobiliprotein gene expression that may be correlated with cellular protein content. In a previous study (Schomaker, Richardson, & Dudycha, unpublished), we found that the cellular pigment concentration of phycoerythrin in *R. salina* does not match expression patterns for the phycoerythrin α and beta subunits across different light spectra. Not only that, but we found that the α and beta subunits are not expressed at similar levels, which is unexpected given that they are needed in a one-to-one ratio for the construction of the protein. When comparing *H. andersenii* to these results, we see a similar pattern. The phycoerythrin α subunit was expressed at a much higher level (~15 TPM) compared to the beta subunit (less than 1 TPM). For *R. salina*, the average expression for the α subunit gene was ~1,670 TPM, while the beta subunit gene exhibited an expression of ~78 TPM. It is interesting that, one, the α and beta subunits are not expressed at similar levels in given that they are needed at a 1:1 molar ratio in both species; and, two, that the disparity between the two subunits is similar for both species (the α subunit is expressed at a ~17-fold difference). Additionally, for both species, the expression patterns observed at the level of gene expression did not match that of what was observed in the cellular pigment concentrations across spectra, and the expression trends across spectra for the α and beta subunits were not similar.

This difference is observed in the opposite direction for our other phycoerythrin-containing cryptophyte, *C. ovata.* In *C. ovata,* the phycoerythrin beta subunit was expressed at a higher level than the α subunit, with the beta having an average of

~135,000 TPM and the α having an average of ~22,000 TPM, yielding a 6-fold difference in expression. Not only did we see the opposite trend in expression for *C. ovata* compared to *R. salina* and *H. andersenii,* but the expression trends across spectra were similar for the α and beta subunits in *C. ovata* while they were not for the other two phycoerythrin species, with both the α and beta subunits exhibiting extremely low expression in blue light compared to all other light environments. This is particularly interesting because we observed the highest concentration of phycoerythrin in blue light in *C. ovata.* Combined, these observations suggest that there may be post-transcriptional and post-translational regulation occurring in all these species that is leading to a difference in the observed expression and the cellular pigment concentrations (Rochaix 1992, 1996; Gruissem *et al.* 1993). Additionally, we saw multiple genes related to RNA processing and regulation that were significantly differentially expressed within multiple species, further suggesting that post-transcriptional and post-translational control may be related to differences observed in expression and pigment patterns.

These results suggest that the specific type of phycobilin that the cryptophytes maintain may be related to their expression and pigment patterns. *R. salina* and *H. andersenii* exhibit similar responses at both the cellular pigment and expression level, and both species are native in marine habitats and exhibit a striking, bright-pink coloration with similar Cr-PE maximum-absorption peaks in the green-region of the visible light spectrum, while *C. ovata* is a freshwater species that appears olive-green in color and has a maximum absorption peak that is further into the yellow-region of the spectrum. *H. tepida,* our Cr-PC containing cryptophyte, exhibited the highest α subunit expression in red light (~958 TPM), which is consistent with the cellular Cr-PC concentrations we observed. However, we did see high concentrations of both subunits in

green light whereas we saw the lowest Cr-PC concentrations overall in green light, so the subunit expression and the pigment concentrations do not correlate across all of the spectra, just like in the phycoerythrin-containing species. These absorption characteristics may be resulting in the similarities and differences we are observing among species. This is particularly interesting because *Hemiselmis* species and *Rhodomonas* species consistently fall into unique clades in the cryptophyte phylogenetic tree, yet they exhibit similar responses to changes in light spectrum at the physiological level (Greenwold *et al.* 2019). This, combined with the difference in *H. tepida's* response compared to *H. andersenii's* response to different light spectra suggests that pigment type and coloration is a stronger driver in the organisms' plastic response than phylogenetic relationship.

How do photosynthesis-related genes respond to light spectrum at the transcript level across species with different phycobilin types?

The responsiveness of photosynthesis-related genes to light spectrum seems to vary with species. In *R. salina*, we saw changes in expression of phycoerythrin subunits and chlorophyll binding proteins across spectra, along with various photosystem I and II encoding proteins. Overall, we saw few significant differences in expression of pigment-related genes across the different light spectrum, which is interesting given that we saw significant differences in pigment concentration in *R. salina* across the various spectral environments. We believe that this discrepancy between gene expression and pigment composition may be a result of post-transcriptional and post-translational modification. In *H. andersenii*, we found one ATP-synthase subunit to be upregulated in green light no matter what other color of light it was compared to, and we also found a gene related to photosystem I protein synthesis was upregulated in green light compared to red light. In

H. tepida, the only photosynthesis-related gene that was significantly differentially expressed in any of the comparisons was the same photosystem I protein that was upregulated in *H. andersenii* in green light compared to red light, except in *H. tepida*, it was upregulated in blue light compared to red. Both green and blue light are spectra that have higher energy levels than red light does, and this might suggest that expression of some photosynthesis-related genes are regulated by higher energy levels compared to others, which could be a high-energy light acclimation response. It's possible that after exposure to a certain "threshold" of high-energy light that certain photosynthesis-related gene expression is altered. In the cyanobacterium, *Synechocystis* sp. PCC 6803, there is a major shift in photosynthesis-related gene expression when cultures are transferred to high-light conditions (note that "high-light conditions" for different algal groups will vary). *Synechosystis* sp. exhibits downregulation of genes related to photosystem function and the phycobilisomes to avoid absorbing excess light energy, while there is upregulation of genes related to carbon dioxide fixation and cellular metabolism to increase energy consumption (reviewed in Muramatsu and Hihara 2012). This has also been shown in terrestrial plants, where exposure to high-light leads to a shift from photosynthesis to other metabolic processes, which is directly related to regulating light energy to control the production of reactive oxygen species which can be harmful to the organism (Tikkanen *et al.* 2014).

While the other three species exhibited few significantly differentially expressed photosynthesis-related genes across light environments, we found that *C. ovata* showed significantly differential expression for 26 of the 99 photosynthesis-related genes in every comparison that we performed. All of these genes were regulated in blue light compared to the other light environments in the same direction; 14 of the 26 were downregulated in

blue light no matter what other spectrum they were compared to, and 12 were always upregulated in blue light. Those that were downregulated in blue light included both phycoerythrin subunit genes, the RuBisCo large subunit gene (rbcL), genes related to photosystem I protein components, and one gene coding for a cytochrome b_6-f complex subunit. It's particularly interesting that both phycoerythrin subunit genes were consistently downregulated in blue light in *C. ovata* given that we saw the highest concentration of Cr-PE 566 in blue light for this species. This is further evidence of post-transcriptional and post-translational modification occurring for the major light-harvesting pigments in cryptophytes.

Of the 12 that were consistently upregulated in blue light in *C. ovata*, 4 were genes coding for cytochrome b_6-f complex proteins, 3 were genes coding for photosystem II protein complexes, and the others included the RuBisCo small subunit gene (rbcS), a high-light inducible protein, a sec translocase gene, and a gene coding for magnesium chelatase. Combined with the downregulated genes, these observations suggest that there may be a high-light energy acclimation response occurring in *C. ovata* that is resulting in a shift in energy allocation between the photosystems. In blue light, genes related to photosystem I were downregulated, while those related to photosystem II were upregulated, along with the upregulation in genes coding for cytochrome b6-f proteins. The cytochrome b6-f complex may be related to redox responses during photosynthesis. It has been suggested to be a possible candidate as a "redox sensing site" for genes encoding photosystem I and phycobilisomes subunits in cyanobacteria, where these genes are repressed when the redox state of electron transfer components downstream of the plastoquinones (electron transporters involved in the electron transport chain in oxygenic photosynthesis) is in a reduced state (reviewed in Muramatsu and Hiharu 2012). This is

consistent with our findings, where we see a shift in expression of genes related to each photosystem and the cytochrome b6-f complex in blue light in *C. ovata.* This is particularly interesting because freshwater ecosystems like those that *C. ovata* is generally found in tend to exhibit spectra that are red-dominated, while marine systems where *R. salina, H. andersenii,* and *H. tepida* tend to be blue- or green-dominated (Kirk 1994; Schwarz & Markager 1999). It's possible that this difference in habitat history plays a role in how different cryptophytes respond to light spectrum. The species which are naturally found in waters that are dominated by higher-energy light colors may be less responsive to exposure to blue- and green-dominated spectra because they have evolved to exist within those light habitats, while *C. ovata* has not, and thus is exhibiting a more apparent high-energy light acclimation response to protect itself from harmful redox reactions and reactive oxygen species. Additionally, freshwater ecosystems where *C. ovata* is often found tend to be more transient and ephemeral compared to open-ocean waters, and as a result the organisms that exist within these ecosystems need to be able to adjust to more frequent and drastic changes than those in marine systems (Cuthbert *et al.* 2018). As a result, the gene expression patterns observed in freshwater species may be more plastic than those in marine species.

What other functions respond to light spectrum at the transcript level?

When examining the gene expression of the complete gene set, we saw many genes that were sensitive to light spectrum that had no obvious function in the photosynthesis pathway, suggesting that light spectrum may regulate a wide range of molecular and cellular pathways. For both *R. salina* and *H. andersenii,* we saw the greatest number of significant upregulation in higher-energy light compared to lower

energy light (blue in the red vs. blue comparison; green in the red vs. green comparison; and blue in the green vs. blue comparison). This further suggests that the energetic characteristics of different light spectra seem to influence gene expression. However, we saw this opposite result in *H. tepida*, where we saw a great number of upregulated genes in red light compared to blue light in the red vs. blue comparison. This difference could be attributed to the differences in absorption characteristics between the various cryptophytes, where more genes may be responsive to red light in *H. tepida* because that is the light that its major light harvesting pigment absorbs best, while both *R. salina* and *H. andersenii* absorb higher-energy lights more efficiently. It is unknown whether our *C .ovata*, would also follow a similar trend as *H. tepida* or the other phycoerythrin-containing cryptophytes given that we did not have enough power to detect significant differential expression in any of the comparisons for the complete gene set in *C. ovata* given it's assembly size.

Additionally, our annotation pipeline uncovered multiple genes in all four species that have functions related to sexual reproduction and cellular differentiation in other algal species. We found 56, 28, 25, and 94 genes with annotations matching RWP-RK domains in *R. salina, H. andersenii, H. tepida,* and *C. ovata,* respectively. In other algal species and terrestrial plants, RWP-RK protein domains are related to nitrogen responses and reproductive development (Lin and Goodenough 2007; Chardin *et al.* 2014; Liu *et al.* 2021). In *Chlamydomonas reinhardtii*, the mating type (either plus, "female, or minus, "male") is controlled by a complex locus that has a sequence similarity to terrestrial plant RWP-RK proteins and are related to nitrogen-sensitive developmental processes (Lin and Goodenough 2007). These RWP-RK transcription factors are a part of what is known as the *MT* (mating type) and *MID* (minus dominance) loci in other algae and are necessary

to convert *plus*-type gametes to *minus*-type (Lin and Goodenough 2007; Hamaji *et al.* 2018). While we did not have any annotations for *MT* or *MID* loci identified in our assemblies, the identification of the RWP-RK genes has been linked to sexual reproduction in many groups of photosynthetic organisms within the green-lineage, including terrestrial plants such as *Arabidopsis* and *Arachis* spp. (Koi *et al.* 2016; Liu *et al.* 2020), and algal groups such as *Chlamydomonas, Ulva, Volvox (*Lin and Goodenough 2007; Ferris *et al.* 2010; Chardin *et al.* 2014; Liu *et al.* 2020*).* As such, the identification of these genes suggests the potential for sexual reproduction and cellular differentiation in cryptophytes. Sexual reproduction in cryptophytes has been suggested, but the mechanisms by which is occurs and the genetic architecture underlying the potential function is unknown (Hoef-Emden & Archibald 2016). It is unclear if the RWP-RK genes that were identified in our four species exhibit any sequence similarities to each other or how conserved these genes are across the cryptophyte lineage, but these genes are strong candidates for studying the potential for sexual reproduction in cryptophytes.

Conclusion

Cryptophytes have evolved a great diversity of coloration and pigmentation, and they are also found in a wide variety of natural aquatic habitats which vary in spectral characteristics. Here, we have examined how this diversity of pigments is related to the plasticity in response to changes in available light spectrum. Overall, it appears that the type of phycobiliprotein and the coloration that the cryptophyte species exhibit may be related to how they respond to changes in light habitat. *R. salina* and *H. andersenii* exhibited similar responses when examining the phycobiliprotein subunit gene expression, while *H. andersenii* and *C. ovata* exhibited the opposite response; we

attribute this to the absorption characteristics of the various phycobiliproteins that each cryptophyte has. *R. salina* and *H. andersenii* both have a narrow absorption spectrum with a maximum absorption peak from 545-555, while *C. ovata* and *H. tepida* have a wider absorption range that is shifted towards the red end of the spectrum. Even so, all four species showed differences between expression pigment-related genes and pigment composition, suggesting post-transcriptional and post-translation mechanisms at play across all four species.

Additionally, it appears that natural habitat history may play a role in how cryptophytes respond to differences in light spectrum. The photosynthesis-related genes of *R. salina, H. andersenii,* and *H. tepida,* all marine species, were less responsive than *C. ovata* was when exposed to higher-energy light. Because *C. ovata*'s natural habitat tends to be red-dominated, it exhibited a more plastic change in gene expression in blue light likely related to photoprotective and high-energy light acclimation strategies that the three marine species don't exhibit because they have evolved to survive in these habitats.

Last, we found many genes that were functionally non-photosynthetic which were responsive to light spectrum across all species, and we also identified multiple genes that are related to sexual reproduction in other photosynthetic organisms within the assemblies of all four species. Combined, these results suggest that a large part of the cryptophytes' response to light color is unrelated to photosynthesis, and that non-photosynthesis genes play a role in their acclimation to change in light habitat. Additionally, these results suggest that cryptophytes maintain the genetic architecture to support sexual reproduction, but more information is needed to understand how these genes may be directly involved and to determine what leads to shifts in reproductive modes in cryptophytes.

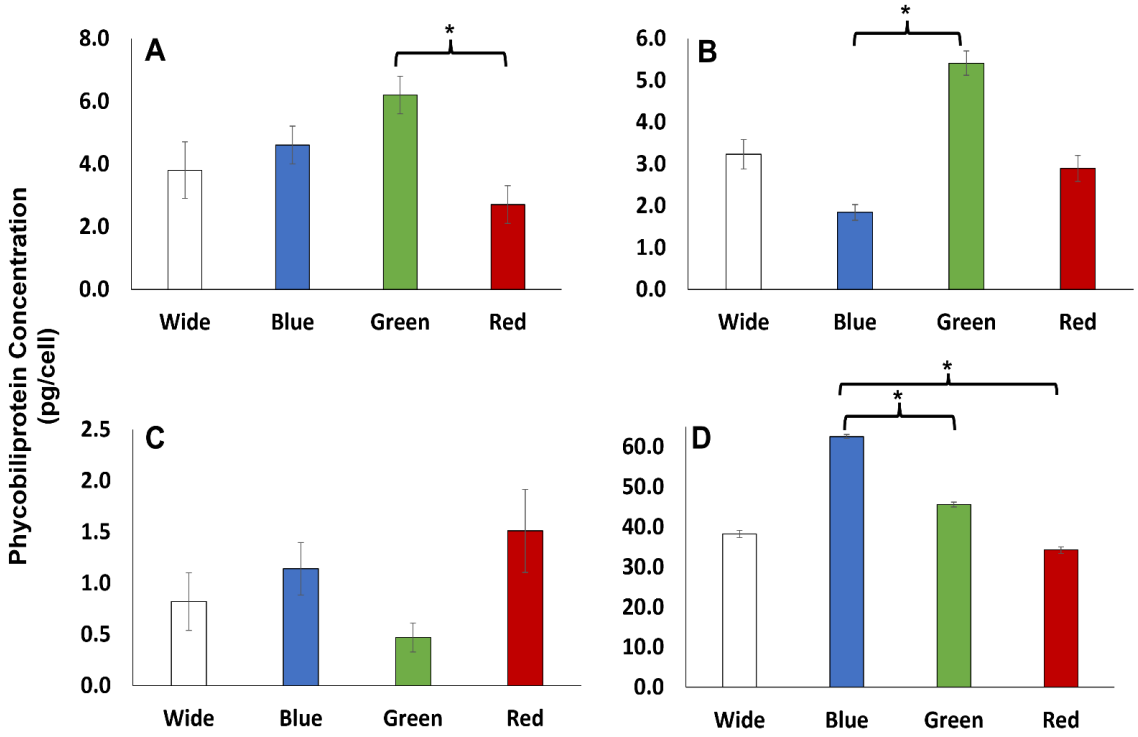

Figure 2.1: Phycobiliprotein concentrations for all four species in wide-spectrum, blue, green, and red light. **A:** *R. salina* phycoerythrin (Cr-PE 545) concentrations (pg/cell). **B:** *H. andersenii* phycoerythrin (Cr-PE 555) concentration (pg/cell). **C:** *H. tepida* phycocyanin (Cr-PC 615) concentrations (pg/cell). **D.** *C. ovata* phycoerythrin (Cr-PE 566) concentrations (pg/cell). Asterisks indicate significant differences (p-value < 0.05). Error bars designate standard error. Note that the y-axes are on different scales.

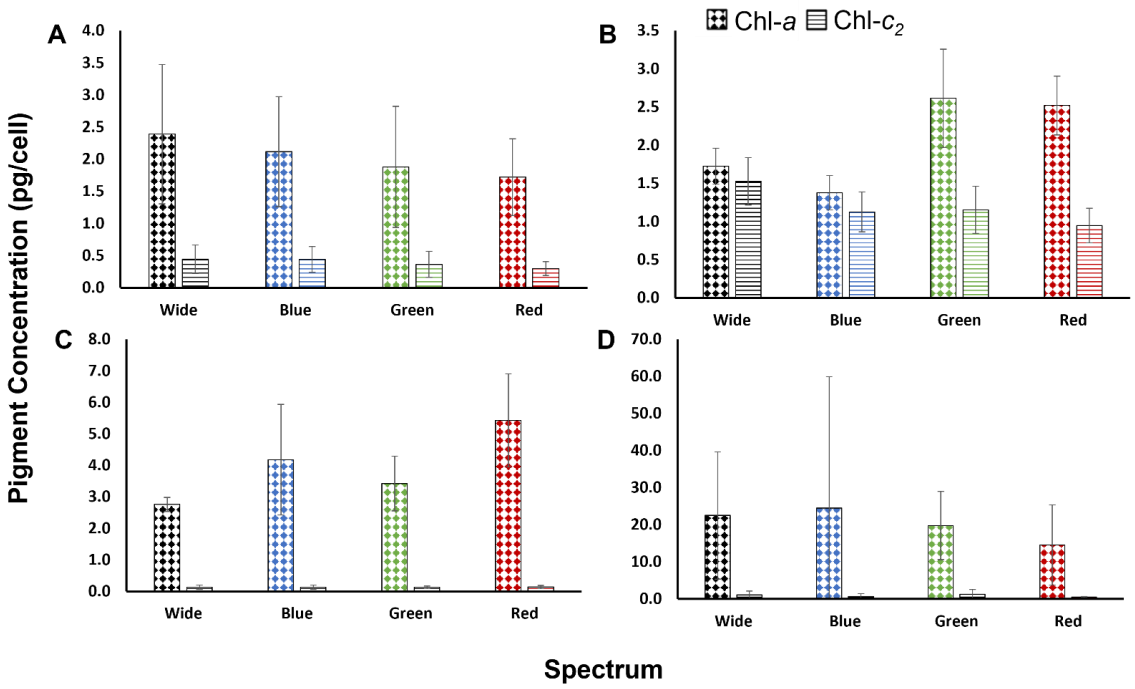

Figure 2.2: Chlorophyll-*a* and chlorophyll-c_2 concentrations (pg/cell) in wide-spectrum, blue, green, and red light for: **A:** *H. andersenii;* **B:** *R. salina;* **C:** *H. tepida;* and **D:** *C. ovata.* Error bars are standard error. Note the differences in scale of the y-axes. The only significant differences were observed between chl-*a* concentrations of *R. salina* cultures grown in red and blue light.

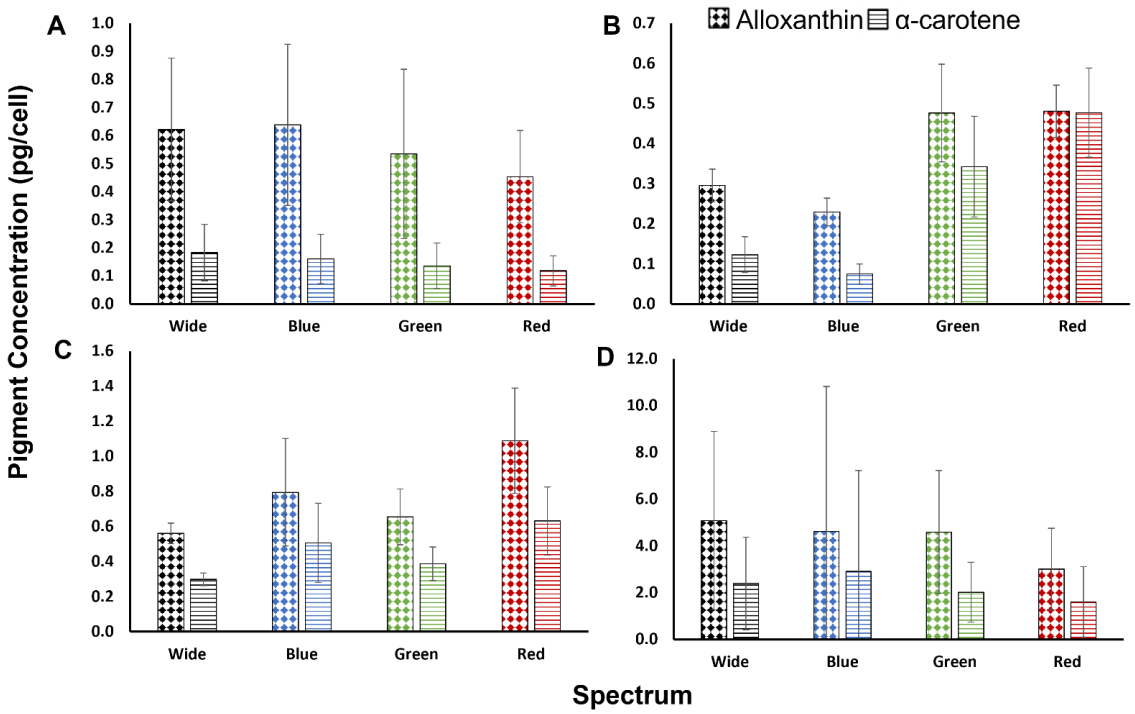

Figure 2.3: Photoprotective pigment concentrations (pg/cell) in wide-spectrum, blue, green, and red light for: **A:** *H. andersenii;* **B:** *R. salina;* **C:** *H. tepida;* and **D:** *C. ovata.* Error bars are standard error. Note the differences in scale of the y-axes. Significant differences were observed in both alloxanthin and α-carotene concentrations of *R. salina* cultures grown in red and blue light.

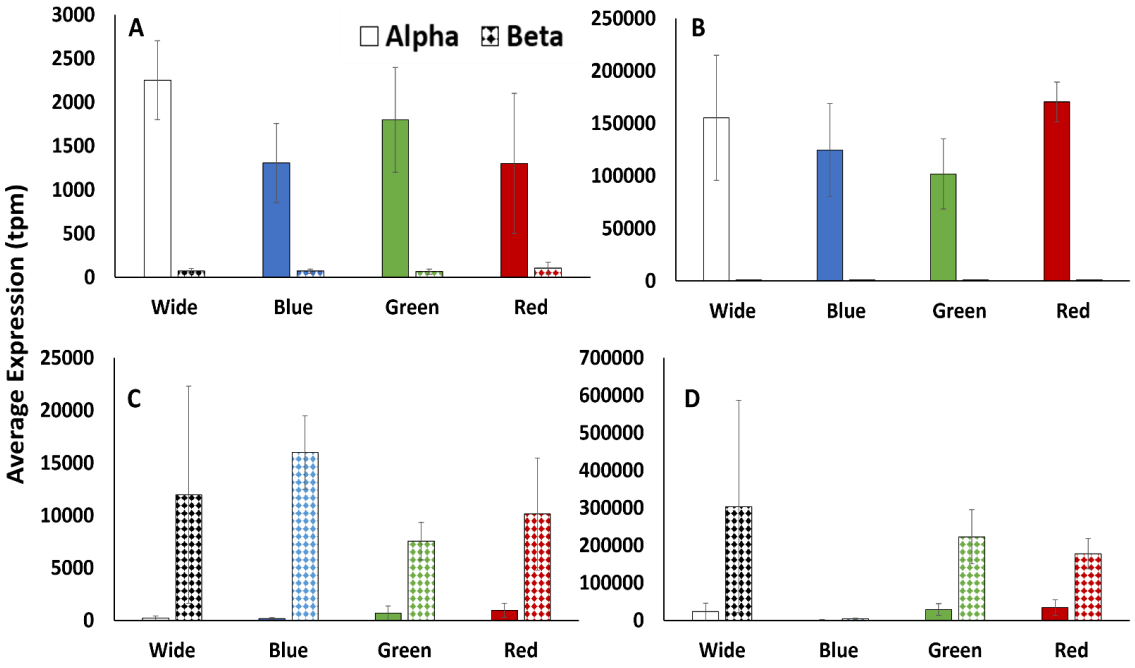

Figure 2.4: Phycobiliprotein alpha and beta subunit expression comparisons for each species across each light environment. Expression is in transcripts per million (tpm). **A:** Expression of cryptophyte phycoerythrin (Cr-PE 545) subunit genes in *R. salina*. **B:** Expression of cryptophyte phycoerythrin (Cr-PE 555) subunit genes in *H. andersenii.* **C:** Expression of cryptophyte phycocyanin (Cr-PC 615) subunit genes in *H. tepida.* **D:** Expression of cryptophyte phycoerythrin (Cr-PE 566) subunit genes in *C. ovata.* Error bars are standard error. Note that the y-axes are at different scales.

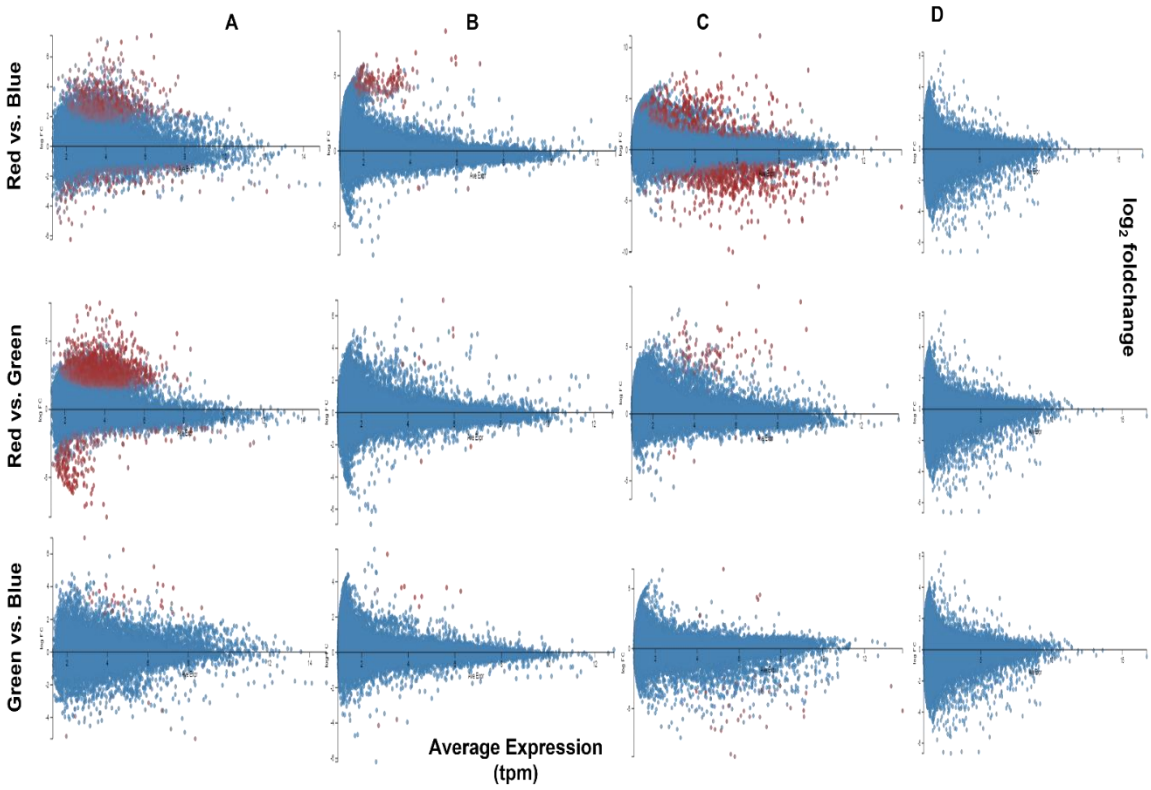

Figure 2.5: MA plots of gene expression for the complete gene set for each species for the following comparisons: red vs. blue, red vs. green, and green vs. blue. For the red vs. blue plots, blue expression is plotted relative to red expression; for the red vs. green plots, green expression is plotted relative to red expression; for the green vs. blue plots; blue expression is plotted relative to green expression. The y-axes are all in $\log_2$ foldchange and the x-axes are the average expression in transcripts per million (tpm) (note the different scales for both axes). **A:** *R. salina.* **B:** *H. andersenii.* **C:** *H. tepida.* **D:** *C. ovata.* Significantly differentially expressed genes (FDR p-value < 0.05 and $\log_2$ foldchange ≥ 2) are designated by red dots.

Table 2.1: Intrinsic population growth rates for *R. salina, H. andersenii, H. tepida,* and *C. ovata* grown in wide-spectrum, blue, green, and red light.

Species	**Wide-spectrum growth rate (per day)**	**Blue growth rate (per day)**	**Green growth rate (per day)**	**Red growth rate (per day)**
Rhodomonas salina	0.40	0.52	0.43	0.43
Hemiselmis andersenii	0.43	0.59	0.51	0.45
Hemiselmis tepida	0.50	0.49	0.36	0.37
Cryptomonas ovata	0.20	0.25	0.17	0.26

Table 2.2: Transcriptome assembly statistics for each of the species used in this study.

Species	**Number of contigs**	**Average contig length**	**N50**	**GC %**	**% of genes annotated**
R. salina	24,167	1,560bp	2,431bp	58.8%	54.5%
H. andersenii	39,221	1,008bp	1,525bp	59.9%	42.2%
H. tepida	20,553	990bp	1,456bp	62.8%	43.9%
C. ovata	155,790	820bp	1,154bp	59.8%	24.6%

Table 2.3: BUSCO results breakdown of the completed cryptophyte assemblies against the eukaryote database. C = Complete; S = Complete and single-copy; D = Complete and duplicated; F = Fragmented; M = Missing.

Species	**Complete BUSCOs (C)**	**Complete and single-copy BUSCOs (S)**	**Complete d and duplicated BUSCOs (D)**	**Fragmented BUSCOs (F)**	**Missing BUSCOs (M)**	**Total BUSCO groups searched**
R. salina	191	158	33	21	91	303
H. andersenii	169	120	49	31	55	255
H. tepida	103	94	9	45	107	255
C. ovata	219	119	100	21	15	255

Table 2.4: BUSCO results breakdown of the completed cryptophyte assemblies against the protist database. C = Complete; S = Complete and single-copy; D = Complete and duplicated; F = Fragmented; M = Missing.

Species	**Complete BUSCOs (C)**	**Complete and single-copy BUSCOs (S)**	**Completed and duplicated BUSCOs (D)**	**Fragmented BUSCOs (F)**	**Missing BUSCOs (M)**	**Total BUSCO groups searched**
R. salina	100	86	14	0	115	215
H. anderseni i	131	93	38	3	81	215
H. tepida	90	78	12	5	120	215
C. ovata	173	76	97	3	39	215

CHAPTER 3: TRADE-OFFS IN GROWTH RATE, BIOVOLUME, AND PIGMENT CONCENTRATION IN RESPONSE TO LIGHT AND CARBON AVAILABILITY IN CRYPTOPHYTES

Abstract

Overall, we investigated the potential plasticity of trophic strategies in cryptophytes by analyzing how growth rates, biovolumes, and phycobiliprotein concentrations responded to carbon and light availability. Given cryptophyte evolutionary history, we expected that cryptophytes would be able to survive in the light and in darkness with added glucose (selecting for osmotrophy) or bacteria (selecting for phagotrophy) as carbon sources, but we expected that responses would vary with clade and with cell size. We expected that larger cells would be more likely to survive in the dark with added bacteria, while smaller cells would be strict autotrophs or would be able to survive in the dark with added glucose. We grew large and small representatives of cryptophytes across each clade (*Chroomonas, Cryptomonas, Guillardia, Hemiselmis, Rhodomonas,* and *Goniomonas*) in light deplete and light replete conditions with the addition of bacteria or glucose as a carbon source. We found that growth, biovolume, and pigment concentration varied greatly with species and treatment. Both *Cryptomonas* species, *Rhodomonas abbreviata,* and *Hanusia phi* exhibited positive growth rates in the dark with added glucose but did not survive with added bacteria. The other species did not survive without light but did exhibit shifts in growth rate with the addition of glucose or bacteria. Interestingly, the species that were not able to survive in the dark exhibited

increased phycobiliprotein concentrations in the dark compared to cultures grown in the light, suggesting a low-light acclimation survival response. Cultures that were able to survive in the dark exhibited lower pigment concentrations in the dark compared to the light, suggesting potential shifts in trophic strategies from autotrophy to heterotrophy. Biovolumes were consistently larger for cultures grown with glucose compared to cultures with no added carbon or with added bacteria, regardless of light availability, suggesting that glucose presence leads to a cellular shift in cell size. Combined, these results show that the response to light and carbon availability in cryptophytes is plastic and diverse, and that the evolution of diversity in algal trophic strategies is not straightforward.

Introduction

Traditional models of aquatic microbial communities and nutrient cycling are structured with a autotroph-heterotroph, or phytoplankton-zooplankton, dichotomy which assume mixotrophs, organisms which can perform both autotrophy and heterotrophy, to be less prevalent in aquatic ecosystems than autotrophs or heterotrophs (Flynn et al. 2013; Ward & Follows 2016). However, recent studies suggest (Flynn et al. 2013; Caron 2016; Stoecker & Lavrentyev 2018) that mixotrophs are more abundant than previously thought and that community dynamics may be misinterpreted by traditional models. As a result, identifying mixotrophic organisms and understanding how mixotrophy functions is now an area of great scientific challenge (Gonzalez-Olalla et al. 2019; Mansour & Anestis 2021)

Strict autotrophs and strict heterotrophs can be considered trophic specialists, whereas mixotrophs are trophic generalists or opportunists, and there are tradeoffs

associated with each trophic strategy. Autotrophs incur costs for maintaining photosynthetic machinery (Raven 1984, 1997; Mansour & Anestis 2021), but tend to be smaller in size and have more inorganic nutrient transporters than heterotrophs and mixotrophs, increasing their overall nutrient affinity (Menge and Weitz 2009). Thus, strict autotrophs tend to outcompete heterotrophs and mixotrophs when light and nutrients are replete (Niel *et al.* 1993; Jansson *et al.* 1996). Heterotrophs incur costs related to maintaining mechanisms to internalize food particles and tend to dominate when inorganic nutrients are limiting but prey is abundant. For phagotrophic heterotrophy, costs are associated with prey detection, capture, and digestion, and for osmotrophic heterotrophy, these costs are related to maintaining membrane transporters to take in dissolved organic carbon (Andersen *et al.* 2015). The tradeoffs for mixotrophy are not as well understood because mixotrophic function is flexible, e.g., some mixotrophs are photosynthetic and use heterotrophy to supplement their growth (these mixotrophs are "more photosynthetic"); others are primarily heterotrophic but use phototrophy when prey is limiting (these are "more heterotrophic); and in some cases, organisms are considered obligate mixotrophs (they must perform both autotrophy and heterotrophy in order to survive) (Raven 1997; Mitra *et al*. 2016). However, mixotrophs have been shown to outcompete trophic specialists in oligotrophic environments because they can meet metabolic demands through a mixture of photosynthesis and external carbon supplementation (Stoecker *et al.* 2017). This flexibility in mixotrophic function has major implications for aquatic community interactions. Mixotrophs that are "more photosynthetic" increase the overall primary production of a community (which can support greater biodiversity and energy transfer to higher trophic levels), while mixotrophs that are "more heterotrophic" contribute to prey consumption but cause less

energy loss at higher trophic levels compared to strict heterotrophs because they are able to offset respiratory losses via photosynthesis (Ward & Follows 2016). These consequences of mixotrophy have led to a conceptual paradigm shift and an increased need for understanding the diversity of mixotrophic function and the conditions that select for it (Flynn et al. 2019).

Cryptophytes are single-celled algae which act as important primary producers and prey species in both marine and freshwater environments (Klaveness 1988). Cryptophytes evolved via secondary endosymbiosis between a hypothesized phagotrophic ancestor and a red algal cell, and as a result, they maintain a host of uniquely complex genomes, including the nucleus and mitochondria which originated from the heterotrophic ancestor and a nucleomorph and chloroplast which came from the red algal endosymbiont (Kim et al. 2017). Most cryptophytes are characterized as strict autotrophs, but some may also be strict heterotrophs. The *Goniomonas* clade is known to be bacterivorous (i.e., it consumes bacteria via phagotrophy), though it did not evolve via secondary endosymbiosis like the other cryptophyte clades. *Cryptomonas paramecium* was once mixotrophic but has lost the ability to photosynthesize even though it maintains a leucoplast and some genes related to photosynthetic function (Sepsenwol 1973; Donaher et al. 2009). Other *Cryptomonas* species have been suggested to be mixotrophic (Lewitus et al. 1991; Marshall & Laybourn-Parry 2002), and some species within the *Rhodomonas* and *Teleaulax* clades have been shown to take up dissolved organic carbon under conditions of light limitation (Lewitus 1991; Yoo *et al.* 2017).

Cryptophytes exhibit a range of pigmentations as well as cell volumes, both which can affect their growth and metabolic processes. Cell volume has been suggested to be related to trophic function (Ward *et al.* 2012; Barton *et al.* 2013; Ward *et al.* 2017),

where smaller cells, with a larger surface-area-to-volume ratio, are best at absorbing dissolved organic compounds via osmotrophy (Litchman *et al.* 2007), while larger cells have a greater capacity for phagotrophic heterotrophy or mixotrophy (Hansen *et al.* 1997). Smaller volumes tend to favor photosynthetic function as well because smaller cells can absorb other nutrients needed for growth and photosynthetic function and size influences light absorption efficiency (Finkel *et al.* 2010). Given this variation in size and potential trophic function in the cryptophyte lineage, our goal was to investigate the diversity and plasticity of trophic function in the cryptophyte lineage. We grew a "large" and "small" (relative to each other) species representative from each cryptophyte clade in light and dark treatments with different carbon sources (bacteria to test for phagotrophy; dissolved glucose to test for osmotrophy) in order to determine 1) how diverse trophic strategies are across the cryptophyte phylogeny and 2) how this function varies with size.

Methods

Species of Interest. We used two species from each cryptophyte clade in this study: *Chroomonas* (*Chroomonas placoidea* and *Chroomonas mesostigmatica*); *Cryptomonas* (*Cryptomonas ovata* and *Cryptomonas ozolini*); *Guillardia* (*Guillardia theta* and *Hanusia phi*); *Hemiselmis* (*Hemiselmis rufescens* and *Hemiselmis andersenii*); *Rhodomonas* (*Rhodomonas salina* and *Rhodomonas abbreviata*); and *Goniomonas* (*Goniomonas avonlea* and *Goniomonas truncata).* Culture collection, strain number, and growth medium for each species can be found in Table 3.1. Species were chosen based on preliminary size measurements (length and width) and growth temperature ranges so that all species could be grown in the same temperature and chamber. Preliminary size measurements are shown on the condensed cryptophyte phylogeny in Figure 3.1.

Growth and Treatment Conditions. We first acclimated stock cultures of each species to a full-spectrum light environment (LμmiBar Pro LED Light strip, LU50001; LμmiGrow, Emeryville, CA, USA) on a 12 hr light:12 hr dark in a Conviron walk-in incubator (Controlled Environments, Inc., Manitoba, Canada) kept at 20°C. To obtain and maintain as minimal bacterial contamination as possible, we first filter-sterilized and microwaved all media for 10 minutes and then it allowed to cool prior to inoculation as detailed in Keller *et al.* (1988). Cultures were left to acclimate for 10 generations (Parkhill *et al.* 2001). Each species was grown in 150mL of its optimal culture medium in 250 mL flasks. Each culture was swirled by hand daily to prevent settling and help aeration. After acclimation, we used a Z2 Beckman Coulter Particle Counter and Size Analyzer to measure the density (in cells/mL) of each stock culture. We used these density measurements to inoculate 4 biological replicates of each species so that each replicate had an approximate starting cell density of 10,000 cells/mL.

We had six treatments in total: light only; light with added glucose; light with added bacteria; darkness only; dark with added glucose; and dark with added bacteria. All treatments with light had a photoperiod of 12 hr of full-spectrum light:12 hr darkness with a light intensity of of 30 μmol m^2 s^{-1}. Cultures grown in the dark treatments were given 0 hr light:24 hr darkness by wrapping bottles with black electrical tape and covering them with black felt. To test for osmotrophy, organic carbon was added as 0.3 g glucose (D-Glucose (Dextrose) Anhydrous, VWR) to 150 mL of media for a final concentration of 0.01 M (Kong *et al*. 2013). Phagotrophy was assessed by inoculating 5.5 x 10^6 cells/mL of bacteria isolated from the original non-axenic cultures into 150 mL of sterile media. Briefly, we isolated and maintained these bacterial cultures by taking 1mL of a non-axenic stock culture of each species and inoculated it into 10 mL of AC broth

(BD Difco) to enrich and select for bacterial growth. This was done for each individual species that was used in this study, resulting in 12 separate bacterial cultures. We let each bacterial culture grow for one week, and then took 1 mL of each bacterial culture and transferred it into 10 mL of new, sterile AC broth, creating 12 new pure bacterial cultures. These bacterial cultures that remained were used to feed cryptophytes when testing for phagotrophy. We chose to create bacterial cultures from the non-axenic cryptophyte cultures to use as the phagotrophy carbon source to ensure that we were 1) using prey species that co-exist with the given species and 2) not introducing bacterial species into each culture they may potentially be harmful to the cryptophytes themselves (Yoo *et al.* 2017). Initial bacterial densities were determined by measuring the optical density of the bacterial stock cultures.

Growth Experiments. We grew each replicate culture for each species until they reached mid-exponential phase, which was determined by plotting the cell density of the cultures on an exponential growth curve throughout the experiment and varied with species. We took population density measurements of each replicate for each species every other day using a Z2 Beckman Coulter Particle Counter and Size Analyzer. All cell counts used for cell density measurements were taken at a 100-fold dilution.

Cryptophyte Phycoerythrin (Cr-PE) Analysis. We took 15 mL aliquots of each replicate culture and centrifuged them at 2,054 g in a Sorvall RC-4B centrifuge for 10 minutes, and then poured off the supernatant and resuspended the pellet in 0.1 M phosphate buffer (pH = 6). Each sample was mixed thoroughly to ensure that the entire cell pellet was resuspended, and then was frozen at -20°C for a minimum of 24 hrs. After freezing, we thawed the samples at 5°C for 24 hrs. Two mL of each thawed sample was then centrifuged at 11,000 g in a Beckman Coulter 19 microfuge for 5 minutes to remove

any remaining cell debris from the extracted pigment. We measured absorbance of the remaining supernatant against a phosphate buffer blank in a 1 cm quartz cuvette using a Shimadzu UV-VIS 2,450 dual-beam spectrophotometer from 400 to 750 nm in 1 nm intervals. We scatter-corrected the data by subtracting the absorbance at 750 nm from the maximum absorption peak (Lawrenz et al. 2011), and then calculated cryptophyte phycobiliprotein concentrations using the following equation:

$$C = \frac{A}{\varepsilon * d}\ x\ MW\ x\ \frac{Vbuffer}{Vsample} x\ \frac{10^{12}}{N}$$

Where A = absorbance of sample, ε = the extinction coefficient for cryptophyte phycobiliprotein (Cr-PE = 5.67 x 10^5 L ·mol^{-1} · cm^{-1}; Cr-PC = 5.70 x 10^5 L ·mol^{-1} · cm^{-1}; MacColl et al. 1976), *d* = path length of the cuvette in cm, MW = molecular weight of cryptophyte phycoerythrin (45,000 Da; MacColl *et al.* 1973, 1976), V_{buffer} = volume of buffer, V_{sample} = volume of sample, and N = concentration of cells (cells/L). The 10^{12} is the conversion factor to convert the results into pg/cell. We did not perform this calculation for the *Goniomonas* clade because both species are heterotrophic and do not produce phycobiliprotein.

We also calculated pigment concentrations per biovolume along with phycobiliprotein per cell. For this conversion, we divided the average cryptophyte-phycobiliprotein concentration in pg/cell by the cell volume in μm^3 to get $pg/\mu m^3$.

Cell Volumes. We took pictures of 200 cells from each treatment at 40x magnification using a Luminera Infinity One camera connected to a Nikon Eclipse TS100 inverted microscope using Teledyne Luminera Infinity Analyze 7 software. To obtain 200 cells for each treatment, we took pictures of 50 cells per each replicate. We used ImageJ to measure length and width of each cell using a picture of a micrometer taken at

either 20X or 40X to calibrate, depending on the species' size. We calculated volumes assuming each cell was a prolate spheroid with the following equation (Hillebrand et al. 1999):

$$V = pi/6 * h * d^2$$

Where h = the length of the cell in µm and d = the diameter (width) of the cell in µm.

Statistical Analysis. We ran a two-way Analysis of Variance (ANOVA) to test for significant differences in pigment concentrations, growth rates, and cell volumes across all four treatments. Comparisons between light only vs. light with bacteria or light only vs. light with glucose allowed us to determine the effect of the added food source on growth and pigment concentration when light was replete. Comparisons between darkness only vs. dark with bacteria or darkness only vs. dark with glucose allowed us to determine the effect of the added food sources on growth and pigmentation when light was limiting. Comparisons between light with glucose vs. light with bacteria as well as dark with glucose vs. dark with bacteria allowed us to determine the effects of the two different food sources regardless of light presence. Comparisons between species allowed us to determine if there were any significant differences between how species with different cell volumes respond to food and light availability.

Results

Growth Experiments.

Growth rates varied with species and with treatment. Growth rates for each species grown in each treatment are shown in Table 3.1. Significant differences for each clade across treatments are summarized in Tables 3.2A-F. For the *Chroomonas* clade,

adding glucose to *C. placoidea* cultures in both light and dark treatments exhibited a significant effect on growth rate (*p*-value < 0.05), and we saw significant differences between *C. placoidea's* growth rate when in grown in light or in dark with the two different carbon sources (Figure 3.2). For *C. mesostigmatica,* we saw a significant difference in growth rate when the cultures were grown in light with the two different carbon sources.

For the *Cryptomonas* clade, we observed a significant difference in how *C. ovata* and *C. ozolini* respond when grown in darkness with bacteria as a carbon source (*p*-value = 0.001). We also saw significant differences between *C. ovata* cultures grown in darkness with and without added bacteria (*p*-value = 4.91x10-6) and between cultures grown in darkness with glucose and darkness with bacteria (*p*-value = 4.45x10-9) (Figure 3.3).

G. theta did not survive long enough to obtain a growth measurement when grown in darkness with added glucose (Figure 3.4), but *H. phi* did. *H. phi* exhibited a stark contrast in growth rates of cultures grown in darkness without any additional carbon (average growth rate = -0.51 ± 0.04) compared to cultures grown in darkness with added bacteria (average growth rate = -0.17 ± 0.05) (*p*-value = 4.96x10-6) or darkness with added glucose (average growth rate = 0.26 ± 0.11) (*p*-value = 6.99x10-14). Cultures grown in light with added glucose (average growth rate = 0.23 ± 0.10) were comparable to those grown in darkness with added glucose. *H. phi* cultures grown in darkness with glucose compared to cultures grown in darkness with bacteria also were significant different (*p*-value = 5.69x10-8).

Neither *H. andersenii* nor *H. rufescens* survived long enough to obtain a growth measurement when grown in the darkness with added bacteria, but both survived long

enough for growth measurements when grown in darkness without any added carbon (*H. andersenii* average growth rate = -0.05 ± 0.04; *H. rufescens* average growth rate = -0.09 ± 0.13) and darkness with glucose (*H. andersenii* average growth rate = -0.13 ± 0.01; *H. rufescens* average growth rate = -0.17 ± 0.04). There were no significant differences between *H. andersenii* or *H. rufescens* growth in the light without added carbon and light with added bacteria, but both species saw a decrease in growth rate when glucose was added to cultures grown in the light (Figure 3.5). Both species also saw a significant difference between cultures grown in light with bacteria and cultures grown in light with glucose (*H. andersenii p*-value = 2.84x10-11; *H. rufescens p*-value = 5.61x10-14). Interestingly, even though cultures in the dark with bacteria did not survive for either species, the addition of bacteria in the light did not incur any significant effects on growth. Additionally, the addition of glucose in light for both *H. rufescens* and *H. andersenii* resulted in decreased growth compared to the other two light treatments just as in darkness.

There were clear shifts in growth rates of species in the *Rhodomonas* clade (Figure 3.6), but only cultures of *R. abbreviata* grown in dark without added carbon compared to cultures in the dark with added bacteria were significantly different (*p*-value = 0.000752). Our heterotrophic clade, *Goniomonas,* only exhibited significant differences in growth for *G. avonlea* when grown in light without added carbon and light with added bacteria (*p*-value = 0.01644) (Figure 3.7). For the light treatments, growth was slowest for both species when no added carbon was available. The growth rates of each species in the dark varied with species. We were not able to obtain growth measurements for *G. truncata* grown in light with added glucose because of persistent fungal contamination that occurred in all our biological replicates before growth experiments were complete.

Cryptophyte-Phycobiliprotein Concentrations.

Cryptophyte-phycobiliprotein concentrations varied depending on species and treatment. Interestingly, multiple species exhibited increased phycobiliprotein concentrations (per cell and per biovolume) when grown in glucose or bacteria compared to the light only or dark only treatments, and some exhibited higher phycobiliprotein concentrations in the dark treatments compared to the light (Figure 3.8A and 3.38B), though not all of these observations were significant.

The phycobiliprotein concentrations per cell for each species in each treatment are summarized in Table 3.3A. There were no significant differences observed between treatment or species for the *Chroomonas* clade or for the *Guillardia* clade, those the *Guillardia* clade exhibited much lower phycobiliprotein concentrations overall (Figure .8) compared to the other clades. For the *Cryptomonas* clade, there were significant differences attributed both to species and treatment. *C. ovata* exhibited a significantly higher Cr-PBP concentration than *C. ozolini* in light with added bacteria (*p*-value = 9.85×10^{-7}), but *C. ozolini* had a significantly higher concentration in light with added glucose compared to *C. ovata* (*p*-value = 0.0027). *C. ovata* had a significantly higher Cr-PBP concentration when grown in light with bacteria compared to when grown in light with glucose (*p*-value = 0.00027), while *C. ozolini* had a significantly higher concentration of Cr-PBP when grown in light with glucose compared to both light only and light with bacteria (*p*-value = 0.00032 and 1.56×10^{-5}, respectively).

The *Hemiselmis* clade exhibited similar trends across species across the treatments. Both *H. andersenii* and *H. rufescens* exhibited higher concentrations of Cr-PBP when grown in darkness without added carbon compared to dark with glucose (*p*-value = 1.13×10^{-7} for *H. rufescens* and *p*-value = 2.98×10^{-6} for *H. andersenii*). Both

species did not survive when grown in the dark with bacteria, and all other treatments exhibited similar Cr-PBP concentrations.

The *Rhodomonas* clade showed great variation in Cr-PBP concentrations across species and treatments. There was as significant difference in the Cr-PBP concentration between *R. salina* and *R. abbreviata* grown in dark with glucose (*p*-value = 0.0083), with *R. salina* exhibiting a higher concentration over *R. abbreviata*, and there was a significant difference in the Cr-PBP concentrations between the two species when grown in light with bacteria (*p*-value = 0.014), with *R. abbreviata* exhibiting the highest concentration compared to *R. salina*. *R. salina* showed similar Cr-PBP concentrations in both dark with glucose and dark with bacteria treatments, which were both significantly higher than *R. salina* cultures grown in darkness only. *R. abbreviata* did not exhibit any significant differences across the darkness treatments, but did have significant differences in Cr-PBP concentrations in cultures grown in light with glucose and light with bacteria compared to light only, with concentrations in light with glucose higher than light only (*p*-value = 0.004), and concentrations in light with bacteria lower than light only (*p*-value = 0.023).

We also calculated pigment concentrations and ran statistical analysis for cryptophyte-phycobiliprotein concentrations per biovolume to check for any significant differences due to size effects (Table 3.3B). When we calculated pigment per biovolume, we see a shift in the significant trends in phycobiliprotein concentration, suggesting that biovolume and phycobiliprotein concentrations are correlated. When considering differences in volume, we saw no significant differences in phycobiliprotein concentrations for either species in the *Chroomonas* clade nor for those in the *Guillardia* clade, though there was a shift in phycobiliprotein concentrations with light availability. For the *Cryptomonas* clade, we observed significantly higher Cr-PBP concentrations in

C. ozolini when grown in multiple of the dark treatments compared to the light treatments for cultures frown in the darkness with no added carbon and those grown in darkness with added glucose, with cultures grown in complete darkness having the greatest concentration of phycobiliprotein. We also saw that there was a significant difference between *C. ozolini* cultures grown in the darkness with no added carbon and cultures of *C. ovata* grown in the same treatment, and that *C. ovata,* while having significant shifts in grown rate and cell volume, did not exhibit any significant changes in phycobiliprotein concentration.

We also saw significant changes in the Cr-PBP concentrations when standardized to cell volume in the *Hemiselmis* and *Rhodomonas* clades. Interestingly, both *Hemiselmis* species exhibited significantly greater concentrations of Cr-PBP in the dark without added carbon compared to all other treatments. Both *Rhodomonas* species had significantly more Cr-PBP in treatments with added bacteria compared to their no-carbon controls, and *R. salina* produced more phycobiliprotein in the dark with bacteria compared to when it was grown in the light with bacteria, as well as when it was grown in the dark with no added carbon source. *R. abbreviata* also exhibited increased phycobiliprotein concentrations in the presence of bacteria than with no added carbon or with added glucose.

Cell volumes

The average cell volumes for all species across all treatments are summarized in Table 3.4. Except for the *Goniomonas* clade, all clades exhibited significant (*p*-value < 0.05) differences in the cell volumes attributed to the different treatments we grew our cultures in. In particular, the addition of glucose seemed to have an effect on cell volume

for multiple species. *C. mesostigmatica* exhibited significantly larger cell volumes in the dark with glucose (170.80 µm ± 1.77) compared to both darkness only (76.93µm ± 9.50) and dark with bacteria (62.6µm ± 4.94) and had significantly larger cell volumes in the light with glucose (125.15µm ± 7.38) compared to light only (77.60µm ± 14.21) and light with bacteria (81.24µm ± 7.14). There were no significant differences between cultures of *C. placoidea* grown in any of the treatments.

C. ovata exhibited significantly smaller cell volumes in dark with glucose (199.17µm ± 51.60) compared to *C. ovata* cultures grown in dark with bacteria (620.79µm ± 29.60) and darkness only (586.64µm ± 50.34). *C. placoidea* did not have any significant differences in cell volumes across treatments. *G. theta* had significantly larger cell volumes when grown in the light with added glucose (179.07µm ± 63.67) compared to cultures grown in light only (64.84µm ± 5.55) and cultures grown in light with bacteria (7140µm ± 12.38). *H. phi* did not exhibit any significant changes in cell biovolume.

H. andersenii was also significantly larger when grown in dark with glucose (191.85µm ± 70.90) compared to darkness only (73.94µm ± 26.60) and when grown in light with glucose (152.73µm ± 33.98) compared to light only (27.94µm ± 1.75) and light with bacteria (27.65µm ± 1.74). *R. abbreviata* was significantly smaller when grown in the light with added glucose (128.84µm 13.18) compared to cultures grown in the light only (282.70µm ± 28.05) and cultures grown in the light with added bacteria (269.15µm ± 46.94), and it was also significantly smaller in darkness with added glucose (74.12µm) compared to dark only (178.35µm ± 10.51) and the dark with added bacteria (175.26µm ± 18.69).

Discussion

Algal growth rate can be used as a measure of fitness, and these rates can be affected by resource availability and resource acquisition ability, which is related to cell volume. We used volume as a potential indicator for trophic strategy in our study, examining whether fitness (growth rate) changes with light and carbon availability (Ward *et al.* 2017). We found that cryptophyte growth rates varied greatly with clade and resource availability. There were four photosynthetic species that exhibited positive growth rates in complete darkness with added carbon: *H. phi* from the *Guillardia* clade, *R. abbreviata* from the *Rhodomonas* clade, and both *Cryptomonas* species, *C. ovata* and *C. ozolini.* All of these species were able to survive in the darkness with added glucose at comparable or faster growth rates than our heterotrophic species, which both had positive growth rates in the presence of glucose and bacteria that were comparable regardless of the presence of light. This suggests that each of these species were able to maintain growth and survival under dark conditions due to the assumed uptake of glucose via osmotrophic means. To our knowledge, this is the first account of the *Guillardia* clade exhibiting any potential for heterotrophic function, but both the *Cryptomonas* and *Rhodomonas* clades have been suggested to be mixotrophic in the past (Lewitus *et al.* 1991).

Cryptophytes are generally thought to be low-light specialists (Doust *et al.* 2006), and *Cryptomonas* species are the most well-adapted to low-light environments (Gervais 2001). This low-light adaptation has been suggested to be a pre-adaptation to surviving near freshwater chemoclines where many *Cryptomonas* species are usually found where nutrients, light, and carbon availability are variable (Gervais 2001). As such, *Cryptomonas* species are hypothesized to be mixotrophic and are often discussed in field

studies because they tend to increase in abundance when there is a bacterial bloom in the water column, suggesting that *Cryptomonas* species are phagotrophic (Gervais 1998, 2001). Gervais (2001) found that *Cryptomonas* species isolated from the field were able to take up dissolved glucose when grown in batch culture but were more efficient at taking up cellular carbon. While our *Cryptomonas* species did not exhibit a positive growth rate in the dark with added bacteria, it's possible that there is a prey preference for these algae, and the bacteria that we fed our *Cryptomonas* species are not ones they selectively feed upon. However, previous studies that have tried to induce phagotrophy in cryptophytes have found that it takes extreme conditions to induce the function, such as low light, low organic carbon, and low nutrient concentrations in combination, and it's possible that our nutrient replete conditions could prohibit phagotrophy from occurring, suggesting that phagotrophy may be triggered via a different mechanism than carbon or light limitation (Sanders & Porter 1988; Roberts & Laybourn-Parry 2001).

For some species, we saw that the addition of carbon regardless of light availability led to decreased growth rates. *C. placoidea* in particular exhibited a slow growth rate when both bacteria and glucose was added to the cultures, and *C. mesostigmatica* exhibited a similar trend when glucose was added in the presence of light. Both *Chroomonas* species were not able to survive in the darkness and exhibited decreased growth rates. Both *Hemiselmis* species also didn't survive in the dark and adding glucose to the *Hemiselmis* cultures when light was available led to negative growth rates for both species. This suggests that the presence of glucose had a negative effect on fitness for both the *Chroomonas* clade and the *Hemiselmis* clade. This is particularly interesting because for many other algal species, the addition of glucose leads to increased growth rates even when light is available. For example, *Spirulina platensis*

grows fastest when cultured with glucose and high light intensities until hit becomes photoinhibited (Chen *et al.* 1996), and *Chlorella* sp. and *Nannochloropsis* sp. both exhibit increased growth rates when grown under photoheterotrophic conditions with light and glucose, as well (Cheirsilp & Torpee 2012). While these previous studies are not focused on cryptophytes, it's interesting that we see such a diverse response to the addition of dissolved organics to these various algal cultures and within our study, with some species responding positively to the addition of glucose and others responding negatively. It's possible that these differences are related to biochemical pathways related to carbon metabolism, or, alternatively, the addition of glucose could lead to the suppression of photosynthesis in some species, which has been shown to occur in some species of red and green algae (Stadnichuk *et al.* 1998; Roth *et al.* 2019). We hypothesize that this photosynthetic repression may be occurring, particularly because *H. phi* exhibited similar growth rates when glucose was added regardless of if the cultures were grown in the light or in the dark, which suggests that the presence of dissolved organics leads to a potential shift in trophic function regardless of light availability. However, further investigation into the photosynthetic and glycolysis pathways would be needed to determine this.

The *Rhodomonas* clade exhibited interesting shifts in growth rates that varied greatly dependent upon the presence of light. Both *R. salina* and *R. abbreviata* showed similar growth trends in the dark, but when they were grown in the light, they had opposite responses. *R. abbreviata* had an increased growth rate when both bacteria and glucose were added in the light, while *R. salina* showed a decreased growth rate when bacteria and glucose were added in the presence of light. This suggests that there is great variation in how species respond to the presence of different carbon sources even within the same clade, consistent with the results we observed within the other clades. Overall,

we did not observe any clear trends in response to carbon and light availability across clades, and some clades appear to have more potential for mixotrophic function than others given that some are able to survive in the darkness while others do not, and there is also variation in how species within the same clade respond to carbon and light availability. Because cryptophytes had to exhibit a mixotrophic ancestral state given that they evolved via the assimilation of a heterotroph and an autotroph, this suggests that this ability has likely been lost in many clades (or was lost entirely and then regained in some species). We hypothesized that variation in growth rate and potential mixotrophic function would be correlated with cell volume, expecting that larger cells would be more likely to exhibit phagotrophic mixotrophy, while smaller cells would be more likely to exhibit osmotrophic phagotrophy. Thus, assuming mixotrophic function, we expected to see a shift in cell volume selected for in different treatments, where larger cells in cultures grown with added bacteria and smaller cells in cultures grown with glucose because smaller cells have a larger surface-area-to-volume ratio which increases their nutrient affinity (Litchman *et al.* 2007). However, we saw the opposite of this expectation. There was a consistent trend where multiple species grown with the addition of glucose exhibited greater biovolumes than those grown without additional carbon or with added bacteria, regardless of the presence of light. Stadnichuk *et al.* (1998) grew *Galdieria partita*, a red alga, in autotrophic (light only) and heterotrophic (complete darkness) conditions with added glucose and found both that the addition of glucose suppressed photosynthetic pigment production, but also that it led to larger cells in cultures grown with glucose. Sanders *et al.* (2001) found that grown of *Ochromonas* sp. with and without light resulted in shifts in cell size, where cultures grown in the light were significantly larger than those in the dark, which is consistent with our results for all

species in our experiment, and they also found that vitamin and nutrient concentration effected cell size, where nutrient deplete conditions led to smaller cell sizes. This suggests that cell size is potentially mediated by multiple traits that are related depending on the environmental conditions, and that the response to the addition of dissolved organics differs from that of nutrient availability.

Interestingly, for some of the species that did not exhibit positive growth or heterotrophic function in the dark (*R. salina, H. andersenii*, *H. rufescens, G. theta, C. placoidea,* and *C. mesostigmatica*), we saw the greatest phycobiliprotein content per cell. Opposite of this, we saw that the species that were able to survive in the darkness (*H. phi, C. ovata, C. ozolini,* and *R. abbreviata*) did not exhibit significant increases in pigment concentration when grown in the dark compared to cultures grown in the light, and generally had the highest phycobiliprotein concentrations when light was present. We also saw shifts in Cr-PBP phycobiliprotein concentrations when we normalized to cell volume, where multiple species exhibited greater concentrations when grown in the dark environments or in environments with added carbon compared to the no-carbon controls. We hypothesize that these observed shifts in pigment concentration between light environments is a result of a low-light acclimation response, where the species that were not able to survive in the darkness were potentially increasing pigment production to capture whatever photons might be available, though we would have needed to measure the rate of pigment production to determine this. However, this has been shown to occur in other species of algae, where light limitation leads to higher pigment concentrations, as well as a higher lipid concentration and greater biomass overall (Leeuwe *et al.* 2014; reviewed in Hu *et al.* 2018). For the species that were able to survive in the dark, we expect that they invested less in pigments because they were able to offset the lack of

light with heterotrophic function, which has been shown to occur in other mixotrophic algae (Yang *et al.* 2000). We also hypothesize that the presence of added carbon influences phycobiliprotein concentrations, but the effect is dependent upon species. For instance, we saw that the addition of glucose to *C. placoidea* cultures grown in the dark led to increase concentrations of phycobiliprotein compared to the dark control and to all cultures grown in the light, but *C. ovata* did not exhibit this same response, instead having concentrations that were lower than the controls when glucose was added. Additionally, we also saw that both *R. salina* and *G. theta* had higher phycobiliprotein concentrations when grown with bacteria compared to the controls, suggesting that the addition of bacteria may influence pigment concentrations. The addition of dissolved carbon has been used frequently as a method to increase intracellular protein and lipid concentrations for algal species used in biofuel studies (Marquez *et al.* 1995; reviewed in Hu *et al.* 2018), suggesting that there may be a link between extracellular carbon content and the biosynthesis reactions.

Overall, we saw that not only does trophic function seem to be plastic in cryptophytes, but also that the degree of plasticity varies across the clades in complex ways. While other studies have suggested that cryptophytes are capable of phagotrophy, we did not see any significant differences attributed to bacterial addition in our study. However, we did see significant changes in growth rate and cell volume in many cultures grown with glucose both in the light and the dark, and we did see significant changes in biovolume and growth attributed to light availability. These results show that the response to light and carbon availability in cryptophytes is plastic, and that the drivers of trophic strategies are complex and likely interconnected.

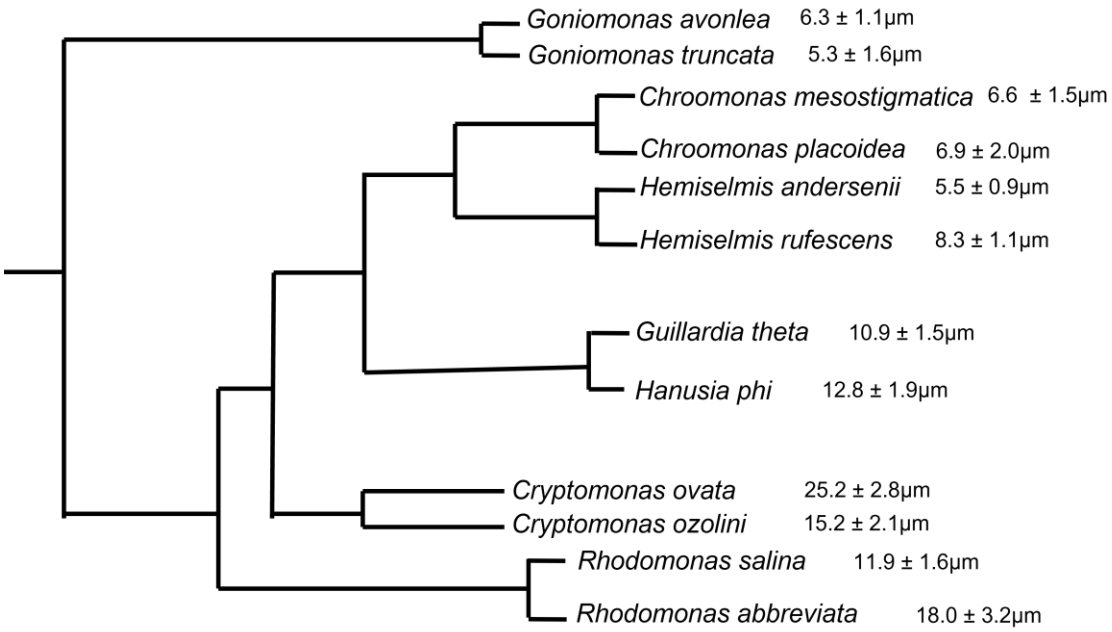

Figure 3.1: Condensed phylogenetic tree of the cryptophyte phylogeny, indicating the species used in this experiment and their preliminary lengths (µm ± standard deviation).

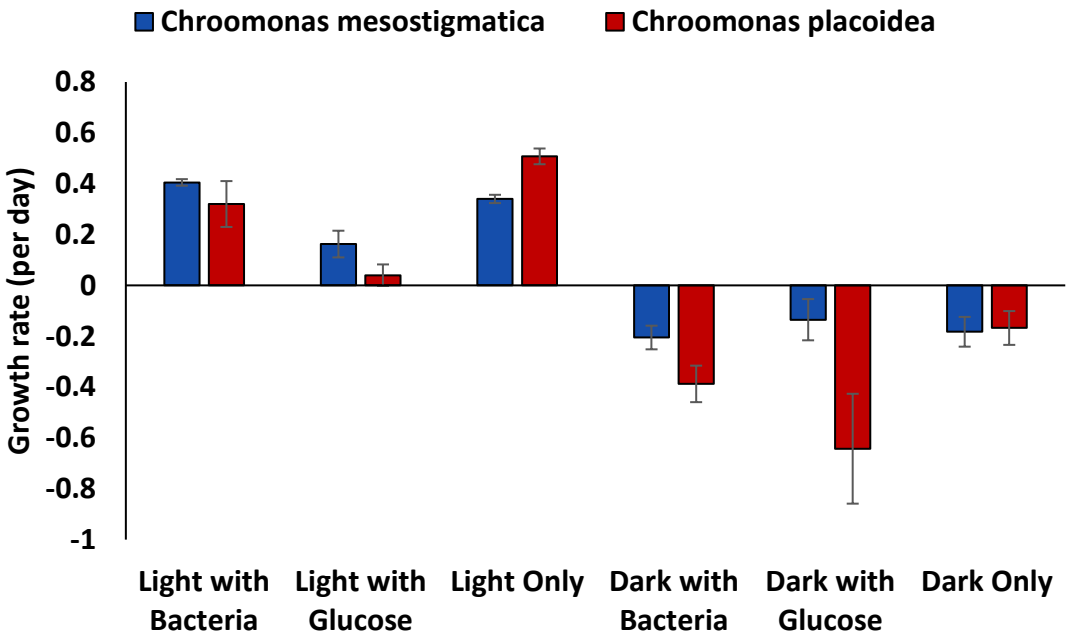

Figure 3.2: Growth rates (per day) of the *Chroomonas* clade grown in the light and the dark with and without added bacteria or carbon as carbon sources. Left: dark treatments; right: light treatments. Columns in blue represent the larger species; columns in orange represent the smaller species.

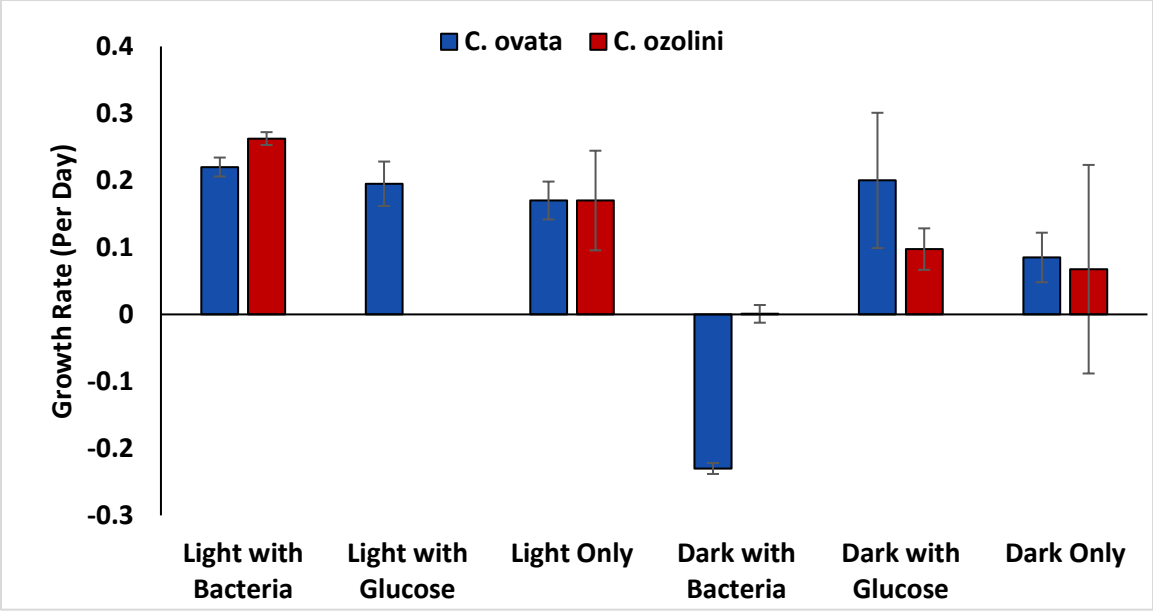

Figure 3.3: Growth rates (per day) of the *Cryptomonas* clade grown in the light and the dark with and without added bacteria or carbon as carbon sources. Left: dark treatments; right: light treatments. Columns in blue represent the larger species; columns in orange represent the smaller species.

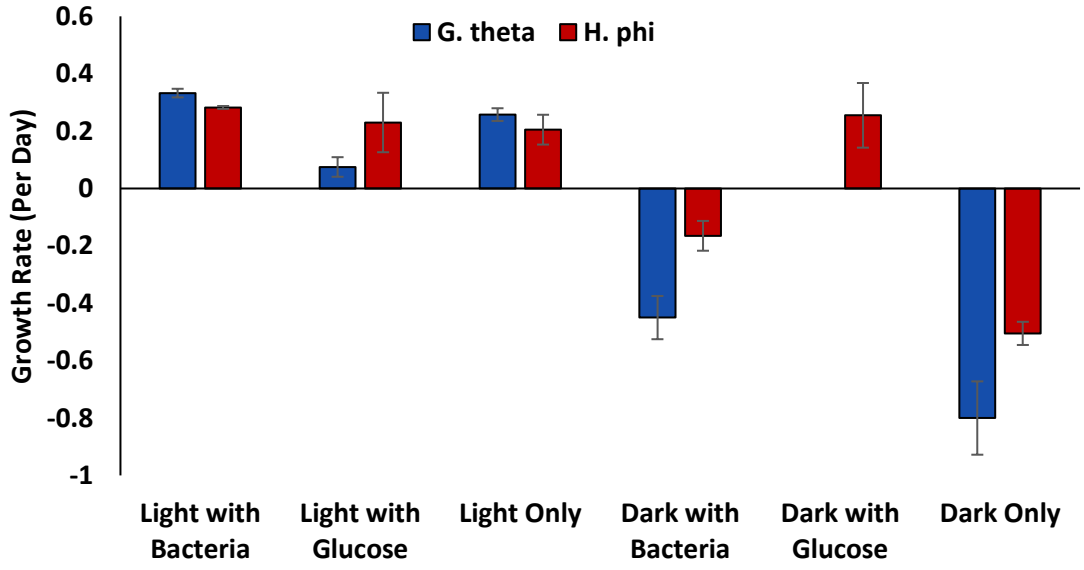

Figure 3.4: Growth rates (per day) of the *Guillardia* clade grown in the light and the dark with and without added bacteria or carbon as carbon sources. Left: dark treatments; right: light treatments. Columns in blue represent the larger species; columns in orange represent the smaller species.

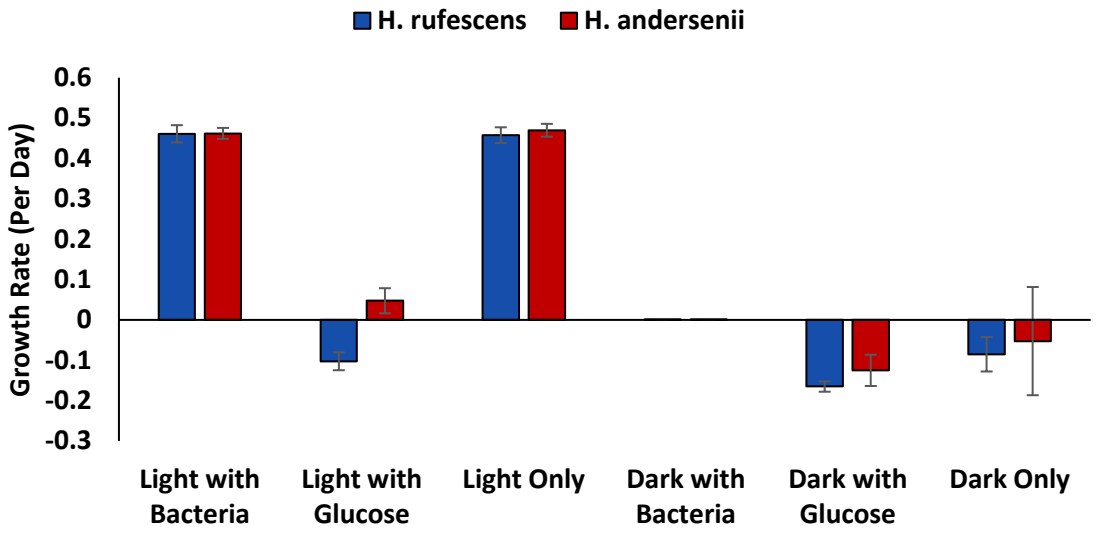

Figure 3.5: Growth rates (per day) of the *Hemiselmis* clade grown in the light and the dark with and without added bacteria or carbon as carbon sources. Left: dark treatments; right: light treatments. Columns in blue represent the larger species; columns in orange represent the smaller species.

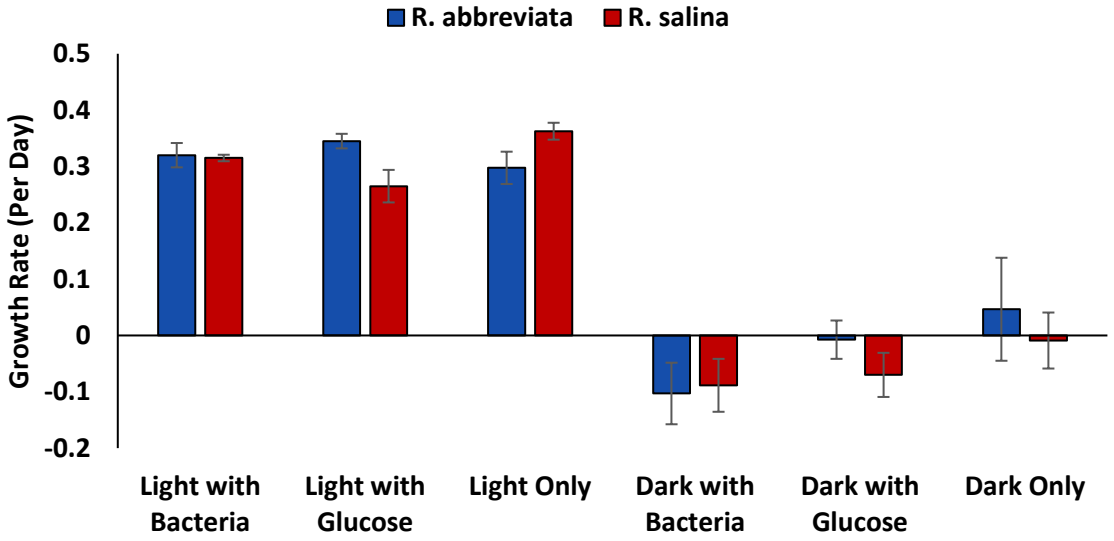

Figure 3.6: Growth rates (per day) of the *Rhodomonas* clade grown in the light and the dark with and without added bacteria or carbon as carbon sources. Left: dark treatments; right: light treatments. Columns in blue represent the larger species; columns in orange represent the smaller species.

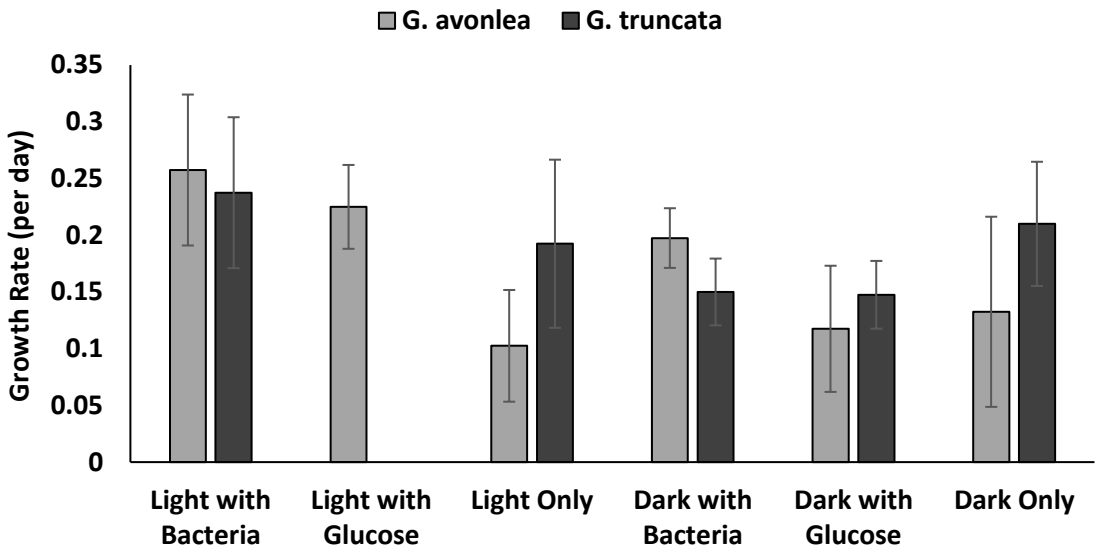

Figure 3.7: Growth rates (per day) of the *Goniomonas* clade grown in the light and the dark with and without added bacteria or carbon as carbon sources. Left: dark treatments; right: light treatments. Note the different scales on the y-axes.

A:

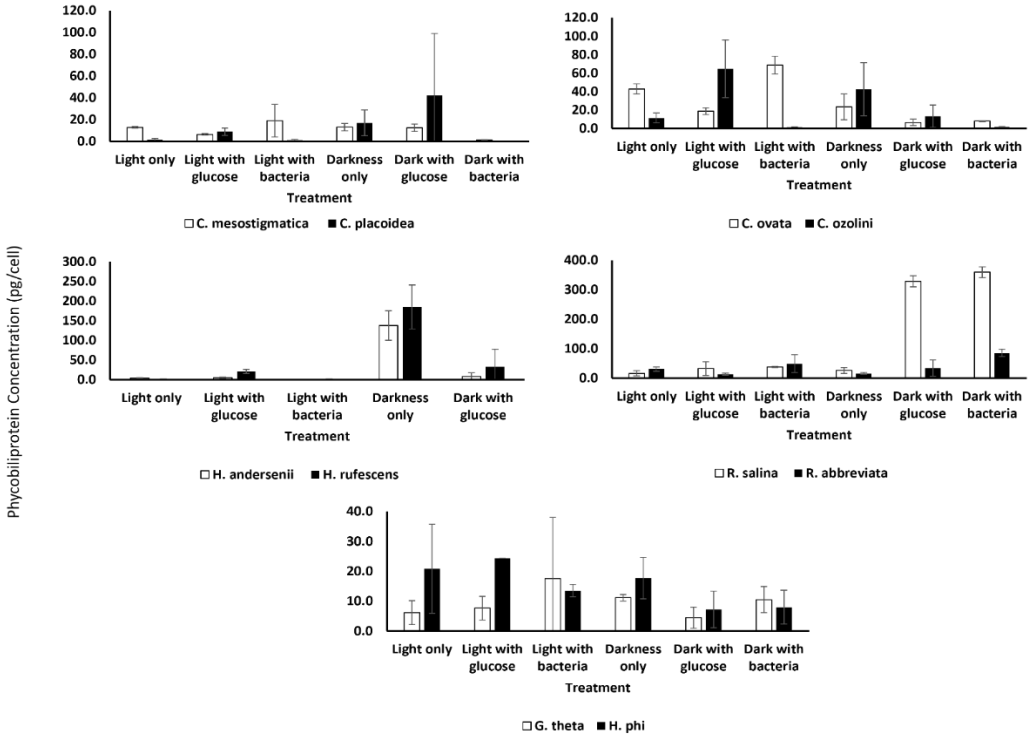

B:

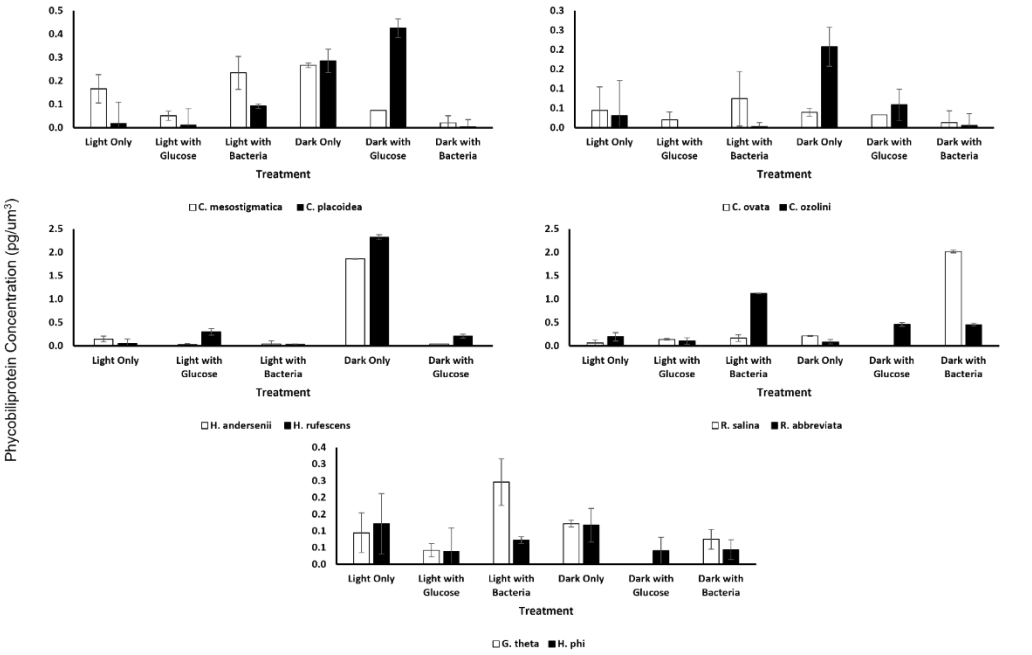

Figure 3.8: A. Phycobiliprotein concentrations (pg/cell) for all photosynthetic organisms included in this study across each treatment. Error bars represent standard deviation. **B:** Phycobiliprotein concentrations (pg/um^3) for all photosynthetic organisms included in this study across each treatment. Error bars represent standard deviation.

Table 3.1: Average growth rates (per day ± standard deviation) for all species grown in all six treatments.

Species	Light Only	Light with Bacteria	Light with Glucose	Dark Only	Dark with Bacteria	Dark with Glucose
Chroomonas placoidea	0.51 ± 0.03	0.32 ± 0.09	0.04 ± 0.04	-0.17 ± 0.07	-0.40 ± 0.07	-0.64 ± 0.22
Chroomonas mesostigmatica	0.34 ± 0.02	0.41 ± 0.01	0.17 ± 0.05	-0.18 ± 0.06	-0.21 ± 0.05	-0.14 ± 0.08
Cryptomonas ovata	0.17 ± 0.03	0.22 ± 0.14	0.20 ± 0.03	0.09 ± 0.04	-0.23 ± 0.008	0.2 ± 0.1
Cryptomonas ozolini	0.17 ± 0.07	0.27 ± 0.01	NA	0.07 ±0.16	0.0008 ± 0.01	0.10 ± 0.03
Guillardia theta	0.26 ± 0.02	0.33 ± 0.02	0.075 ± 0.03	-0.8 ± 0.13	-0.45 ± 0.08	NA
Hanusia phi	0.21 ± 0.06	0.28 ± 0.005	0.23 ± 0.10	-0.51 ± 0.04	-0.17 ± 0.05	0.26 ± 0.11
Hemiselmis andersenii	0.47 ± 0.02	0.46 ± 0.02	0.05 ± 0.02	-0.05 ± 0.04	NA	-0.13 ± 0.01
Hemiselmis rufescens	0.46 ± 0.02	0.46 ± 0.01	-0.10 ± 0.03	-0.09 ± 0.13	NA	-0.17 ± 0.04
Rhodomonas salina	0.36 ± 0.02	0.32 ± 0.01	0.27 ± 0.03	-0.009 ± 0.04	-0.09 ± 0.05	-0.07 ± 0.04
Rhodomonas abbreviata	0.30 ± 0.03	0.32 ± 0.02	0.35 ± 0.01	0.05 ± 0.09	-0.1 ± 0.05	-0.01 ± 0.03
Goniomonas truncata	0.19 ± 0.07	0.24 ± 0.07	NA	0.21 ± 0.05	0.15 ± 0.03	0.15 ± 0.03
Goniomonas avonlea	0.10 ± 0.05	0.26 ± 0.07	0.23 ± 0.04	0.13 ± 0.07	0.20 ± 0.03	0.12 ± 0.06

Table 3.2: Summary of significant two-way ANOVA comparisons and interpretations for each clade across treatments. **A.** *Chroomonas* clade; **B:** *Cryptomonas* clade*;* **C.** *Guillardia* clade; **D.** *Hemiselmis* clade; **E.** *Rhodomonas* clade; **F.** *Goniomonas* clade.

A. *Chroomonas* clade.

Comparison	***p*-value**	**Interpretation**
C. placoidea darkness only vs. *C. placoidea* dark with glucose	7.78E-08	There is a significant difference between how *C. placoidea* grows in the dark with and without glucose
C. placoidea darkness only vs *C. placoidea* dark with bacteria	2.61E-02	There is a significant difference in how *C. placoidea* grows in the dark with and without bacteria
C. placoidea dark with glucose vs. *C. placoidea* dark with bacteria	5.24E-03	There is a significant difference between how C. placoidea grows in the dark with glucose and in the dark with bacteria
C. placoidea light only vs. *C. placoidea* light with glucose	1.13E-07	There is a significant difference between how *C. placoidea* grows in the light with and without glucose
C. placoidea light with glucose vs. *C. placoidea* light with bacteria	1.55E-03	There is a significant difference between how *C. placoidea* grows in the light with glucose and in the light with bacteria
C. placoidea dark with glucose vs. *C. mesostigmatica* dark with glucose	1.59E-08	There is a significant difference in how each *Chroomonas* species response to dark with added glucose
C. mesostigmatica light with glucose vs. *C. mesostigmatica* light with bacteria	9.45E-03	There is a significant difference in how *C. mesostigmatica* grows in the light with glucose and in the light with bacteria

B. *Cryptomonas* clade.

Comparison	*p*-value	Interpretation
C. ovata dark with glucose vs. *C. ovata* dark with bacteria	4.447E-09	There is a significant difference in growth of *C. ovata* in dark with glucose and in the dark with bacteria
C. ovata darkness only vs. *C. ovata* dark with bacteria	4.914E-06	There is a significant difference in growth of *C. ovata* in the dark with and without bacteria
C. ovata dark with bacteria vs. *C. ozolini* dark with bacteria	1.013E-03	There is a significant difference in how the two *Cryptomonas* species respond when grown in the dark with bacteria

C. *Guillardia* clade.

Comparison	*p*-value	Interpretation
H. phi darkness only vs. *H. phi* dark with glucose	6.990E-14	There is a significant difference between *H. phi* grown in dark with and without added glucose
H. phi dark with glucose vs. *H. phi* dark with bacteria	5.690E-08	There is a significant difference between *H. phi* grown in dark with added glucose or added bacteria
G. theta darkness only vs. *G. theta* dark with bacteria	2.800E-06	There is a significant difference between *G. theta* grown in dark with and without added bacteria
H. phi darkness only vs *H. phi* dark with bacteria	4.960E-06	There is a significant difference between *H. phi* grown in dark with and without added bacteria
H. phi darkness only vs. *G. theta* darkness only	6.660E-05	There is a significant difference in how the two *Guillardia* clade species respond to darkness only
H. phi dark with bacteria vs. *G. theta* dark with bacteria	1.189E-04	There is a significant difference in how the two *Guillardia* clade species respond to dark with bacteria
G. theta light with glucose vs. *G. theta* light with bacteria	5.810E-04	There is a significant difference between *G. theta* grown in light with bacteria or in the light with glucose
G theta light only vs. *G. theta* light with glucose	3.404E-02	There is a significant difference between *G. theta* grown in light with and without added glucose

D. *Hemiselmis* clade.

Comparison	*p*-value	Interpretation
H. rufescens light with glucose vs. *H. rufescens* light with bacteria	5.607E-14	There is a significant difference in growth of *H. rufescens* in light with bacteria or light with glucose
H. rufescens light only vs. *H. rufescens* light with glucose	5.762E-14	There is a significant difference in growth of *H. rufescens* in light with and without added glucose
H. andersenii light only vs. *H. andersenii* light with glucose	1.789E-11	There is a significant difference in growth of H. andersenii in light with and without added glucose
H. andersenii light with glucose vs. *H. andersenii* light with bacteria	2.835E-11	There is a significant difference between growth of *H. andersenii* light with bacteria or glucose

H. rufescens light with glucose vs. *H. andersenii* light with glucose	5.314E-03	There is a significant difference in how the two *Hemiselmis* species grow in light with added glucose

E. *Rhodomonas* clade.

Comparison	*p*-value	Interpretation
R. abbreviata darkness only vs. *R. abbreviata* dark with bacteria	7.52E-04	There is a significant difference in how *R. abbreviata* grows in dark with and without added bacteria

F. *Goniomonas* clade.

Comparison	*p*-value	Interpretation
G. avonlea light only vs. *G. avonlea* light with bacteria	0.016441	There is a significant difference in how *G. avonlea* grows in light with and without added bacteria

Table 3.3: A: Average Cryptophyte-phycobiliprotein concentrations (pg/cell ± standard deviation) for all photosynthetic species grown in all six treatments. **B:** Average Cryptophyte-phycobiliprotein concentrations (pg/um^3 ± standard deviation) for all photosynthetic species grown in all six treatments.

A:

Species	Light Only	Light with Bacteria	Light with Glucose	Dark Only	Dark with Bacteria	Dark with Glucose
Chroomonas placoidea	1.47 ± 1.09	8.91 ± 3.39	1.10 ± 0.66	22.00 ± 11.83	0.34 ± 0.14	42.10 ± 56.94
Chroomonas mesostigmatica	12.88 ± 0.73	19.01 ± 14.9	6.35 ± 0.77	13.02 ± 3.29	1.31 ± 0.05	12.56 ± 3.35
Cryptomonas ovata	42.76 ± 5.40	68.57 ± 9.75	18.64 ± 3.72	23.33 ± 14.02	7.9 ± 0.38	6.43 ± 3.5
Cryptomonas ozolini	11.29 ± 5.31	1.1 ± 0.66	NA	42.40 ± 28.73	1.57 ± 0.40	13.25 ± 12.03
Guillardia theta	6.13 ± 3.98	17.57 ± 20.42	7.61 ± 3.98	11.12 ± 1.06	10.47 ± 7.94	NA
Hanusia phi	20.8 ± 14.93	13.51 ± 2.03	24.29 ± 13.20	17.21 ± 6.93	7.94 ± 4.4	7.21 ± 3.58
Hemiselmis andersenii	4.17 ± 0.66	1.08 ± 0.13	4.82 ± 1.67	137.58 ± 37.41	NA	8.27 ± 9.24
Hemiselmis rufescens	1.81 ± 0.69	0.99 ± 0.40	21.02 ± 4.91	184.91 ± 56.02	NA	32.66 ± 45.12
Rhodomonas salina	16.41 ± 9.11	43.79 ± 11.30	32.18 ± 23.91	25.98 ± 9.59	312.95 ± 32.64	328.48 ± 19.09
Rhodomonas abbreviata	55.57 ± 50.01	303.04 ± 303.96	13.53 ± 3.62	15.95 ± 16.38	80.20 ± 17.79	34.17 ± 27.27

B:

Species	Light Only	Light with Bacteria	Light with Glucose	Dark Only	Dark with Bacteria	Dark with Glucose
Chroomonas placoidea	0.02 ± 0.01	0.06 ± 0.04	0.01 ± 0.07	0.29 ± 0.15	0.005 ± 0.002	0.42 ± 0.57
Chroomonas mesostigmatica	0.17 ± 0.009	0.23 ± 0.18	0.05 ± 0.006	0.27 ± 0.07	0.02 ± 0.0008	0.07 ± 0.02
Cryptomonas ovata	0.04 ± 0.006	0.07 ± 0.01	0.02 ± 0.004	0.04 ± 0.02	0.013 ± 0.0006	0.03 ± 0.02
Cryptomonas ozolini	0.03 ± 0.01	0.003 ± 0.002	NA	0.21 ± 0.14	0.006 ± 0.002	0.06 ± 0.05
Guillardia theta	0.09 ± 0.06	0.25 ± 0.07	0.04 ± 0.02	0.12 ± 0.01	0.08 ± 0.03	NA

Hanusia phi	0.12 ± 0.09	0.07 ± 0.01	0.13 ± 0.07	0.12 ± 0.05	0.04 ± 0.03	0.04 ± 0.04
Hemiselmis andersenii	0.15 ± 0.02	0.04 ± 0.005	0.03 ± 0.01	1.86 ± 0.51	NA	0.04 ± 0.05
Hemiselmis rufescens	0.06 ± 0.02	0.04 ± 0.01	0.31 ± 0.07	2.33 ± 0.71	NA	0.21 ± 0.29
Rhodomonas salina	0.07 ± 0.04	0.17 ± 0.04	0.14 ± 0.11	0.22 ± 0.08	2.01 ± 0.21	2.58 ± 0.15
Rhodomonas abbreviata	0.20 ± 018	1.13 ± 1.13	0.11 ± 0.03	0.09 ± 0.09	0.46 ± 0.10	0.46 ± 0.37

Table 3.4: Average volume calculations (μm^3 ± standard deviation) for all species grown in all six treatments.

Species	Light Only	Light with Bacteria	Light with Glucose	Dark Only	Dark with Bacteria	Dark with Glucose
Chroomonas placoidea	78.71 ± 3.49	96.60 ± 4.82	99.03 ± 25.39	76.93 ± 9.50	70.67 ± 0.30	99.12 ± 22.51
Chroomonas mesostigmatica	77.60 ± 14.21	81.24 ± 7.14	125.15 ± 7.38	76.93 ± 9.50	62.6 ± 4.94	170.80 ± 1.77
Cryptomonas ovata	957.56 ± 71.32	924.91 ± 48.83	931.76 ± 256.75	586.64 ± 50.34	620.79 ± 29.60	199.17 ± 51.60
Cryptomonas ozolini	369.93 ± 42.87	326.93 ± 42.83	312.89 ± 73.87	204.21 ± 13.09	253.83 ± 43.56	225.20 ± 70.74
Guillardia theta	64.84 ± 5.55	71.40 ± 12.38	179.07 ± 63.67	90.95 ± 0.32	139.32 ± 16.87	NA
Hanusia phi	170.94 ± 23.24	185.91 ± 19.11	193.88 ± 55.42	150.55 ± 12.81	180.19 ± 17.80	174.45 ± 71.44
Hemiselmis andersenii	27.94 ± 1.75	27.65 ± 1.74	152.73 ± 33.98	73.94 ± 26.60	NA	191.85 ± 70.90
Hemiselmis rufescens	27.65 ± 1.74	27.86 ± 2.81	68.72 ± 17.43	79.38 ± 32.92	NA	154.09 ± 69.61
Rhodomonas salina	248.05± 19.88	259.18 ± 60.04	225.04 ± 92.98	119.99 ± 18.32	155.09 ± 19.72	127.32 ± 71.22
Rhodomonas abbreviata	282.7 ± 28.05	269.15± 46.94	128.84± 13.18	178.35 ± 10.51	175.26 ± 18.69	74.12 ± 37.95
Goniomonas avonlea	101.26 ± 11.77	77.60 ± 14.21	81.24 ± 7.14	90.96 ± 0.31	76.93 ± 9.50	79.55 ± 9.6
Goniomonas truncata	89.83 ± 4.71	96.60 ± 4.82	99.03 ± 25.39	90.01 ± 2.10	77.64 ± 8.85	99.11 ± 22.51

REFERENCES

CHAPTER 1 AND 2

Aguilera J, Gordillo FJL, Karsten U, Figueroa FL, & Niell FX. (2000). Light quality effect on photosynthesis and efficiency of carbon assimilation in the red alga Porphyra leucosticta. Journal of Plant Physiology. 157:96-92.

Algarra P, de la Vina G, & Niell J. (1991). Effects of light quality and irradiance level interactions on short-term pigment response of the red alga Corallina elongata. Marine Ecology Progress Series. 74:27-32.

Allen JF, de Paula WBM, Puthiyaveetil S. & Nield J. (2011). A structural phylogenetic map for chloroplast photosynthesis. Trends Plant Sci. 16:645-655.

Andrews S. (2010). FastQC: a quality control tool for high throughput sequence data. Babraham Institute. http://www.bioinformatics.babraham.ac.uk/projects/fastqc/.

Apt KE, Collier JL, & Grossman AR. (1995). Evolution of the phycobiliproteins. J. of Molecular Biology. 248(1):79-96.

Armbruster U, Ruhle T, Kreller R, Strotbek C, Zuhlke J, Tadini L, … Leister D. (2013). The photosynthesis affected mutant68-like protein evolved from a PSII assembly factor to mediate assembly of the chloroplast NAD(P)H dehydrogenase complex in 3943.

Balvanera, P., A. B. Pfisterer, N. Buchmann, J. S. He, T. Nakashizuka, D. Raffaelli, & B. Schmid. (2006). Quantifying the evidence for biodiversity effects on ecosystem functioning and services. Ecology Letters 9: 1146– 1156.

Beck, C. F., & Haring, M. A. (1996). Gametic Differentiation of Chlamydomonas. International Review of Cytology. 168: 259-302

BioBam Bioinformatics. (2019). OmicsBox – Bioinformatics made easy. https://www.biobam.com/omicsbox

Blankenship, R.E. (2002). Molecular Mechanisms of Photosynthesis. Blackwell Science Ltd., UK.

Blinks LR. (1954). The photosynthetic function of pigments other than chlorophyll. Annual Review of Plant Physiology. 5(1):93-114.

Bolger AM, Lohse M, & Usadel B. (2014). Trimmomatic: A flexible trimmer for Illumina Sequence Data. Bioinformatics 30(15):2114-20. https://doi.org/10.1093/bioinformatics/btu170

Bray NL, Pimentel H, Melsted P, & Pachter L. (2016). Near-optimal probabilistic RNA-seq quantification. Nature Biotechnology. 34:525-527.

Cardinale BJ. (2011). Biodiversity improves water quality through niche partitioning. Nature.
472:86-89.

Cardinale, B. J., D. S. Srivastava, J. E. Duffy, J. P. Wright, A. L. Downing, M. Sankaran, & C. Jouseau. (2006). Effects of biodiversity on the functioning of trophic groups and ecosystems. Nature 443: 989– 992.

Caron DA, Sanders RW, Lim EL, Marrase C, Amaral LA, Whitney S, Aoki RB, & Porter KG. (1993). Light-dependent phagotrophy in the freshwater mixotrophic chrysophyte dinobryon cylindricum. Microbial Ecology. 25(1):93-111.

Celedon JM & Cline K. (2013). Intra-plastid protein trafficking: How plant cells adapted prokaryotic mechanisms to the eukaryotic condition. Biochim. Biophys. Acta. 4833:341-351.

Chardin, C., Girin, T., Roudier, F., Meyer, C., & Krapp, A. (2014). The plant RWP-RK transcription factors: key regulators of nitrogen responses and of gametophyte development. Journal of experimental botany, 65(19), 5577–5587.

Cunningham BR., Greenwold MJ., Lachenmyer EM., Heidenreich KM., Davis AC., Dudycha JL., Richardson TL. (2019). Light capture and pigment diversity in marine and freshwater cryptophytes. *J. of Phycology*, 55(3):552-564.

Curtis BA, Tanifuji G, Burki F, Gruber A, Irimia M, Maruyama S, … Archibald J. (2012). Algal genomes reveal evolutionary mosaicism and the fate of nucleomorphs. Nature. 492:59-65.

Cuthbert, RN, Dalu, T, Wasserman, RJ, et al. (2019). Sex-skewed trophic impacts in ephemeral wetlands. *Freshw Biol*, 64: 359– 366. https://doi.org/10.1111/fwb.13228

Dammeyer T. & Frenkenberg-Dinkel N. (2008). Function and distribution of bilinbiosynthesis enzymes in photosynthetic organisms. Photochemical and Photobiological Sciences, 7:1121-1130.

Das P, Lei W, Aziz, SS, & Obbard JP. (2011). Enhanced algae growth in both phototrophic and mixotrophic culture under blue light. Bioresource Technology. 102(4):3883-3887.

Deng XW, Tonkyn JC, Peter GF, Thornber JP, & Gruissem W. (1989). Post-transcriptional control of plastid mRNA accumulation during adaptation of chloroplasts to different light quality environments. The Plant Cell. 1:645-654.

Deng Y, Yao J, Wang X, Guo H, & Duan D. (2012). Transcriptome sequencing and comparative analysis Saccharina japonica (Laminariales, Phaeophyceae) under blue light induction. PLoS One.

Dittami SM., Michel G., Collen J., Boyen C., Tonon T. (2010). Chlorophyll-binding proteins revisited – a multigenic family of light-harvesting and stress proteins from a brown algal perspective. BMC Evolutionary Biology, 10.

Douglas SE & Penny SL. (1999). The plastid genome of the cryptophyte alga, Guillardia theta: complete sequence and conserved synteny groups confirm its common ancestry with red algae. J. Mol Evol. 48:236-244.

Donaher N, Tanifuju G, Onodera N, Malfatti S, Chain P, Hara Y, & Archibald JM. (2009). The complete plastid genome sequence of the secondarily nonphotosynthetic alga Cryptomonas paramecium: Reduction, compaction, and accelerated evolutionary rate. Genome Biology and Evolution. 1:439-448.

Dring MJ. (1987). Marine plants and blue light. In Blue Light Responses: Phenomena and Occurrence in Plants and Microorganisms (Edited by H. Senger), pp. 121-140. CRC Press, Boca Raton, FL.

Dutkiewicz, S., A. E. Hickman, O. Jahn, S. Henson, C. Beaulieu, & E. Monier. (2019). Ocean colour signature of climate change. Nature Communications 10: 578.

Eberhard S, Finazzi G, & Wollman FA. (2008). The dynamics of photosynthesis. Ann. Rev. Genetics. 42:463-515.

Engelmann, T.W. (1883). Farbe und Assimilation. Assimilation findet nur in den

farbstoffhaltigen Plasmathielchen statt. II. Näherer Zusamennhang awischen Lichtabsorption und Assimilation. Bot Z 41:1-13.

Eskins K, Kiang CZ, & Shibles R. (1991). Light-quality and irradiance effects on pigments, light-harvesting proteins and Rubisco activity in a chlorophyll- and light-harvesting-deficient soybean mutant. Physiologia Plantarum. 83:27-53.

Ferris, P. J., & Goodenough, U. W. (1997). Mating type in Chlamydomonas is specified by mid, the minus-dominance gene. Genetics. 146(3): 859–869.

Ferris P, Olson BJSC, … Umen JG. (2010). Evolution of an expanded sex-determining locus in *Volvox. Science*, 328(5976):351-354.

Gaidukov, N. (1903). Die Farbervänderung bei den Prozessen der Komplementären chromatischen Adaptation. Ber. Deutsch Bot. Ges. 21:3517-522.

Gantt E. (1980). Structure and function of phycobilisomes: Light harvesting pigment complexes in red and blue-green algae. International Review of Cytology. 66:45-80.

Gantt E. (1996). Pigment protein complexes and the concept of the photosynthetic unit: Chlorophyll complexes and phycobilisomes. Photosynthesis Research, 28:47-53.

Gervais F. (1997). Cryptomonas undulata spec., nov., a new freshwater cryptophyte living near the chemocline. Nova Hedwigia. 65(1-4):353-364.

Gilbert D. (2013). EvidentialGene:tr2aacds, mRNA transcript assembly software. http://arthropods.eugenes.org/EvidentialGene/about/EvidentialGene_trassembly_pipe.html

Glazer, A.N. (1977). Structure and molecular organization of the photosynthetic accessory pigments of cyanobacteria and red algae. Mol Cell Biochem 18, 125–140.

Glazer, A.N. (1983). Comparative biochemistry of photosynthetic light harvesting systems. Ann. Rev. Biochem. 52: 125-127.

Gould S, Fan E, Hempel F, Maier U, & Klosgen RB. (2007). Translocation of a phycoerythrin a subunit across five biological membranes. J. of Biol. Chem. 282(41):P30295-30302.

Grabherr MG, Haas BJ, Yassour M, Levin JZ, Thompson DA, Amit I, … Regev A. (2011). Full-length transcriptome assembly from RNA-seq data without a reference genome. Nat Biotechnol, 29(7):644-652. https://doi.org/10.1038/nbt.1883

Greenwold MJ, Cunningham BR, Lachenmeyer EM, Pullman JM, Richardson TL, & Dudycha JL. (2019). Diversification of light capture ability was accompanied by the evolution of phycobiliproteins in cryptophyte algae. Proc. R. Soc. B. 286.

Grossman, A.R. (2003). A molecular understanding of complementary chromatic adaptation. Photosyn. Res. 76:207-215.

Gruissem W & Schuster G: Control of mRNA degradation in organelles. (1993). In: Brawerman G, Belasco J (eds) Control of Messenger RNA Stability, pp. 329-365. Academic Press, Orlando, FL.

Guillard, R.R.L. & Ryther, J.H. (1962). Studies on Marine Planktonic Diatoms I. Cyclotella nana Hustedt and Detonula confervacea (Cleve) Gran. Canadian Journal of Microbiology. 8, 229-239.

Gurevich A, Savelieve V, Vyahhi N, & Tesler G. (2013). QUAST: quality assessment tool for genome assemblies. Bioinformatics. 29(8):1072-1075.

Hamaji T, Kawai-Toyooka H, Uchimura H, Suzuki M, Noguchi H, Minakuchi Y, Toyoda A, Fujiyama A, Miyagishima S, Umen JG, Nozaki H. (2018) Anisogamy evolved with a reduced sex-determining region in volvocine green algae. *Communications Biology*, 1(17).

Harrop ST, Wilk KE, Dinshaw R, Collini E, Mirkovic T, Ying Teng C, … & Curmi P. (2014). Single-residue and exciton states of cryptophyte light-harvesting proteins. PNAS. 111(26):E2666-E2675.

Heidenreich KM & Richardson TL. (2019). Photopigment, absorption, and growth responses of marine cryptophytes to varying spectral irradiance. Journal of Phycology. 56(2): 507-520.

Hermsmeier D, Mala E, Schulz R, Thielmann J, Galland P, & Senger H. (1991). Antagonistic blue- and red-light regulation of cab-gene expression during photosynthetic adaptation in Scenedesmus obliquus. J. of Photochemistry and Photobiology B: Biology. 11(2):189-202.

Hey D. & Grimm B. (2020). One-helix protein1 and 2 form heterodimers to bind chlorophyll in photosystem II biogenesis. Plant Physiology,183(1):179-193.

Hill, DRA & Rowan, KS. (1989). The biliproteins of the Cryptophyceae. Phycologia 28:455-463.

Hill DRA & Wetherbee R. (1986). Proteomonas sulcata gen. et sp. nov. (Cryptophyceae), a cryptomonad with two morphologically distinct and alternating forms. Phycologia, 25:521-543.

Hillaert J, Hovestadt T, Vandegehuchte ML, & Bonte D. (2018). Size-dependent movement explains why bigger is better in fragmented landscapes. Ecol Evol. 8(22):10754-10767.

Ho CL, Teoh S, Teo SS, Rahim RA, & Phang SM. (2009). Profiling the transcriptome of Gracilaria changii (Rhodophyta) in Response to Light Deprivation. Mar Biotechnol. 11:513-519.

Hoef-Emden, K. & Archibald JM. (2016). Handbook of the Protists: Cryptophyte (Cryptomonads).

Hoef-Emden, K., & Melkonian, M. (2003). Revision of the genus Cryptomonas (Cryptophyceae): A combination of molecular phylogeny and morphology provides insights into a long-hidden dimorphism. Protist, 154(3–4), 371–409. Corrigendum: Hoef-Emden, K., & Melkonian, M. (2008). Protist, 159(3), 507.

Hoham RD, Kang KY, Hasselwander AJ, Behrstock AF, Blackburn IR, Johnson RC, & Shlag EM. (1997). The effects of light intensitiy and blu, green and red wavelengths on mating strategies in the snow alga, Chloromonas sp. -d, from the Tughill Plateau, New York State. Western Snow Conference.

Hoham, R.W., Marcarelli, A.M., Rogers, H.S., Ragan, M.D., Petre, B.M., Ungerer, M.D., Barnes, J.M. & Francis, D.O. (2000). The importance of light and photoperiod in sexual reproduction and geographical distribution in the green snow alga, Chloromonas sp.-D (Chlorophyceae, Volvocales). Hydrol. Process., 14: 3309-3321.

Hosler JP, Wurtz EA, Harris EH, Gillham NW, Boynton JE. (1989). Relationship between gene dosage and gene-expression in the chloroplast of Chlamydomonas reinhardtii. Plant Physiol. 91:648-655.

Huang, X., Barrios, L.A.M., Vonkhorporn, P., Honda, S., Albertson, D.G., & Hecht, R.M. (1989). Genomic organization of the glyceraldehyde-3-phosphate dehydrogenase gene family of Caenorhabditis elegans. Journal of Molecular Biology. 206(3): 411-424.

Jarvis P & Soll J. (2001). Toc, Tic, and chloroplast protein import. Biochim. Biophys. Acta. 1541:64-79.

Kamiya, A. & Miyachi, S. (1984a). Effects of light quality on formation of 5-aminolevulinic acid, phycoerythrin and chlorophyll in Cryptomonas sp. cells collected from the subsurface chlorophyll layer. Plant Cell Physiol. 25:831–9.

Kamiya, A. & Miyachi, S. (1984b). Blue-green and green light adaptations on photosynthetic activity in some algae collected from subsurface chlorophyll layer in the western Pacific Ocean. In Senger, H. [Ed.] Blue Light Effects in Biological Systems. Springer, Berlin, Heidelberg, pp. 517–28.

Kana R, Kotabova E, Sobotka R, & Prasil O. (2012). Non-photochemical quenching in cryptophyte alga Rhodomonas salina is located in chlorophyll a/c antennae. PLoS ONE. 7(1): https://doi.org/10.1371/journal.pone.0029700

Khan H, Parks N, Kozera C, Curtis BA, Parsons BJ, Bowman S, Archibald JM. (2007). Plastid Genome Sequence of the Cryptophyte Alga Rhodomonas salina CCMP1319: Lateral Transfer of Putative DNA Replication Machinery and a Test of Chromist Plastid Phylogeny. Molecular Biology and Evolution. 24(8):1832–1842.

Kim DG, Lee C, Park SM, & Choi YE. (2014). Manipulation of light wavelength at appropriate growth stage to enhance biomass productivity and fatty acid methyl ester yield using Chlorella vulgaris. Bioresource Technology. 159:240-248.

Kim JI, Yoon HS, Yi G, Kim HS, Yih W, & Shin W. (2015). The plastid genome of the cryptomonad Teleaulax amphioxeia. PlosOne. https://doi.org/10.1371/journal.pone.0129284

Kim JI, Moore CE, Archibald JM, Bhattacharya D, Yi G, Yoon HS, & Shin W. (2017). Evolutionary dynamics of cryptophyte plastid genomes. Genome Biology and Evolution. 9(7):1859-1872.

Kim JH, Choi SJ, & Lee S. (2019). Effects of temperature and light on photosynthesis and growth of red alga Pyropia dentata (Bangiales, Rhodophyta) in a conchocelis phase. Aquaculture. 505(30):167-172.

Kim MY, Christopher DA, & Mullet JE. (1993). Direct evidence for selective modulation of psbA, rpoA, rbcL and 16s-RNA stability during barley chloroplast development. Plant Molec. Biol. 22:447-463.

Kirk, J. (1994). Light and Photosynthesis in Aquatic Ecosystems (2nd ed.). Cambridge: Cambridge University Press. doi:10.1017/CBO9780511623370

Koi S, Hisanaga T, Sato K, … Ishizaki K, Kohchi T. (2016). An evolutionarily conserved plant RKD factor controls germ cell differentiation. *Current Biology*, 26(13):1775-1781.

Konishi M & Yanagisawa S. (2013). Arabidopsis NIN-like transcription factors have a central role in nitrate signalling. Nature Communications. 4:1-9.

Korbee N, Figueroa FL, & Aguilera J. (2005). Effect of light quality on the accumulation of photosynthetic pigments, proteins, and mycosporine-like amino acids in the red alga Porphyra leucosticte (Bangiales, Rhodophyta). Journal of Photochemistry and Photobiology B: Biology. 80(2):71-78.

Koziol AG., Borza T., Ishida KI, Keeling P, Lee RW, & Durnford D. (2007). Plant Physiology. 143:18.2-1816.

Kritzberg, ES. (2017). Centennial-long trends of lake browning show major effect of afforestation. Limnology and Oceanography Letters 2:105–112.

Kugrens, P. & Lee, R.E. (1988). Ultrastructure of fertilization in a cryptomonad. J. of Phycol. 24(3):385-393.

Kugrens, P. & Lee, R.E. (1990). Ultrastructural Evidence for Bacterial Incorporation and Myxotrophy in the Photosynthetic Cryptomonad Chroomonas Pochmanni Huber-P estalozzi (Chyptomonadida). The Journal of Protozoology. 37: 263-267.

Lawrenz E & Richardson TL. (2017). Differential effects of changes in spectral irradiance on photoacclimation, primary productivity and growth in Rhodomonas salina (Cryptophyceae) and Skeletonema costatum (Baccilariophyceae) in simulated blackwater environments. Journal of Phycology. 53(6): 1241-1254.

Lawrenz E, Fedewa EJ, & Richardson TL. (2011). Extraction protocols for the quantification of phycobilins in aqueous phytoplankton extracts. Journal of Applied Phycology. 23: 865-871.

Lee C, Ahn JW, Kim JB, Kim JY, & Choi YE. (2018). Comparative transcriptome analysis of Haematococcus pluvialis on astaxanthin biosynthesis in response to irradiation with red or blue LED wavelength. World Journal of Microbiology and Biotechnology. 34(96).

Lewitus, A.J., Caron, D.A. & Miller, K.R. (1991). EFFECTS OF LIGHT AND GLYCEROL ON THE ORGANIZATION OF THE PHOTOSYNTHETIC APPARATUS IN THE FACULTATIVE HETEROTROPH PYRENOMONAS SALINA (CRYPTOPHYCEAE)1. Journal of Phycology. 27: 578-587.

Li, Y., Gu, W., Huang, A., Xie, X., Wu, S. & Wang, G. (2019). Transcriptome analysis reveals regulation of gene expression during photoacclimation to high irradiance levels in Dunaliella salina (Chlorophyceae). Phycological Res., 67: 291-302.

Li Y, Cai X, Gu W, & Wang G. (2020). Transcriptome analysis of carotenoid biosynthesis in Dunaliella salina under red and blue light. J. of Oceanology and Limnology. 38:177-185.

Lin, H., & Goodenough, U. W. (2007). Gametogenesis in the Chlamydomonas reinhardtii minus mating type is controlled by two genes, MID and MTD1. Genetics, 176(2), 913–925.

Lopez-Figueroa F. (1991). Red, green and blue light photoreceptors controlling chlorophyll a, biliprotein and total protein synthesis in the red alga Chondrus crispus. British Phycological Journal. 26:383-393.

Losi A, Gartner W. (2008). Shedding (blue) light on algal gene expression. PNAS. 105(1):7-8.

Lu S, Wang J, Chitsaz F, Derbyshire MK, Geer RC, Gonzales NR, … Marchler-Bauer A. (2020). CDD/SPARCLE: the conserved domain database in 2020. Nucleic Acids Res. 48(D1):D265-D268.

Liu C, Yuan D, Liu T, Xing M, Xu W, Zhang H, Jin H, Cai C, Li S. (2020). Characterization and comparative analysis of RWP-RK proteins from *Arachis duranensis, Arachis ipaensis,* and *Arachis hypogaea. International J. of Genomics.*

Liu X, Blomme J, Bogaert K, D'hondt S, Wichard T, De Clerk O. (in review). Transcriptional profiling of gametogenesis in the green seaweed *Ulva mutabalis*

identifies an RWP-RK transcription factors linked to reproduction. *BMC Plant Biology*.

Luimstra, V. M., Verspagen, J. M. H., Xu, T., Schuurmans, J. M., & Huisman, J. (2020). Changes in water color shift competition between phytoplankton species with contrasting light-harvesting strategies. Ecology 101(3):e02951. 10.1002/ecy.2951

Mackinney G. (1941). Absorption of light by chlorophyll solutions. The Journal of Biological Chemistry.

Martin M. Cutadapt removes adapter sequences from high-throughput sequencing reads. Technical Notes.

McKie-Krisberg, Z.M., Gast, R.J. & Sanders, R.W. (2015). Physiological Responses of Three Species of Antarctic Mixotrophic Phytoflagellates to Changes in Light and Dissolved Nutrients. Microb Ecol. 70: 21–29.

Menghini D & Aubry S. (2021). De novo transcriptome assembly data of the marine bioluminescent dinoflagellate *Pyrocystis lunula. Data in Brief*, 37.

Mouget JL, Rosa P, & Tremblin G. (2004). Acclimation of Haslea ostrearia to light of different spectral qualities – confirmation of 'chromatic adaptation' in diatoms. Journal of Photochemistry and Photobiology B: Biology. 75(1-2):1-11.

Muramatsu M & Hihara Y. (2012). Acclimation to high-light conditions in cyanobacteria: from gene expression to physiological responses. *J. of Plant Research,* 125:11-39.

Nan F, Feng J, Lv J, Liu Q, & Xie S. (2018). Transcriptome analysis of the typical freshwater rhodophytes Sheathia arcuate grown under different light intensities. PLoS One.

Neilson JAD, Rangrikitphoti P, Durnford DG. (2017). Evolution and regulation of Bigelowiella natans light-harvesting antenna system. J. of Plant Physiology. 217:68-76.

Ojala, A. (1993). The influence of light quality on growth and phycobiliprotein/chlorophyll a fluorescence quotients of some species of freshwater algae in culture. Phycologia 32:22- 28.

Ota S, Oshima K, Yamazaki T, Takeshita T, Bisova K, Zachleder V, Hattori M, & Kawano S. (2019). The Parachlorella genome and transcriptome endorse active RWP-RK, meiosis and flagellar genes in Trebouxiophycean algae. Cytologia. 84(4):323-330.

Overkamp KE, Gasper R, Kock K, Herrman C, Hofmann E, & Frankenberg-Dinkel N. (2014). Insights into the biosynthesis and assembly of cryptophycean phycobiliproteins. J. of Biological Chemicstry. 289(39):26691-26707.

Park, S., Jung, G., Hwang, Y. & Jin E. (2010). Dynamic response of the transcriptome of a psychrophilic diatom, Chaetoceros neogracile, to high irradiance. Planta 231-249.

Parkhill JP., Maillet G., Cullen JJ. (2001). Fluorescence-Based maximal quantum yield for PSII as a diagnostic of nutrient stress. J. of Phycol., 37:517-529.

Patel M & Berry JO. (2008). Rubisco gene expression in C4 plants. J. of Experimental Botany. 59(7): 1625-1634.

Pichard SL, Frischer ME, & Paul JH. Ribulose bisphosphate carboxylase gene expression in subtropical marine phytoplankton populations. Marine Ecology Progress Series. 101:55-65.

Pichard SL, Campbell L, Kang JB, Tabita FR, & Paul JH. (1996). Regulation of ribulose bisphosphate carboxylase gene expression in natural phytoplankton communities. I. Diel rhythms. Marine Ecology Progress Series. 139:257-265.

Pinckney JL, Millie DF, Howe KE, Paerl HW, & Hurley JP. (1996). Flow scintillation counting of 14C-labeled microalgal photosynthetic pigments. Journal of Planktonic Research. 18:1867-1880.

Powell DR. Degust: interactive RNA-seq analysis. DOI: 10.5281/zenodo.3258932.

Qiu, X.C. Mukai K, Shimasaki Y, Wu M, Chen C, Lu Y… Oshima Y. (2020). Diurnal variations in expression of photosynthesis-related proteins in the harmful

Raphidophyceae Chattonella marina var. Antiqua. Journal of Experimental Marine Biology and Ecology. 527

Quast C, Pruesse E, Yilmaz P, Gerken J, Schweer T, Yarza P, Peplies J, & Glockner FO. (2013). The SILVA ribosomal RNA gene database project: Improved data processing and web-based tools. Nucl Acids Res 41(D1):D591-596. https://dx.doi.org/10.1093%2Fnar%2Fgks1219

Rivkin RB. (1989). Influence of irradiance and spectral quality on the carbon metabolism of phytoplankton. I. Photosynthesis, chemical composition and growth. Marine Ecology Progress Series. 55:291-304.

Roberts, E.C. & Laybourn-Parry, J. (1999), Mixotrophic cryptophytes and their predators in the Dry Valley lakes of Antarctica. Freshwater Biology, 41: 737-746.

Rochaix JD. (1992). Post-transcriptional steps in the expression of chloroplast genes. Annu. Rev. Cell Biol. 8:1-28.

Rochaix JD. (1996). Post-transcriptional regulation of chloroplast gene expression in Chlamydomonas reinhardtii. Plant Molec. Biol. 32:327-341.

Rottberger J, Gruber A, Boenigk J, & Kroth PG. (2013). Influence of nutrients and light on autotrophic, mixotrophic and heterotrophic freshwater chrysophytes. Aquat Microb Ecol 71:179-191.

Roulet, N., & T. R. Moore. (2006). Browning the waters. Nature 444:283–284.

Sanfilippo JE, Garczarek L, Partensky F, & Kehoe DM. (2019). Chromatic acclimation in cyanobacteria: A diverse and widespread process for optimizing photosynthesis. Annual Review of Microbiology. 73: 407-433.

Schulz MH, Zerbino DR, Vingron M, & Birney E. (2012). Oases: Robust de novo RNA-seq assembly across the dynamic range of expression levels. Bioinformatics 28(8):1086-92. https://doi.org/10.1093/bioinformatics/bts094

Schwarz A & Markager S. (1999). Light absorption and photosynthesis of a benthic moss community: importance of spectral quality of light and implications of changing light attenuation in the water column. *Freshwater Biology.* 42:609-623.

Sebelik V, West R, Trskova EK, Kana R, & Polivka T. (2020). Energy transfer pathways in the CAC light-harvesting complex of Rhodomonas salina. BBA – Bioenergetics. 1861(11).

Simao FA, Waterhouse RM, Ioannidis P, Kriventseva EV, & Zdobnov EM. (2015). BUSCO: Assessing genome assembly and annotation completeness with single-copy orthologs. Bioinformatics 31(19):3210-2. https://doi.org/10.1093/bioinformatics/btv351

Sirover, M.A. (1998). Role of the glycolytic protein, glyceraldehyde-3-phosphate dehydrogenase, in normal cell function and in cell pathology. Journal of Cellular Biochemistry. 66(2): 133-140.

Stengel DB, Connan S, Popper ZA. (2011). Algal chemodiversity and bioactivity: sources of natural variability and implications for commercial application. *Biotechnol Adv*.,29(5):483-501.

Stomp M, Huisman J, Johng FD, Veraart AJ, Gerla D, Rijkeboer M, … Stal LJ. (2004). Adaptive divergence in pigment composition promotes phytoplankton biodiversity. Nature. 432: 104-107.

Stomp M, Huisman J, Voros L, Pick FR, Laamanen M, Haverkamp T, & Stal LJ. (2007). Colourful coexistence of red and green picocyanobacterial in lakes and seas. Ecology Letters. 10: 290-298.

Takahashi F, Yamagata D, Ishikawa M, Fukamatsu Y, Ogura Y, Kasahara M, … Kataoka H. (2007). AUREOCHROME, a photoreceptor required for photomorphogenesis in stramenopiles. PNAS. 104(49):19625-19630.

Takaichi S. (2011). Carotenoids in algae: Distributions, biosynthesis and functions. Mar. Drugs. 9:1101-1118.

Tardu M, Dikbas UM, Baris I, & Kavakli IH. (2016). RNA-seq analysis of the transcriptional response to blue and red light in the extremophilic red alga, Cyanidioschyzon merolae. Functional & Integrative Genomics. 16:657-669.

Tedeschi F, Rizzo P, Rutten T, Altschmied L, & Baumlein H. (2016). RWP-RK domain-containing transcription factors control cell differentiation during female gametophyte d evelopment in Arabidopsis. New Phytologist. 213(4):1909-1924.

Toth VR & Palmer SCJ. (2016). Acclimation of Potamogeton perfoliatus L. to periphyton accumulation-induced spectral changes in irradiance. Hydrobiologia. 766: 293-304.

Ullrich WR, J. Lazarová, C.I. Ullrich, F.G. Witt, & P.J. Aparicio. (1998). Nitrate uptake and extracellular alkalinization by the green alga Hydrodictyon reticulatum in blue and red light, Journal of Experimental Botany. 49(324):1157–1162

Vadiveloo A, Moheimani NR, Cosgrove JJ, Bahri PA, & Parlevliet D. (2015). Effect of different light spectra on the growth and productivity of acclimated Nannochloropsis sp. (Eustigmatophyceae). Algal Research. 8:121-127.

Vadiveloo A, Moheimani NR, Cosgrove JJ, Parlevliet C, & Bahri PA. (2017). Effects of different light spectra on the growth, productivity and photosynthesis of two acclimated strains of Nannochloropsis sp. Journal of Applied Phycology. 29:1765-1774.

Vesk, M., Dwarte, D., Fowler, S., & Hiller, R. G. (1992). Freeze-fracture immunocytochemistry of light havesting pigment complexes in a cryptophyte. Protoplasma 170, 166-176.

Wallen DG & Geen GH. (1971). Light quality in relation to growth, photosynthetic rates and carbon metabolism in two species of marine plankton algae. Marine Biology. 10:34-43.

Ward B & Follows MJ. (2016). Marine mixotrophy increases trophic transfer efficiency, mean organism size, and vertical carbon flux. PNAS. 113(11):2958-2963.

Wang WJ, Wang FJ, Sun XT, Liu FL, & Liang ZR. (2013). Comparative transcriptome under red and blue light culture of Saccharina japonica (Phaeophyceae). Planta. 237:1123-1133.

Xiang, T., Nelson, W., Rodriguez, J., Tolleter, D. & Grossman, A.R. (2015). Symbiodinium transcriptome and global responses of cells to immediate changes in light intensity when grown under autotrophic or mixotrophic conditions. Plant J, 82: 67-80.

Yocum, CS & Blinks LR. (1957). Light-induced efficiency and pigment alterations in red algae. J. Gen. Physiol. 41(6):1113-1117.

Yoo YD, Seong KA, Jeong HJ, Yih W, Rho JR, Nam SW, & Kim HW. (2017). Mixotrophy in the marine red-tide cryptophyte Teleaulax amphioxeia and ingestion and

grazing impact of cryptophytes on natural popoulations of bacteria in Korean coastal waters. Harmful Algae. 68:105-117.

CHAPTER 3

Andersen R, Charvet S, Hansen PJ. 2018. Mixotrophy in Chlorophytes and Haptophytes—Effect of Irradiance, Macronutrient, Micronutrient and VitaminLimitation. *Frontiers in Microbiology Aquatic Microbiology.*

Barton, A. D., Finkel, Z. V., Ward, B. A., Johns, D. G., & Follows, M. J. (2013). On the roles of cell size and trophic strategy in North Atlantic diatom and dinoflagellate communities. *Limnology and Oceanography*, *58*(1), 254–266.

Caron DA. 2016. Mixotrophy stirs up our understanding of marine food webs. *PNAS*, 113(1):2806-2808.

Cheirsilp B, Torpee S. 2012. Enhance growth and lipid production of microalgae under mixotrophic culture condition: Effect of light intensity, glucose concentration and fed-batch cultivation. *Bioresource Technology*, 110:510-516.

Chen, F., Zhang, Y. & Guo, S. Growth and phycocyanin formation of *Spirulina platensis* in photoheterotrophic culture. *Biotechnol Lett* **18,** 603–608 (1996).

Donaher N, Goro Tanifuji, Naoko T. Onodera, Stephanie A. Malfatti, Patrick S. G. Chain, Yoshiaki Hara, John M. Archibald, The Complete Plastid Genome Sequence of

the Secondarily Nonphotosynthetic Alga *Cryptomonas paramecium*: Reduction, Compaction, and Accelerated Evolutionary Rate, *Genome Biology and Evolution*, Volume 1, 2009, Pages 439–448

Doust AG, Wilk KE, Curmi PMG, Scholes GD. 2006. The photophysics of cryptophyte light-harvesting. *J. of Photochemistry and Photobiology A: Chemistry,* 184(1-2):1-17.

Flynn KJ., Stoecker DK., Mitra A, Raven JA, Glibert PM., Hansen PJ., Graneli E., Burkholder JM. 2013. Misuse of the phytoplankton-zooplankton dichotomy: the need to assign organisms as mixotrophs within plankton functional groups. *J. of Plankton Research*, 35(1):3-11.

Gervais, F. (1997), LIGHT-DEPENDENT GROWTH, DARK SURVIVAL, AND GLUCOSE UPTAKE BY CRYPTOPHYTES ISOLATED FROM A FRESHWATER CHEMOCLINE. Journal of Phycology, 33: 18-25

Gervais, F. (1998), Ecology of cryptophytes coexisting near a freshwater chemocline. Freshwater Biology, 39: 61-78.

González-Olalla, J.M., Medina-Sánchez, J.M. and Carrillo, P. (2019), Mixotrophic trade-off under warming and UVR in a marine and a freshwater alga. J. Phycol., 55: 1028-1040.

Hansen PJ, Peter Koefoed, Bjørnsen, Hansen, Benni Winding, (1997), Zooplankton grazing and growth: Scaling within the 2-2,-µm body size range, Limnology and Oceanography, 42

Hu J, Nagarajan D, Zhang Q, Chang J, Lee D. 2018. Heterotrophic cultivation of microalgae for pigment production: A review. *Biotechnology Advances,* 36(1):54-67.

Jansson, Mats, Blomqvist, Peter, Jonsson, Anders, BergstrÖm, Ann-Kristin, (1996), Nutrient limitation of bacterioplankton, autotrophic and mixotrophic phytoplankton, and heterotrophic nanoflagellates in Lake Örträsket, *Limnology and Oceanography*, 41.

Keller MD, Bellows WK, Guillard RRL. 1988. Microwave treatment for sterilization of phytoplankton culture media. *J. of Experimental Marine Biology and Ecology,* 117(3):279-283.

Kim JI, Moore CE, Archibald JM, Bhattacharya D, Yi G, Yoon HS, & Shin W. (2017). Evolutionary dynamics of cryptophyte plastid genomes. *Genome Biology and Evolution.* 9(7):1859-1872.

Klaveness D. 2013. Biology and ecology of the Cryptophyceae: Status and challenges. *Biological Oceanography*, 6(3-4):257-270.

Leeuwe, M.A., Visser, R.J. and Stefels, J. (2014), The pigment composition of *Phaeocystis antarctica* (Haptophyceae) under various conditions of light, temperature, salinity, and iron. J. Phycol., 50: 1070-1080.

Lewitus, A.J., Caron, D.A. and Miller, K.R. (1991), EFFECTS OF LIGHT AND GLYCEROL ON THE ORGANIZATION OF THE PHOTOSYNTHETIC APPARATUS IN THE FACULTATIVE HETEROTROPH *PYRENOMONAS SALINA* (CRYPTOPHYCEAE). Journal of Phycology, 27: 578-587

Litchman, E., Klausmeier, C.A., Schofield, O.M. and Falkowski, P.G. (2007), The role of functional traits and trade-offs in structuring phytoplankton communities: scaling from cellular to ecosystem level. Ecology Letters, 10: 1170-1181.

Mansour JS and Anestis K. 2021. Eco-Evolutionary Perspectives on Mixoplankton. *Frontiers in Marine Science: Marine Biology.*

Marquez, F.J., Nishio, N., Nagai, S. and Sasaki, K. (1995), Enhancement of biomass and Pigment production during growth of *Spirulina platensis* in mixotrophic culture. J. Chem. Technol. Biotechnol., 62: 159-164.

Marshall, W. and Laybourn-Parry, J. (2002), The balance between photosynthesis and grazing in Antarctic mixotrophic cryptophytes during summer. Freshwater Biology, 47: 2060-20704

Menge DNL, Weitz JS. 2009. Dangerous nutrients: Evolution of phytoplankton resource uptake subject to virus attack. *J. of Theoretical Biology*, 257(1):104-115.

Mitra A., Flynn KJ., Tillman U., Raven JA., Caron D., Stoecker DK…. Lundgren V. 2016. Defining planktonic protist functional groups on mechanisms for energy and nutrient acquisition: Incorporation of diverse mixotrophic strategies. *Protist,* 167(2):106-120.

Niel EWJ, P.A.M. Arts, B.J. Wesselink, L.A. Robertson, J.G. Kuenen, Competition between heterotrophic and autotrophic nitrifiers for ammonia in chemostat cultures, *FEMS Microbiology Ecology*, Volume 11, Issue 2, February 1993, Pages 109–118

Parkhill, J.-P., Maillet, G. and Cullen, J.J. (2001), FLUORESCENCE-BASED MAXIMAL QUANTUM YIELD FOR PSII AS A DIAGNOSTIC OF NUTRIENT STRESS. Journal of Phycology, 37: 517-529

Raven, J.A. (1984), A COST-BENEFIT ANALYSIS OF PHOTON ABSORPTION BY PHOTOSYNTHETIC UNICELLS. New Phytologist, 98: 593-625

Raven, J. A., (1997), Phagotrophy in phototrophs, *Limnology and Oceanography,* 42.

Roberts, E.C. and Laybourn-Parry, J. (1999), Mixotrophic cryptophytes and their predators in the Dry Valley lakes of Antarctica. Freshwater Biology, 41: 737-746

Roth, M.S., Westcott, D.J., Iwai, M. *et al.* Hexokinase is necessary for glucose-mediated photosynthesis repression and lipid accumulation in a green alga. *Commun Biol* **2,** 347 (2019).

Sanders, R., Caron, D., Davidson, J. *et al.* Nutrient Acquisition and Population Growth of a Mixotrophic Alga in Axenic and Bacterized Cultures. *Microb Ecol* **42,** 513–523 (2001).

Sepsenwol, S. 1973. "Leucoplast of the cryptomonad Chilomonas paramecium. Evidence for presence of a true plastid in a colorless flagellate." Exp. Cell Research. 76: 395-409

Stadnichuk IN, Rakhimberdieva MG, Bolychevtseva YV, Yurina NP, Karapetyan NV, Selyakh IO. 1998. Inhibition by glucose of chlorophyll a and phycocyanobilin biosynthesis in the unicellular red alga *Galdieria partita* at the stage of coproporphyrinogen III formation. *Plant Science*, 136(1):11-23.

Stoecker DK and Lavrentyev PJ. 2018. Mixotrophic plankton in the Polar Seas: A pan-arctic review. *Frontiers in Marine Science: Marine Ecosystem Ecology.*

Stoecker DK., Hansen PJ, Caron DA, Mitra A. 2017. Mixotrophy in the Marine Plankton. *Annual Review of Marine Science*, 9(1):311-335.

Ward BA. & Follows MJ. 2016. Marine mixotrophy increases trophic transfer efficiency, mean organism size, and vertical carbon flux. *PNAS*, 113(11):2958-2963.

Ward, B. A., Dutkiewicz, S., Jahn, O., & Follows, M. J. (2012). A size-structured food-web model for he global ocean. *Limnology and Oceanography*, *57*(6), 1877–1891.

Ward BA, Maranon E, Sauterey B, Rault J, Claessen D. 2017. The size dependence of phytoplankton growth rates: A trade-off between nutrient uptake and metabolism. *The American Naturalist,* 189(2).

Yang C, Hua Q, Shimizu K. 2000. Energetics and carbon metabolism during growth of microalgal cells under photoautotrophic, mixotrophic and cyclic light-autotrophic/dark-heterotrophic conditions. *Biochemical Engineering Journal*, 6(2):87-102.

Yoo YD, Seong KA, Jeong HJ, Yi W, Rho JR, Nam SW, Kim HS. 2017. Mixotrophy in the marine red-tide cryptophyte *Teleaulax amphioxeia* and ingestion and grazing impact of cryptophytes on natural populations of bacteria in Korean coastal waters. *Harmful algae,* 68: 105-117.